What Brown saw, and you can too

Philip Pearle,[1] Kenneth Bart,[2] David Bilderback,[3] Brian Collett,[4] Dara Newman,[5] and Scott Samuels[5]

[1]*Emeritus, Department of Physics, Hamilton College, Clinton, NY 13323*
[2]*Department of Biology, Hamilton College, Clinton, NY 13323*
[3]*Emeritus, Division of Biological Sciences, The University of Montana, MT 59812*
[4]*Department of Physics, Hamilton College, Clinton, NY 13323*
[5]*Division of Biological Sciences, The University of Montana, MT 59812*

A thorough discussion is given of the original observations by Robert Brown, of particles undergoing what is now called Brownian motion. Topics scanted in the literature, the nature of those particles, and Brown's thought that he was observing universal organic particles whereas he was observing the Airy disc of his lens, are treated in detail. Also shown is how one may make the same observations, including how to make a ball lens microscope. Appendices contain tutorials on the relevant theory.

PACS numbers:

I. INTRODUCTORY

In June 1827, the celebrated British botanist Robert Brown was observing pollen of the plant *Clarkia pulchella* immersed in water, with his one lens microscope (essentially, a magnifying glass with small diameter and large curvature). He noticed that particles ejected from the pollen were of two shapes: some were oblong and some smaller ones were circular, and they were jiggling about in the water. Thus commenced his investigations, which showed that anything sufficiently small would move similarly. Of course, we now understand, as Brown never did, that the jiggling is due to the irregular impact of water molecules.

Physicists care about particles. This paper arose from curiosity as to the nature of the particles Brown observed. That question is answered here.

Brown was motivated in his investigations by the observation, for all objects he *bruised*, that the smallest bits in motion were circular, and of about the same diameter. He called these bits "molecules" (a word in common usage meaning tiny particle), suggesting that they might be universal building blocks of nature. However, Brown was actually seeing the effects, on the images of sufficiently small objects, of the diffraction and spherical aberration of his lens. A literature search has found this point tersely suggested once[1]. An experimental and theoretical examination of this issue is given here.

Although this paper was initially intended to be brief, it grew with the realization of the richness of the subject matter, a weaving of history, botany and classical physics, with experimental possibilities. We hope that, with appropriate selectivity and emphasis, it may be an interesting and accessible resource for various projects for teachers and students from middle school to college.

Section II, History, discusses *Clarkia pulchella*. It was found by Meriwether Lewis in 1806 on the return trip of the Lewis and Clark expedition. It was named and published in 1814 in England by Frederick Traugott Pursh. Its seeds were first collected and sent to England in 1826 from the northwest Pacific coast by David Douglas. They arrived in London in 1827 and were grown there, providing flowers for Brown's investigations.

Section III, Jiggly, peruses Brown's classic paper.

Section IV is entitled Botany. The question which motivated this paper was answered only when it reached one of the authors (D. B.): the oblong particles Brown saw are amyloplasts (starch organelles, i.e., starch containers) and the spherical particles are spherosomes (lipid organelles, i.e., fat containers). Some history of early pollen research and some physiology of pollen are discussed here.

Section V, Microscopy, discusses how to go about duplicating Brown's observations of *Clarkia* pollen. This was undertaken by the author least capable in this regard, a theoretical physicist (P.P.), in expectation of uncovering difficulties that a novice might face, and is written in the first person. This is followed by a discussion of Brown's lens. It closes with an experimental investigation (by B. C.) of imaging by a 1mm diameter spherical (ball) lens, whose magnification is close to that of Brown's lens.

Section VI, Theory, is meant for advanced physics undergraduates or graduate students and their teachers. It consists of seven theoretical appendices, tutorials on classical physics. Most of this material has been known for over a century. Some of it has found its way into textbooks. Apart from the benefit of finding all the relevant material in one place, in self-contained form, each appendix contains some novel treatment. Some material may suggest further, independent, investigations. The subject matter is A) Brownian motion, B) viscous force and torque, C) WKB derivation of geometrical optics (the eikonal equation) from the wave equation, D) application to mirrors and lenses, E) Huyghens-Fresnel-Kirchhoff construction, F) imaging of a point source of light (diffraction and spherical aberration receiving a unified treatment), and G) imaging of an illuminated hole.

II. HISTORY

This section describes how the plant *Clarkia pulchella* of the American Northwest came to be grown in England.

A. Lewis

In 1778, 1785 and again in 1792, the American botanist Humphrey Marshall (1722-1801) proposed to the American Philosophical Society of Philadelphia that they support a botanical expedition westward to the Pacific ocean[2]. Thomas Jefferson (1743-1826) joined the Society in 1790. He heard the last proposal and tried to advance it in 1793, but the project foundered.

On June 20, 1803, first term President Thomas Jefferson sent a formal letter to his private secretary and aide Meriwether Lewis (1774-1809), a captain in the 1st U. S. Infantry. It requested that he head an expedition up the Missouri River to find a navigable route to the Pacific Ocean. No mention in this letter was made of botany, but Jefferson had it in mind. Following Jefferson's recommendation, as part of his preparation, in Philadelphia, in May and June of 1803, Lewis took a crash course in botany from Benjamin Smith Barton (1766-1815), who had written the first American textbook on the subject.

Lewis was authorized to choose a co-commander, and he chose William Clark (1770-1838), who had earlier been Lewis's commanding officer. On May 14, 1804, the Lewis and Clark expedition set out from St. Louis. They reached the Pacific at the mouth of the Columbia River on Nov. 7, 1805 (*OCEAN in view! Oh! The joy!* wrote Clark in his journal). They returned on September 23, 1806, having accomplished all that was asked of them and more.

On the return journey, while waiting for a month in the Kamiah Valley of Idaho for the snow to melt in the mountains, Lewis wrote on June 1, 1806:

I met with a singular plant today in blume, of which I preserved a specemine. It grows on the steep sides of the fertile hills near this place. . . . I regret very much that the seed of this plant are not yet ripe and it is probable will not be so during my residence in this neighborhood."[3]

and he gave a detailed botanical description of the flower.

B. Pursh

Upon his return, in April 1807, since Barton had failed to do anything with specimens sent on earlier, Lewis sought the advice of Bernard McMahon (1775-1816). He was a Philadelphia seedsman esteemed by Jefferson and entrusted to grow the seeds brought back by Lewis. McMahon suggested employing Frederick Traugott Pursh (1774-1820), the curator (and often collector) of Barton's collection. Lewis hired Pursh to prepare a catalog of the plants he had collected.

Unhappy working for Barton, Pursh moved to the home of McMahon, and had achieved a great deal by 1808. Meanwhile, Jefferson sent Lewis to be Governor of the Louisiana Purchase territory. This was a terribly demanding job, and ultimately led to Lewis's untimely death. Letters sent to Lewis by McMahon, who was personally financing Pursh, went unanswered. Therefore, McMahon recommended Pursh to a distinguished medical doctor and botanist, Dr. David Hosack (1769-1835). Hosack was Alexander Hamilton's family physician, who tried to save Hamilton's life after his duel with Aaron Burr. In 1801, Hosack had bought 20 acres in Manhattan (presently the site of Rockefeller Center), and created Elgin Botanical Gardens, the first such enterprise in America.

Pursh left Philadelphia for New York in April 1809, to be gardener at Elgin. He took his work and many of Lewis's specimens with him. However, the upkeep of Elgin Gardens was too expensive. Hosack sold it to New York State in 1810, after which it soon deteriorated. Pursh left for the West Indies in late 1810, partly for his health and partly to collect plants for Hosack. He returned to the United States in the fall of 1811, and then sailed to London in the winter.

Pursh published his volume *Flora Americae Septentrionalis* in mid-December 1813. In it, he gave the name *Clarkia pulchella* (beautiful Clarkia) to the flower mentioned above, of course, in honor of Clark.

C. Douglas

However seeds of *Clarkia pulchella* only made their way to England in 1826[5]. The plant was apparently not grown before then in the United States, either. It was found on a collecting expedition by the adventurous, indefatigable, assiduous botanical collector, David Douglas (1799-1834), after whom the Douglas fir is named.

Douglas was hired by Joseph Sabine (1770-1837), secretary of the Horticultural Society of London, to collect plants and seeds from the American Northwest. The Hudson's Bay Company also sponsored the trip. Douglas embarked on July 25, 1824, on the Hudson's Bay Company brig *William and Ann*. It left Gravesend on July 27, stopping at a few places (e.g., Rio de Janeiro, for three weeks), and traveled around Cape Horn. It dropped anchor at the mouth of the Columbia River (part of whose meandering length is now the western two-thirds of the border between Oregon and Washington) on April 7, 1825. Douglas wrote in his journal:

At one o'clock noon, we entered the river and passed the sand barrier safely (which is considered dangerous and on which I learn many vessels have been injured and some wrecked). [The *William and Ann*, under another captain, was wrecked on this bar on March 10, 1829,

with all hands lost.] *Thus my long and tedious voyage of 8 months 14 days from England terminated. The joy of viewing land, the hope of in a few days ranging through the long wished-for spot and the pleasure of again resuming my wonted employment may be readily calculated. ... With truth I may count this one of the happy moments of my life.*

The brig anchored on April 12 at Fort George (now in Astoria, Oregon), on the south shore of the Columbia River. However, the fort had recently been abandoned in favor of a new headquarters of the Hudson's Bay Company at Fort Vancouver (now in Vancouver, Washington), 90 miles up the Columbia River. After some botanizing and after collecting his gear from the brig, Douglas disembarked and *with one Canadian and six Indians* left by canoe on April 19. On April 20, he arrived at Fort Vancouver, on the north shore of the river, which became the base for his excursions.

He gathered plants in the neighborhood until June 20, having collected almost 300 specimens, which he lists and briefly describes in his journal[6]. Then, he hitched a boat-ride further up the Columbia River with some Hudson's Bay employees. In a couple of days and 46 miles, they passed what Lewis and Clark had named "The Grand Rapids" (which are now lost, slightly above the Bonneville Dam). Traveling on, they reached what Lewis and Clark had named "The Great Falls" (later called the Celilo Falls, which were lost in 1957 with the construction of the Dalles Dam). He wrote in his journal[7],

From the Grand Rapids to the Great Falls (70 miles) the banks are steep, rocky, and in many places rugged. The hills gradually diminish in elevation ... .As far as the eye can stretch is one dreary waste of barren soil thinly clothed with herbage. In such places are found the beautiful Clarkia pulchella, ...

He stayed in the area above the Great Falls for about a month, and collected around 120 specimens. He writes[8]:

During my journey, I collected the following plants, some very interesting and will, I am sure, amuse the lovers of plants at home.

and lists about 120 more plants, recommencing with number 296. In the list is

(329) Clarkia pulchella *(Pursh), annual; description and figure very good; flowers rose color; abundant on the dry sandy plains near the Great Falls; on the banks of two rivers twenty miles above the rapids; an exceedingly beautiful plant. I hope it may grow in England.*

He left on July 19,

... in an Indian canoe for the purpose of prosecuting my researches on the coast, which was in a great measure frustrated by the tribe among whom I lived going to war ... ,

arriving again at Fort Vancouver on August 5.

Douglas proceeded to dry his plants. He also collected some seeds from plants in the neighborhood that were already in the collection but had not earlier gone to seed. He left on August 19 to go up a tributary of the Columbia for some more collecting, and returned on August 30. On September 1 he made a second trip to the Grand Rapids, again "... to collect seeds of several plants seen in flower in June and July." With 499 plants now on his list[9],

Returned on the 13th ... and learned that the vessel had returned from the North and would be despatched for England without delay. My time must now be taken up packing, arranging, and writing for a short time. From that time till October 3rd employed dividing my seeds and specimens and finishing transcribing my Journal. Wrote today to Jos. Sabine, Esq., ... I am to-morrow morning to leave here to see my boxes safely place in the vessel.

However, he could not go to the *William and Ann*, because he punctured his knee with a nail while packing the crates. So, he sent them on with instructions for their care, *particularly the chest of seed*. The captain sent assurances that he would personally call on Mr. Sabine.

The ship left the mouth of the Columbia River on October 25, 1825, in due course rounding Cape Horn. It arrived at London on April 15, 1826[10], and that is how *Clarkia pulchella* seeds first arrived in England.

Addendum: Douglas had more adventures while collecting plants and animals (and sending them back to England) during 1826. Having wintered over, on March 20, 1827 he embarked on the Columbia River. He was aiming to reach Hudson Bay, and from there return to England. With various companions, collecting plants all the way, he headed first for Kettle Falls, now at the northeast corner of Washington state. Then, they set out for the Canadian Rockies on April 18. They reached the Athabasca Pass, (now at the border between British Columbia and Alberta, around the middle of the western edge of Jasper National Park) on May 1. At midday, while the rest of the group was resting, Douglas became, it has been suggested, the first mountaineer in North America[11]:

After breakfast, about one o'clock, being well refreshed, I set out with the view of ascending what seemed to be the highest peak on the north ... . The view from the summit is of that cast too awful to afford pleasure-nothing as far as the eye can reach in every direction but mountains towering above each other, rugged beyond all description ... . This peak, the highest yet known in the northern continent of America, I felt a sincere pleasure in naming "Mount Brown," in honour of R. Brown, Esq., the illustrious botanist, no less distinguished by the amiable qualities of his refined mind.

He proceeded easterly, through Edmonton, arriving at the settlement of Norway House on the northern end of Lake Winnipeg on June 16. He dawdled in the vicinity

and collected some more plants. Finally, leaving there on August 18, Douglas arrived at the settlement of York Factory on the eastern end of Hudson Bay on July 28, 1827, concluding his journal with:

I sailed from Hudson's Bay on September 15th and arrived at Portmouth on October 11th, having enjoyed a most gratifying trip.

D. Brown

As shall be seen, pollen from *Clarkia pulchella* flowers, grown from the seeds shipped out by Douglas, were put to use by Robert Brown as soon as possible. Biographies of Robert Brown (1773-1858), a comprehensive book[12] as well as short and web-accessible sketches[13][14][16] are available, so only a brief outline shall be given here. Already in his teenage years, Brown had a strong interest in botany. While attending medical school at the University of Edinburgh, he collected plants in Scotland, and befriended people of like interest. He left the university in 1793 without his medical degree and joined the Army in 1794. He was sent in 1795 to serve in Ireland as a surgeon's mate. He spent as much of his time there as he could spare doing botany. He visited London in the summers of 1798 and 1799, networking with other botanists.

At the time, Joseph Banks (1743-1820) was the most influential botanist in England. His initial fame was gained from plant collecting during Captain Cook's first expedition (1768-1771). Banks was president of the Royal Society from 1778 until his death. (He appears as a colleague of Stephen Maturin in the novels of Patrick O'Brian!). He convinced the Admiralty of the desirability of charting the coast of Australia and collecting plants there. Having heard good things about Brown, Banks wrote him a letter on December 12, 1800, offering the post of naturalist on the expedition. Brown accepted with alacrity. He obtained leave from his military duties, traveled to London, and became acquainted with Banks. Brown also met Ferdinand Bauer (1760-1826), a superb botanical illustrator, who was to accompany him on the trip. Brown prepared diligently. The ship *Investigator* set sail for Australia on July 18, 1801. Brown had many adventures as an indefatigable collector of plants (but also of animals, birds, fishes, reptiles, insects and rocks). He returned on October 7, 1805, having found thousands of new species of plants.

Brown's work had been so impressive that, before the year ended, he was chosen to be librarian of the Linnean Society. With salary and free lodgings in prospect, he quit the army. Also, Banks convinced the Admiralty to continue Brown's salary, and that of Bauer, as they codified their work. In the next five years, Brown wrote ground-breaking papers on plant classification, often aided by microscopic observations. In 1810 he published Volume 1 describing his Australian plants. The projected Volume 2 was never published, because the first volume was a financial failure, but much of the remaining material later emerged in various papers. In that year, Banks hired him as the librarian and curator of Banks's herbarium. Together with his arrangement with the Linnean Society, this made him financially secure (the Admiralty stipend ended the following year).

Brown was extremely active professionally, at the hub of botanical research in England, and was increasingly admired throughout Europe, not least because of his remarkably perceptive microscopy. A forte was characterizing plants by the nature of their reproductive organs and seeds, a scheme that was superior to the Linnean system then prevalent.

Banks died in the middle of 1820. He left his library, herbarium, an annuity and eventually the lease to his house to Brown, with the stipulation that Brown take up residence there. The botanical materials were to go eventually to the British Museum, subject to Brown's convenience. He leased half of the house to the Linnean society for their collections and use, and soon resigned from his paid Linnean positions. In 1825 he declined an offer of the Linnean Society, writing that one who occupied the proffered position of Secretary ... *should unquestionably have the habits of a man of business and be perfectly regular in matters of correspondence. That I do not possess such habits at present is but too well known to all my friends and whether I should ever acquire them is at least very doubtful.*

Nonetheless, despite his protestation of lack of business acumen, his negotiations with the Trustees of the British Museum for the transfer of Banks's library, which took more than a year, concluded in September 1827 with satisfying success. He was to become the underlibrarian in charge of the collection. There was a good stipend for two days work a week and a full-time paid assistant John Joseph Bennett (1801-1876) who became a friend and eventually Brown's executor. The terms were such that he retained his rooms, stipend from Banks and control of Banks's herbarium. During these negotiations, Brown was conducting the investigations of concern here.

III. JIGGLY

When the seeds Douglas had shipped out arrived at the Horticultural Society in early spring 1826, they came under the purview of John Lindley (1799-1865)[17]. Lindley had been mentored by Brown: in 1818, Brown gave Lindley a job that lasted a year and a half working in Banks's herbarium[12]. In 1821, the Horticultural Society leased 33 acres in Chiswick for an experimental garden[18]. The next year, Sabine hired Lindley to be assistant secretary of the garden, to superintend the collection of plants and their propagation.

The Natural History Museum in London (which spun off from the British Museum in 1881) has an extensive collection of Brown's papers. In box 24 of Brown's "Slips Catalogue," sheet #224 is labeled Clarkia[19]. Directly

underneath, Brown's (not always legible) handwriting reads *Hort Soc* (Horticultural Society) *Horticult (illegible) Chiswick (illegible)*, and the next line reads *occident* (western) *Amer (illegible) by D Douglas*. Thus, Brown certifies that his *Clarkia pulchella* flowers came directly from the Horticultural Society's garden. Flowers or seeds could be distributed to Fellows of the Society, but Brown was not one. Therefore, he likely received *Clarkia* flowers privately from John Lindley[20].

Sheet #224 contains entries dated June 12, 1827 and June 13, 1827. The first entry begins by describing the pollen[21]:

The grains of Pollen are subspherical or orbiculate-lenticular (circular-lens shaped) *with three equidistant more pellucid and slightly projecting points so that they are obtusely triangular. ...*

Figure 1 shows the pollen viewed under a microscope. Figure 2 is an electron microscope picture of the pollen. It looks vaguely like a pinched tetrahedron with the longest dimension around 100 microns[22] and "pores" at three vertices.

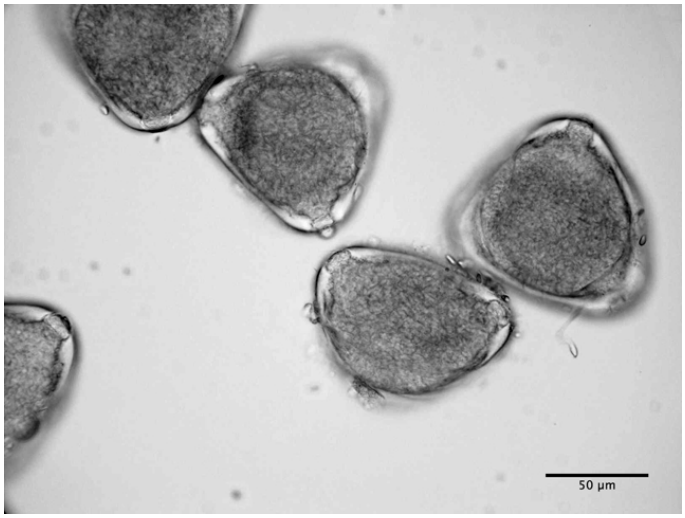

FIG. 1: *Clarkia pulchella* pollen imaged by a microscope at x400.

The entry turns to the contents of the pollen:

The fovilla or granules fill the whole orbicular disk but do not extend to the projecting angles. They are not spherical but oblong or nearly cylindrical. & the particles have a manifest motion. This motion is only visible to my lens which magnifies 370 times. The motion is obscure but yet certain. ...

Thus began the research that resulted in Brown's wonderfully discursive paper[23], dated July 30, 1828, and entitled:

A brief Account of Microscopical Observations made in the Months of June, July and August 1827, on the Particles contained in the Pollen of Plants; and on the general Existence of active Molecules in Organic and Inorganic Bodies.

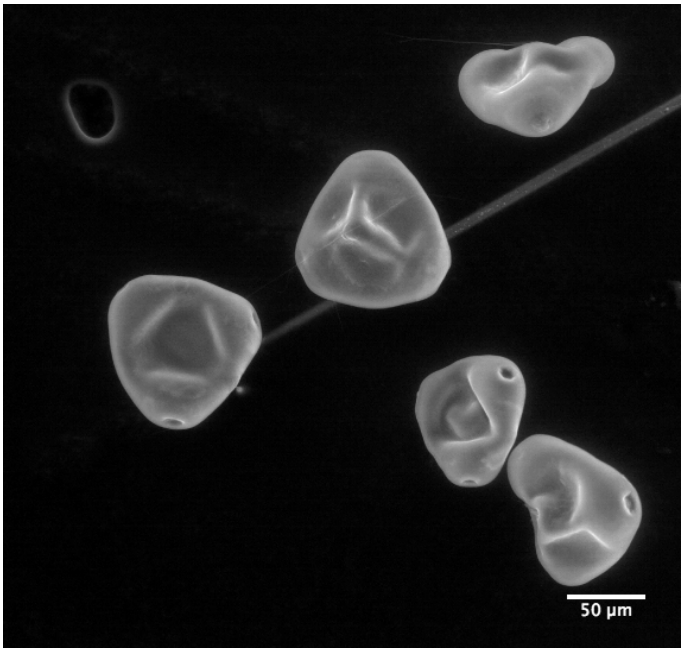

FIG. 2: *Clarkia pulchella* imaged by an electron microscope.

It was first privately published as a pamphlet, treated as a preprint and given to various colleagues. However, it was published in September.

This is a superb example of a researcher of unusual capability and energy delineating his thought processes. Some of its 53 paragraphs shall be treated here in some detail, especially the first nine that describe Brown's interaction with *Clarkia* and the start of a broader investigation.

A. Brown's Microscopes

The paper begins with a description of his microscope in the first paragraph:

The observations, of which it is my object to give a summary in the following pages, have all been made with a simple microscope, and indeed with one and the same lens, the focal length of which is about 1/32 of an inch.

Brown expands in a footnote:

This double convex Lens, which has been several years in my possession, I obtained from Mr. Bancks, optician, in the Strand. After I had made considerable progress in the inquiry, I explained the nature of my subject to Mr. Dollond, who obligingly made for me a simple pocket microscope, having very delicate adjustment, and furnished

with excellent lenses, two of which are of much higher power than than that above mentioned. ...

However, he added that he only used the Dollond microscope *... in investigating several minute points.*

A well known rule of thumb is that a near object is best seen at a distance of 10 inches. This puts the magnification Brown used at $\approx 10/f = 320$, which is not far from Brown's own estimate of ×370 cited above.

The whereabouts of this lens is not known. There does exist a pocket microscope of Brown's made by Bancks, in a box of dimensions less than 1"x2"x5". Upon Brown's death, Bennett gave this microscope *... which he was in the daily habit of using at the museum ...*[24] to a mutual friend, and it has ended up at the Linnean Society. It has a complete set of lenses, the strongest of which has magnification ×170. Bennett gifted another Bancks microscope, used by Brown at home, whose strongest lens has magnification ×160: this is now in the museum at Kew Gardens. These are all the extant microscopes that can definitively be traced to Brown. There is also a pocket microscope at the University Museum of Utrecht, made by Dollond, with highest power lenses ×330 and ×480 magnification that associated documents suggest bears a relationship to Brown's Dollond microscope[24].

The Linnean Society microscope's ×170 lens has been conjectured by Ford to be the one Brown used for his Brownian motion observations[24][25], and the microscope at Utrecht is thought to be essentially identical to Brown's microscope made by Dollond. Ford proposed that Brown meant the working distance of the lens (the distance between the front of the lens and the viewed object) when he stated that the focal length was 1/32 inch. Ford also surmised that the above-mentioned extant microscopes represent Brown's full collection. If so, since the ×170 lens is the strongest Bancks lens extant, it is the best candidate. In addition, Brownian motion can be observed with it[14], albeit of milk fat globules[15]. Indeed, as Brown asserted in his footnote, the ×170 lens is much less powerful than the Utrecht ×330 and ×480 Dollond lenses.

However, these conjectures are doubtful.

The ×170 lens (which therefore has a focal length of 1/17 inch) was measured by Ford to have a working distance of 1.5mm=1/17inch, not 1/32inch[25]. [Regardless, there must be some mistake. Half the lens thickness is the difference between the working distance and the focal length of the lens (which is essentially the object distance, for a magnifying glass). If both these numbers are 1/17 inch, this implies that half the lens thickness is 0!]

Moreover, Brown had many microscopes. Upon his death, the *Gardener's Chronicle* magazine reported that at least 9 microscopes of his were sold, some made by Bancks[36].

Brown likely had two Dollond lenses of power much larger than ×370, as he said in his footnote. The French botanist Alphonse de Candolle (1806-1893) visited Brown in 1828. He wrote to his famous botanist father that Brown had showed him the motion of granules from pollen, and added[27]:

For that he only works with the simple lenses. But it is true that the lenses of English manufacture are as strong as many compound microscopes, because they magnify up to 800 and 1000 times. Mr. Brown has had 30 or 40 made by Dollond and other famous opticians and he chooses from them 5 or 6 in number, with which he usually works. He obtains thus the effect of an ordinary microscope with the clarity and the reliability of a simple lens.

This is supported in a remark contained in an addendum by Brown entitled *Additional Remarks on Active Molecules* written a year later[23]. Brown says that the new work described there

... employed the simple microscope mentioned in the Pamphlet as having been made for me by Mr. Dollond, and of which the three lenses that I have generally used, are of a 40th, 60th and 70th of an inch focus.

Thus, he says he has lenses of power ×600 and ×700, which agrees with his footnoted remark, *two of which are of much higher power* than the ×370 lens.

Brown was the most astute microscopist of his day, and known to be extremely cautious with his statements. We believe he should be taken at his word: he used a ×370 lens.

These are remarkably small lenses, with surface radii, thickness and diameter comparable in size to the focal length. Such lenses are like those of Leeuwenhoek (1632-1723)—a delightful recent paper describes grinding such a lens[28].

Brown apparently preferred simple microscopes rather than compound microscopes. Charles Darwin (1809-1882) visited Brown in 1831, just before the voyage of the Beagle, to consult about what microscope to take. He wrote in his "Life and Letters," *I saw a good deal of Robert Brown ... He seemed to me to be chiefly remarkable for the minuteness of his observations and their perfect accuracy. ....* He was advised to take a Bancks single lens microscope on the voyage, which he did. This microscope is at Darwin's home, Down House in Kent.

The way to construct a compound microscope that was superior to a single lens was not well known at the time, because of spherical aberration. Joseph Jackson Lister (1786-1869) (father of the surgeon Joseph Lister who instigated antiseptic operations, after whom the mouthwash Listerine was named) discovered how to minimize spherical aberration in compound microscopes, by appropriately separating lens elements. He commissioned construction of such a microscope in 1826, but only published the concept in 1830[29].

As is discussed in detail later in this paper, a single lens, with appropriate choice of the exit pupil, can have negligible spherical aberration. In addition, a single lens microscope is more portable. Darwin only replaced

his Beagle microscope, which served the dual purpose of observation and dissection, by two microscopes, a compound microscope in 1847 and a dissecting microscope of his own design in 1848. Concerning the latter, he wrote to a friend: *... I have derived such infinitely great advantage from my new simple microscope, in comparison with the one which I used on the Beagle ... . I really feel quite a personal gratitude to this form of microscope & quite a hatred to my old one.*[30]

B. Observing *Clarkia pulchella*

The second paragraph mentions a paper Brown had published in 1826, which

... led me to attend more minutely than I had before done to the structure of the Pollen, and to inquire into its mode of action on the Pistillum ...

The pistil, the female part of a flower, consists of a vase-like object called the style, containing at its bottom the ovules (immature seeds containing eggs) and a structure on top called the stigma. Others conjectured that, when a pollen grain sticks to the stigma, the grain releases the particles it contains, and these somehow travel down through the style to fertilize the ovules. In his third paragraph, Brown expresses doubts *respecting the mode of action of the pollen in the process of impregnation.*

As explained in the fourth and fifth paragraphs, he had the idea to look into this too late in the year, past the time of flowering:

It was not until late in the autumn of 1826 that I could attend to this subject; and the season was too far advanced to enable me to pursue the investigation. Finding, however, in one of the few plants then examined, the figure of the particles contained in the grain of pollen clearly discernible, and that figure not spherical but oblong, I expected with some confidence to meet with plants in other respects more favorable to the inquiry, in which these particles, from peculiarity of form, might be traced through their whole course ... .

I commenced my study in June 1827, and the first plant examined proved in some respects remarkably well adapted to the object in view.

Thus Brown explains his selection: among a number of flowers apparently chosen by chance, *Clarkia pulchella* pollen clearly contained oblong particles.

For what follows, note that the male part of a flower, the stamen, consists of two parts. There is the anther, which is a sack in which pollen grains develop; it sits on a stalk called the filament, which conveys nutrients from the flower to the anther. When the pollen is ripe, it is released because the anther bursts, splitting longitudinally (in most cases), a process called *dehiscence.*

The sixth paragraphs launches the investigation.

This plant was Clarckia pulchella*, of which the grains of pollen, taken from antherae fully grown before bursting, were filled with particles or granules of unusually large size, varying from 1/4000th to about 1/3000th of an inch in length, and of a figure between cylindrical and oblong, ... While examining the form of these particles immersed in water, I observed many of them very evidently in motion ... . In a few instances the particle was seen to turn on its longer axis. These motions were such as to satisfy me, after frequently repeated observation, that they arose neither from currents in the fluid, nor from its gradual evaporation, but belonged to the particle itself.*

This is the first kind of particle Brown observes, whose length he estimates at about 6 to 8 microns. This is worth noting, since observations discussed later in this paper give these particles shorter lengths. The difference shall be attributed to the alteration of the image by his lens, as mentioned earlier.

In the seventh and eighth paragraphs, he notes the existence of a second kind of particle;

Grains of pollen of the same plant taken from antherae immediately after bursting, contained similar subcylindrical particles, in reduced numbers however, and mixed with other particles, at least as numerous, of much smaller size, apparently spherical, and in rapid oscillatory motion.

These smaller particles, or Molecules as I shall term them, when first seen, I considered to be some of the cylindrical particles swimming vertically in the fluid. But frequent and careful examination lessened my confidence in this supposition; and on continuing to observe them until the water had entirely evaporated, both the cylindrical particles and spherical molecules were found on the stage of my microscope.

C. Seeing Brownian Motion

We emphasize here that Brown was *not* observing the pollen move. He was observing much smaller objects, which reside within the pollen, move. This is well known—see for example the excellent pedagogical article by Layton[31]. Nonetheless, statements that Brown saw the pollen move are rife[32].

A *Clarkia* pollen is $\approx 100\ \mu m$ across[22]. As we shall shortly show, that is too large for its Brownian motion to be readily seen. However, fortunately for Brown, the contents of the pollen are just the right size for their motion to be conveniently observed.

To understand this, one may employ Einstein's famous equation for the mean square distance $\overline{x^2}$ travelled by a sphere of radius R in time t, in one dimension, in a liquid of viscosity η at temperature T, Eq. (A6) with

Eq. (B17):

$$\overline{x^2} = \frac{2kTt}{6\pi\eta R},$$

where k is Boltzmann's constant.

As shown following Eq. (A6), the mean distance travelled is $\overline{|x|} \approx .80\sqrt{\overline{x^2}}$. For an oblong object, as discussed in Appendix B, the equation is the same except that R is to be replaced by an effective radius $R_{\rm eff}$. For example, for an ellipsoid of revolution whose length is $2a$, with maximum cross-section a circle of diameter a, $R_{\rm eff}$ lies approximately in the range $.6a - .7a$, depending upon the angle between the direction of motion and the long axis (Eqs. (B18), (B19)).

Similar results are to be expected even for a weirdly-shaped object like *Clarkia* pollen. For the pollen and its contents, one may estimate using the expression

$$\begin{aligned}\overline{|x|} &\approx .80\sqrt{\frac{2kTt}{6\pi\eta R_{\rm eff}}} \approx 5.2\times 10^{-7}\sqrt{\frac{t_{\rm sec}}{R_{\text{eff-cm}}}} \\ &\approx .52\sqrt{\frac{t_{\rm sec}}{R_{\text{eff}-\mu m}}}\mu m, \end{aligned} \tag{1}$$

where a micron 1 $\mu m = 10^{-3}$ mm. In Eq. (1), $T = 20°\text{C}=293°\text{K}$, and the viscosity coefficient for water at this temperature, $\eta = .01$ gm/cm-sec, were used.

TABLE I: $\overline{|x|}$ in μm for values of $R_{\rm eff}$ in μm and t in sec.

$R_{\rm eff}$	.50	1.0	1.5	2.0	2.5	3.0	3.5	4.0	50
t=1	.74	.52	.43	.37	.33	.30	.28	.26	.07
t=30	4.1	2.9	2.3	2.0	1.8	1.6	1.5	1.4	.41
t=60	5.7	4.0	3.3	2.9	2.6	2.3	2.2	2.0	.57

Table I follows from Eq. (1). The reason for choosing $t = 1$ sec is that the little jiggles on the time scale of about a second are what catches the eye.

TABLE II: $\overline{|\theta|}$ in degrees for values of $R_{\rm eff}$ in μm and t in sec.

$R_{\rm eff}$	.50	1.0	1.5	2.0	2.5	3.0	3.5	4.0	50
t=1	74	26	14	9	7	5	4	3	.01
t=30	402	142	78	50	36	27	22	18	.4
t=60	570	201	110	71	51	39	31	25	.6

[For later use, we have appended here a similar table for the mean angle $\overline{|\theta|}$, Eq. (A8) and Eq. (B26):

$$\overline{|\theta|} \approx .80\sqrt{\frac{2kTt}{8\pi\eta R_{\rm eff}^3}} \approx 26\sqrt{\frac{t_{\rm sec}}{R^3_{\text{eff}-\mu m}}}\text{degrees}, \tag{2}$$

where $R_{\rm eff}$ for rotation about the two ellipse axes is given by Eqs. (B27), (B28).]

It is considered that the human eye is unable to resolve angles less than 1 arcminute$\approx 2.9\times 10^{-4}$ radians[33]. At a distance of 25 cm, this means a displacement less than 73 μm cannot be seen by the eye. This implies that less than a $73/370 \approx .2$ μm displacement cannot be seen by the eye with the help of a lens of magnification $\times 370$. Thus, by this rough criterion (e.g., the perception of motion may involve an altered criterion, illumination matters, and diffraction and aberration of the image has not been taken into account), from Table 1, the pollen contents with $R_{\rm eff} < 4$ μm could be seen to move in 1 sec, but not the pollen with $R_{\rm eff} \approx 50$ μm.

D. Observing Pollen Of Other Plants

In paragraph 9, Brown starts to look at the pollen of other plants, to see if their contents are similar and behave similarly. First, he looks at plants which have a similar classification. In the family *Oenothera* (evening primrose), *Clarkia* is a genus and *C. pulchella* is a species. Another genus in the same family is *Onagraceae*, which Brown calls *Onagrariae*:

In extending my observations to many other plants of the same natural family, namely Onagrariae*, the same general form and similar motions of particles were ascertained to exist, especially in the various species of* Oenothera*, which I examined. I found also in their grains of pollen taken from the antherae immediately after bursting, a manifest reduction in the proportion of the cylindrical or oblong particles, and a corresponding increase in that of the molecules, in a less remarkable degree, however, than in* Clarckia.

In paragraph 10, Brown remarks that this

... reduction in that of the cylindrical particles, before the grain of pollen could possibly have come in contact with the stigma, — were perplexing circumstances in this stage of the inquiry , and certainly not favorable to the supposition of the cylindrical particles acting directly upon the ovulum; an opinion which I was inclined to adopt when I first saw them in motion. ...

In paragraph 11 he is off and running, looking at a variety of flowering plants:

In all these plants particles were found, which in the different families or genera varied in form from oblong to spherical, having manifest motions similar to those already described ... In a great proportion of these plants I also remarked the reduction of the larger particles, and a corresponding increase of the molecules after the bursting of the antherae ...

Prior to discussing the next paragraph, we should emphasize that, so far, Brown had *not* observed the *particles*

or granules moving while they were *within* the *Clarkia pulchella* pollen grain. As he says in paragraphs 6 and 8, he observed them moving in water.

Unfortunately, he doesn't say how they manage to get out of the pollen grain after the grains are put in water. As will be discussed in more detail in Section IV, pollen grains in water—in vitro—may burst open, the contents streaming out under pressure (called turgor). (What happens naturally—in vivo—will be discussed there too.) Moreover, the particles within *Clarkia pulchella* pollen seem to be too packed together to move. And, we have observed that the fluid in which they are packed is so viscous that their motion is impeded when they do emerge. However, paragraph 12 says:

In many plants, belonging to several different families, but especially to Gramineae*, the membrane of the grain of pollen is so transparent that the motion of the larger particles within the entire grain was distinctly visible; ... and in some cases even in the body of the grain in* Onagrariae.

So, Brown *was* able to see particles move within some pollen, but he does not specifically include *Clarkia pulchella*. Sometimes Brown is said to have observed particles moving within the pollen, and the implication is that this was what Brown first observed, which is incorrect[34][15].

The next two paragraphs consider plants with varied kinds of pollen but similar results. Then comes paragraph 15:

Having found motion in the particles of all the living plants which I had examined, I was led next to inquire whether this property continued after the death of the plant, and for what length of time it was retained.

Paragraph 16 reports that, from plants dried or preserved in alcohol, for a few days, to a year, to more than twenty years, to more than a century, the pollen *... still exhibited the molecules or smaller spherical particles in considerable numbers, and in evident motion, ...* .

He next has the idea to look at plants that reproduce by spores: mosses and the horsetail (*Equisetum*). He finds within the moss spores, and sitting on the surface of the *Equisetum* spores, *... minute spherical particles, apparently of the same size with the molecule described in* Onagrariae*, and having equally vivid motion on immersion in water ; ...* .

E. Observing Organics

Then, as described in paragraph 19, an accident occurred. On *bruising* a spore of *Equisetum*, *... which at first happened accidentally, I so greatly increased the number of moving particles that the source of the added quantity could not be doubted.* This leads him to *bruise ... all other parts of those plants ...,* with the same motion observed.

Therefore, the motion had nothing to do with plant reproduction. He says:

... My supposed test of the male organ was therefore necessarily abandoned.

From this comes a hypothesis. The naturalist George-Louis Leclerc, Comte de Buffon (1707-1788), had proposed an atomic-style hypothesis, that there are elementary "organic molecules" (hence Brown's name for the smaller particles he observed) out of which all life is constructed. Brown signs onto this in paragraph 20:

... I now therefore expected to find these molecules in all organic bodies: and accordingly in examining the various animal and vegetable tissues, whether living or dead, they were always found to exist; and merely by bruising these substances in water, I never failed to disengage the molecules in sufficient numbers to ascertain their apparent identity in size, form, and motion, with the smaller particles of the grains of pollen.

Paragraph 21 contains this charming observation:

... I remark here also, partly as a caution to those who may hereafter engage in the same inquiry, that the dust or soot deposited on all bodies in such quantity, especially in London, is entirely composed of these molecules.

He now looks at things that were once organic, gum-resins, pit coal, then fossil wood. He then thinks of mineralized vegetable remains and looks at silicified wood, with similar results. Paragraph 22 concludes:

... But hence I inferred that these molecules were not limited to organic bodies, nor even to their products.

F. Observing Inorganics

So, (paragraphs 23-32) *... to ascertain to what extent the molecules existed in mineral bodies became the next object of inquiry. ....* Starting with *... a minute fragment of window-glass, from which when merely bruised on the stage of the microscope ...*, he tries all kinds of minerals, rocks, and metals, even *... a fragment of the Sphinx*!

... in a word, in every mineral I could reduce to a powder sufficiently fine to be temporarily suspended in water, I found these molecules more or less copiously: ...

When he looks at objects that are not spherical, such as fibers, he conjectures that they are composed of a number of molecules. He heats or burns wood, paper, cloth fiber, hair, quenches them in water and finds "molecules" in motion.

G. Brown's Summary of Observations on Molecules

Paragraphs 33-37 summarize, with commendable caution:

There are three points of great importance which I was anxious to ascertain respecting these molecules, namely, their form, whether they are of uniform size, and their absolute magnitude. I am not, however, entirely satisfied with what I have been able to determine on any of these points.

As to form, I have stated the molecule to be spherical, and this I have done with some confidence; ...

He explains that he judged the size of bodies *... by placing them on a micrometer* (a glass slide with lines ruled on it) *divided to five thousandths of an inch ... .*

The results so obtained can only be regarded as approximations, on which perhaps, for obvious reason, much reliance will not be placed. ... I am upon the whole disposed to believe the simple molecule to be of uniform size, ... its diameter appeared to vary from 1/15,000 to 1/20,000 of an inch.

So, with his microscope, he estimates the molecule size at from 1.7 to 1.3μm. A footnote adds *While this sheet was passing through the press ...* he asked the lens maker Dollond to look at *Equisetum* spores, whose surface he had earlier noted released "molecules,"

... with his compound achromatic microscope, having at its focus a glass divided into 10,000ths of an inch, upon which the object was placed; and although the greater number of particles or molecules seen were about 1/20, 000 of an inch, yet the smallest did not exceed 1/30,000th of an inch.

So, with Dollond's microscope, these particular molecules were mostly 1.3μm, with some estimated at .85μm.

Brown prudently concludes,

I shall not at present enter into additional details, nor shall I hazard any conjectures whatever respecting these molecules ... .

H. Brown's Concluding Remarks

In the final paragraphs of the paper, Brown returns *... to the subject with which my investigations commenced, and which was indeed the only object I originally had in view ...*, namely whether the larger particles acted upon the ovule. *My endeavors, however, to trace them, ... was not attended with success ....* He returned to this problem, with more success, a few years later (Section IV). The paper ends with establishing his priority. He notes: *The observations, of which I have now given a brief account, were made in the months of June, July and August, 1827.* He mentions people to whom he showed the phenomenon (he soon traveled to Europe, and demonstrated it there) and people who had made related observations in the past (the phenomenon was first seen by Leeuwenhoek, and remarked upon by many later microscopists —see comments by Nelson[16]) to but fell short of his results in some way .

Brown issued an addendum the following year[23], *Additional Remarks on Active Molecules*,

... to explain and modify a few of its statements, to advert to some of the remarks already made, either on the correctness or the originality of the observations, and to the causes that have been considered sufficient for the explanation of the phenomena.

He rejects the notion that the molecules are animated, he regrets having introduced hypotheses such as larger objects being made out of molecules, distances himself from the notion that the molecules are identically sized, rejects some explanations of the motion. He says they are *... motions for which I am unable to account.*

He describes an experiment designed to put to rest the idea that it is evaporating water, or interaction among the particles, which produces the motion, He shakes a mixture of oil and water that has previously been filled with particles, obtaining small drops of water surrounded by oil, some of which contain only one particle, and notes that the motion is unabated and continues indefinitely since the water does not evaporate.

He concludes once again by *... noticing the degree in which I consider those observations to have been anticipated*, and discussing other people's earlier work.

IV. BOTANY

A. Early Pollen Research

Unbeknownst to Brown, the mechanism of fertilization of the ovule by pollen he had been looking for had been observed by accident in 1822 by the Italian optical designer, astronomer and botanist Giovanni Battista Amici (1786-1863). Amici was looking at a hair on a stigma[35]:

I happened to observe a hair with a grain of pollen attached to its tip which after some time suddenly exploded and sent out a type of transparent gut. Studying this new organ with attention, I realized that it was a simple tube composed of a subtle membrane, so I was quite surprised to see it filled with small bodies, part of which came out of the grain of pollen and the others which entered after having traveled along the tube or gut.

Thus, what is now called the pollen tube was discovered. Brown became aware of this, and launched an investigation of the germination of pollen grains in orchids in 1831.

He was the first to realize that contact with the stigma causes the pollen to germinate, and he observed the particles from within the pollen flowing into the pollen tube. (Ironically, if in his 1827 work he had decided to observe pollen in vivo, instead of in vitro, he likely would have seen the pollen tube, pursued that, and his Brownian motion observations might never have taken place.) By 1833, he had published his observations that the pollen tube reaches and penetrates the ovule. Brown also was the first to insist upon the importance of insects in pollination[**?**].

During this 1831 work, Brown noticed a structure within cells belonging to an orchid leaf's epidermis, its outer layer. Characteristically he first looked at the internal cells of the plant and made the same observation, and then studied a myriad of other plants, with the same result. Brown had found the cell nucleus, which he named (from the latin word for "little nut"). He also specified that the pollen grain contains a nucleus. [One wonders if the term arose in physics due to Brown. Michael Faraday (1791-1867) used it to describe the center of the atom in 1844: Faraday knew Brown, lectured about Brownian motion in 1829, and letters are extant from Faraday to Brown. The term was adopted by Ernest Rutherford in 1912: one wonders how that came about.]

As we have seen, a pollen grain also contains amyloplasts and spherosomes (starch and fat organelles). Their nature became known within a decade after Brown's publications, but much was still unknown and wrongly conjectured. The two types of particles seen by Brown were described by John Lindley (who earlier had a falling out with Brown, following an article Lindley wrote that was construed to attribute some of Brown's early work to Bauer) in his 1848 book "An Introduction to Botany"[37]:

In consequence of their manifest motion it has been conjectured that the longer particles of the fovilla were the incipients of the embryo, and it is by the the introduction of one or more of these into the ovule that the act of impregnation is accomplished by the deposit of a rudimentary embryo in the ovule. [Wrong!] *But both Fritzsche and Mohl agree in considering many of the smaller particles of the fovilla as minute drops of oil:* [Right!] *the molecular motion has been ascribed to currents in the fluid, in which the fovilla is suspended, and which, according to Fraunhofer, no precautions can possibly prevent;* [Wrong!] *and, what is more important, the larger particles become blue upon the application of iodine, without however losing their property of motion, as Fritzsche has shown: they are therefore starch.*[Right!]

Lindley cites Fritzshe's and Mohl's work, published in 1833 and 1837, respectively.

B. Pollen Physiology

A pollen grain consists of an elaborate, three-layered cell wall surrounding a single, living cell[38], called a tube cell, because it can grow into a pollen tube. The outer layer of the pollen wall is sculptured and ornamented. It consists mainly of a tough, water-insoluble, fatty substance called sporopollenin[39]. Because of its thickness, ornamentation and chemical nature, the pollen grain wall is often optically opaque, and many of the internal contents of fresh pollen grains remain elusive using a light microscope. (However, as we have seen, the oblong amyloplasts of *C. pulchella* can be seen through the pollen wall, which led Brown to start working with that plant.) At particular locations, the cell wall is modified to form one or more apertures or pores. (*C. pulchella, elegans* and *amoena* have three pores). When pollen lands on a flower's stigmatic surface, the pollen absorbs water through the pores. Molecules (such as amino acids, oils and sugars[40],[41]) of the stigma induce the pollen to germinate, with a pollen tube emerging through one of these pores. When, in the laboratory, pollen grains are more uniformly surrounded by an artificial incubation medium, several tubes may emerge from a single pollen grain.

In spite of opacity of a pollen grain's cell wall, ultrastructural studies with an electron microscope reveal the tube cell contents[42]. There is a centrally located nucleus surrounded by the cytoplasm, which consists of a viscous fluid and its contents, membrane-bound structures called organelles (little organs). These organelles include amyloplasts (which store starch), spherosomes (which store lipids), numerous very small ribosomes needed for protein synthesis and a structure called an endoplasmic reticulum, which is involved in transporting proteins.

A small lens-shaped cell, the generative cell, is also found in the cytoplasm of the tube cell. This generative cell is passively transported within the elongating pollen tube and ultimately divides to form two nonmotile sperm. The pollen tube passes through the stigma and down the style, and reaches an ovule. The ovule is surrounded by integuments (a layer that will become the outer coating of the seed) pierced by a hole called a micropyle. The pollen tube passes through the micropyle, and enters the ovule. The ovule contains an egg cell, as well as a neighboring cell called the central cell. When the pollen tube arrives in the vicinity of the egg, a pore forms at the tip of the pollen tube, which bursts, and the two sperm are released[43]. A double fertilization is achieved: one sperm fertilizes the egg to form the embryo (seedling), and the other sperm nucleus unites with the nucleus of the central cell to form a unique nutritive tissue, the endosperm, which will become the food for the embryo or seedling.

Within a few minutes of landing on the receptive stigmatic surface of the flower (or upon being placed in an incubation medium), respiratory activity[44] (oxygen–

dependent reactions that create the energy rich molecule ATP which is the energy currency of the cell) and protein synthesis[45] are initiated within the tube cell. By 15 minutes, RNA synthesis has begun and, even when this RNA synthesis is blocked experimentally, the germination and early growth of the pollen tube proceeds[46]. This suggests that the RNA required for the early phases of germination and tube growth is preformed in the pollen tube cell and is ready for utilization.

Ultrastructural studies of pollen germination and tube growth show that in the few minutes before emergence of the pollen tube, structures called Golgi bodies are activated. These accept proteins from the endoplasmic reticulum and bundle them into more complicated molecules. These molecules are shipped out (so to speak) in packages called vesicles[47], produced by the Golgi bodies. The vesicles migrate and fuse locally with the pollen tube's boundary layer, called the plasma membrane, to form the growing tip of the pollen tube. As they fuse with the plasma membrane, the vesicles release their contents of cell wall material that contribute to the lengthening pollen tube. They also release enzymes that are believed to help dissolve a pathway for the pollen tube through the stylar tissue of the flower's pistil[48],[49]. The starch and lipid, stored in the amyloplasts and spherosomes, respectively, are presumably utilized as energy sources and provide raw materials for the construction of new cell wall material and new plasma membrane during pollen tube elongation.

When pollen grains of many plants are placed in water for microscopic examination, they often will germinate and form a short tube, but then they frequently rupture, to release the cytoplasmic contents of the tube cell into the water. As the cytoplasmic contents disperse into the water, the more numerous and larger amyloplasts and spherosomes are seen. Other organelles are too small (ribosomes are about .02μm) to be seen with the light microscope or too few (nucleus) to be easily spotted.

Jost[50] first suggested that, during pollen germination and pollen tube growth, sugar plays the role of osmotically regulating the swelling and bursting of pollen grains and tubes. However, Bilderback[51] demonstrated that the pollen grains of some plants do not require sugar to stabilize pollen growth and tube elongation. Schumucker[52] recognized that boron plays an active role during pollen tube growth. Its physiological behavior remained unknown until Dickinson[53] found that boron binds in a reversible manner to growth-related sites in the pollen tube. Calcium and potassium[54],[55],[56] also have been found to be essential for stable growth of pollen tubes. Weiseseel and Jaffe[57] were able to show that potassium enters the tips of actively growing pollen tubes. The directed growth of the pollen tube to the plant egg may be due to a gradient of calcium, potassium, hydrogen and chloride within the flower's pistil, extending from the stigma to the egg [58],[59]. The details of pollen tube evolution are an active subject of research[60]. Observation of pollen tube growth makes an engaging student lab[61].

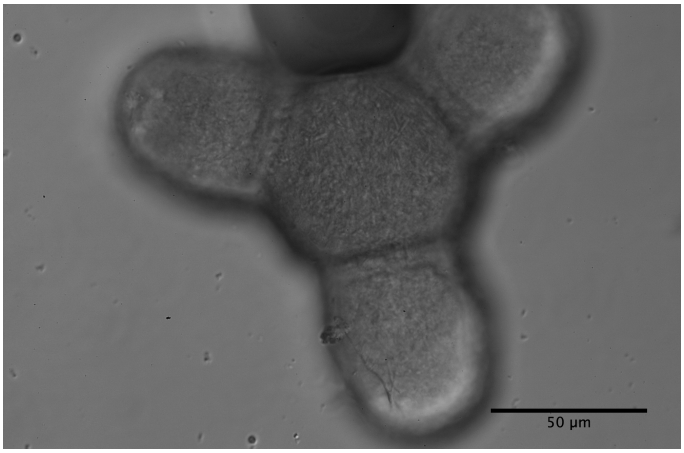

FIG. 3: *Clarkia amoena* pollen under the microscope ×400

Artificial pollen incubation media did not begin to be formulated until the beginning of the twentieth century. Thus, Brown put pollen into water, observed the contents of ruptured pollen grains, and discovered Brownian motion instead of (rediscovering) the pollen tube.

V. MICROSCOPY

As mentioned in the Introduction, this section is written in the first person.

Clarkia pulchella, variously called ragged robin, elkhorn, pinkfairies and deerhorn (because of its four three-pronged petals), is native to western North Amer-

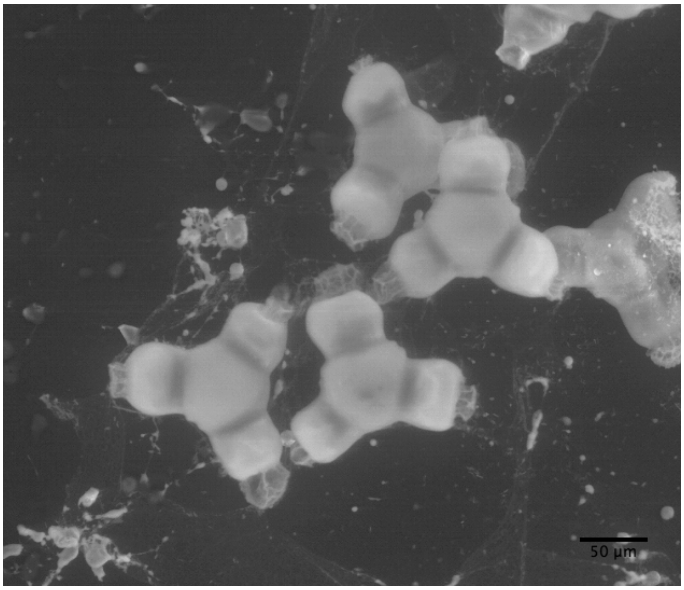

FIG. 4: *Clarkia elegans* pollen under the electron microscope.

ica. It can be found growing wild in parts of British Columbia, Idaho, Montana, South Dakota and Washington[62]. Indeed, I observed some sent to me that grew wild near Missoula, Montana. However, a number of companies sell *Clarkia pulchella* seeds[63], along with seeds of *Clarkia amoena* (also called farewell-to-spring), which grows wild in California, Oregon and Washington, and seeds of *Clarkia elegans* (also called unguiculata, mountain garland) which grows wild in California. Seed packets sell for just a few dollars. (Other *Clarkia* species, of which 41 are known[64], are sold less frequently).

A. Growing *Clarkia*

Seed–growing advice is available on–line and in many gardening books. Growing seeds indoors under lights is not hard. Here is one person's experience, which certainly can be improved upon. My aim was to do as little as possible.

There are many seed growing systems available at gardening stores, such as peat pots. I have had good results with the Lee Valley Self-Watering Seed Starter[65], which contains 24 compartments, watering via a felt capillary mat, and a water level indicator. It can be left for about a week before refilling with water. The mat should be soaked before using. Lee Valley recommends using a soilless mixture containing sphagnum or peat, but I used a commercial potting soil mix with added nutrients.

A shop light fixture with grow–light bulbs, or even ordinary fluorescent bulbs, can be used, with some arrangement to raise the plants or lower the light fixture. However, I used a commercial stand with grow–lights which is reasonably priced[66] and has a mechanism for raising and lowering the fixture. A timer that kept the lights on perhaps 16 hours a day completed the equipment.

Seeds may be meted out to the compartments from the seam of a small folded piece of paper. The seeds germinated in about a week to ten days. The bulbs should be within a few inches of the tops of the plants, else the plants become etoliated, i.e., spindly from lack of sufficient light. After a few weeks to a month, I transferred the seedlings to 4" pots, 24 of which fit in a tray (periodically watered)[65]. As the plants grew, I staked them. Flowers started to bloom after about ten weeks.

B. Qualitative

C. pulchella has four stamens (eight for *elegans* and *amoena*) surrounding the pistil. I used a miniature Swiss army knife scissors (a nail scissors will do as well) to cut each filament so the anther fell on a microscope slide. I used tweezers to hold an anther. If the anther had not yet burst, I sliced it with a long sharp sewing needle to reveal the pollen. If it had burst, usually some pollen had fallen out of the anther and was already on the slide. In either case, I scraped pollen out of the anther with the needle. I enjoyed observing what I was doing through a low power binocular microscope, though this can be done without one. *C. pulchella* pollen are little triangles, which glowed in the light like diamonds.

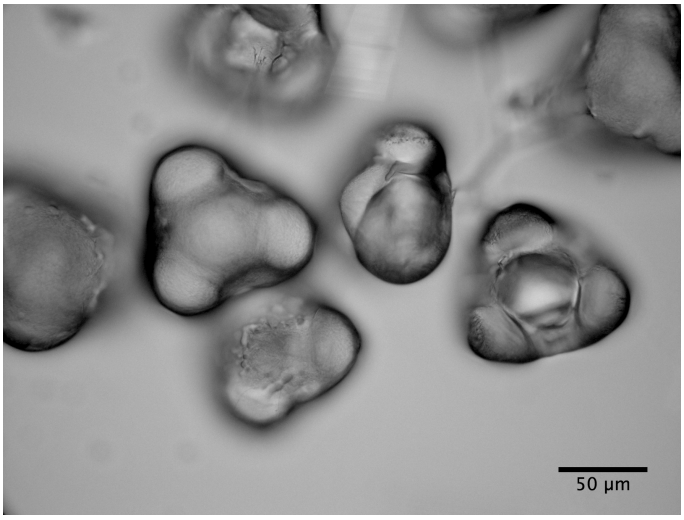

FIG. 5: Desiccated *Clarkia pulchella* pollen

I was surprised when I did the same with *C. amoena* and *C. elegans*. I had not known that species of the same genus could have differently shaped pollen, in this case hexagons with protuberant lobes on alternate edges (Figures 3 and 4). The connection between the two shapes is apparent (see Figure 5) when viewing a dry slide of desiccated *C. pulchella* pollen. Each appears as a membrane surrounding the *C. amoena/C. elegans* pollen shape.

A drop of distilled water is put on the pollen on the slide using a medicine dropper, followed by a cover slip and then observed. One should follow Brown's injunc-

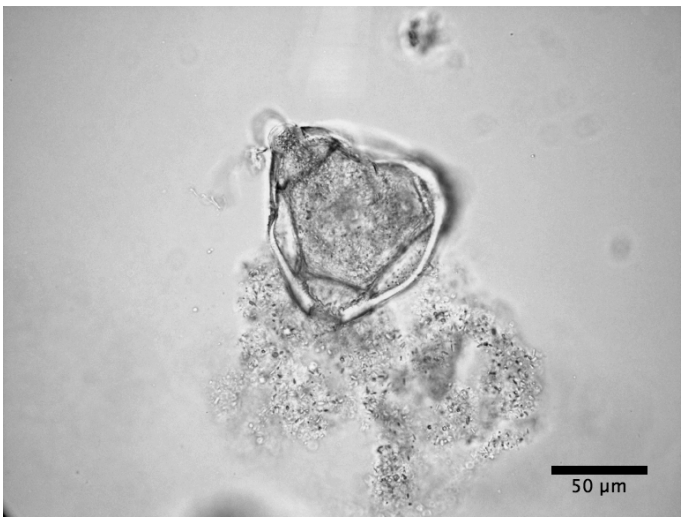

FIG. 6: Bursting *Clarkia pulchella* pollen.

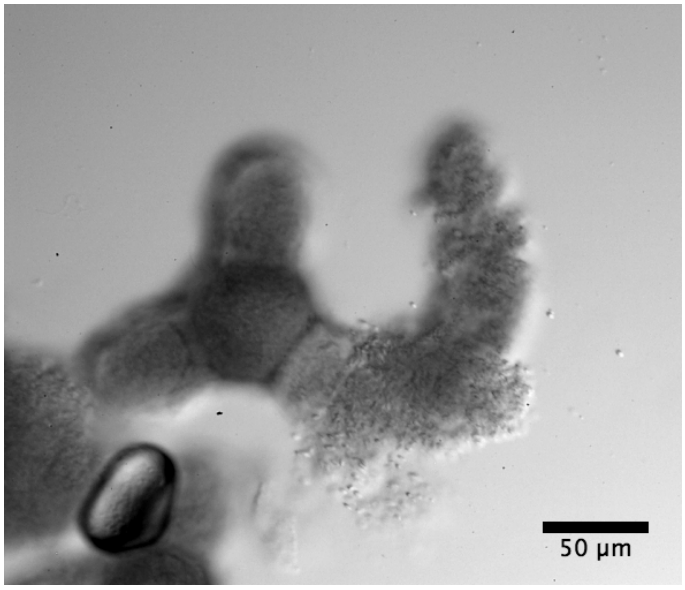

FIG. 7: Bursting *Clarkia elegans* pollen.

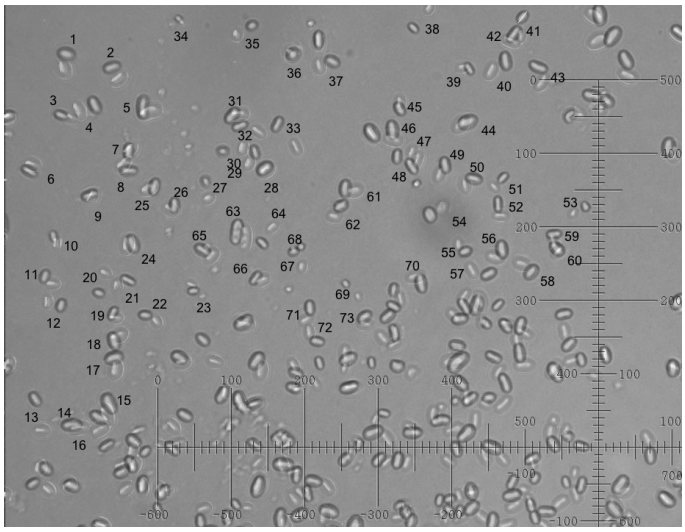

FIG. 8: *Clarkia pulchella* pollen contents before dehiscence, two superimposed photos taken 1 min apart, at ×400. The scale is 2 μm per division.

tion to observe pollen from anthers either before dehiscence (i.e., before the anther has split open, releasing the pollen) or soon thereafter. Most of the pollen do not burst in water, and if one waits too many days after dehiscence to make observations, none may burst, especially for *C. pulchella*. As pollen matures in the anther, its outer membrane may grow more impervious to bursting in water.

When first viewed, particles from the pollen were sometimes seen already on the slide: perhaps the pollen had been damaged by the needle, or the pollen had rapidly burst open as soon as the water was applied. I could also see pollen bursting before my eyes, and the particles streaming out (Figures 6, 7), like logs released from a log–jam, usually in fits and starts. The particles at the log–jam periphery diffuse away from the rest and can be seen undergoing Brownian motion. The remainder are packed closely, and the intracellular medium in which they sit is viscous, so they show little or no Brownian motion until the log–jam disperses.

C. Quantitative

There are many interesting phenomena one can investigate. Here are two brief studies, suggestive but by no means definitive. For the first, we consider the distribution of particle sizes emerging from *Clarkia pulchella* pollen before and after dehiscence. For the second, we consider Brownian motion and Brownian rotation of the amyloplasts.

1. Observations

An Olympus BX-50 microscope, at ×400 was used. Its resolution is cited as .45 μm, and its depth of focus as 2.5 μm. A microscope camera and five different computer applications were employed,.

Fig. 8 shows two superimposed photos of *C. pulchella* particles taken 1 minute apart, from pollen *before* dehiscence. The two pictures were enhanced in contrast and treated differently in brightness and then superimposed, using the program Photoshop Elements 2. A marvelous free program, called ImageJ[67], enables precision measurements on photographs. 73 particles in the upper left quadrant of the viewing area (two time-displaced images of each) were labeled. Each image's long axis length, long axis angle θ, x and y coordinates were measured. ImageJ puts the results in an Excel worksheet.

Fig. 9 shows a photo of *C. pulchella* particles from pollen *after* dehiscence. 89 particles in the lower left quadrant were labeled and their lengths were measured. A graph of number of particles per radius bin (radius $R \equiv 1/2\times$particle length, bin size =.25 μm) for both photos appears in Fig. 10.

Qualitatively, this confirms what Brown said. There are very few spherosomes visible in Fig. 8, taken from pollen before dehiscence. The appearance after dehiscence, in Fig. 9, of many particles of apparent radius $\lesssim 1\mu$m, the "molecules," or spherosomes that so excited Brown, is strikingly apparent. These particles appear as light or dark, depending upon their location with respect to the microscope focal plane.

Fig. 10 presents a graph of what is observed in Figs. 8, 9. The distribution of numbers of particles with radii above 1 μm before and after dehiscence appears to be the same: these are the amyloplasts. However, there is a peak in the number of particles with radii less than 1 μm

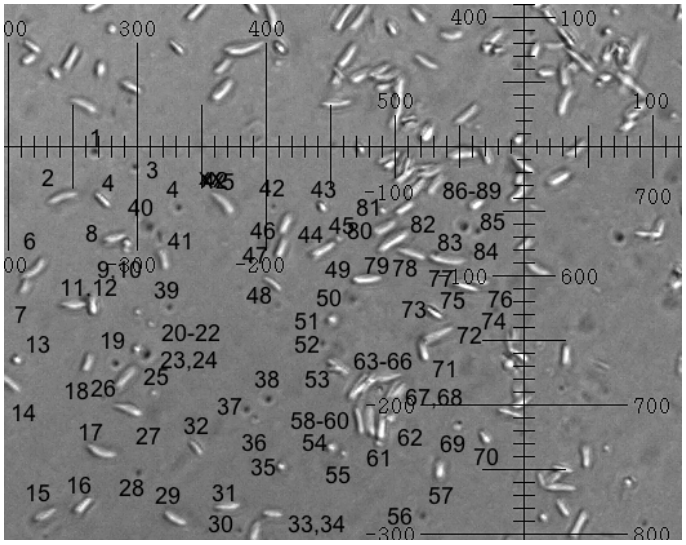

FIG. 9: *Clarkia pulchella* pollen contents after dehiscence. The scale is 2 μm per division.

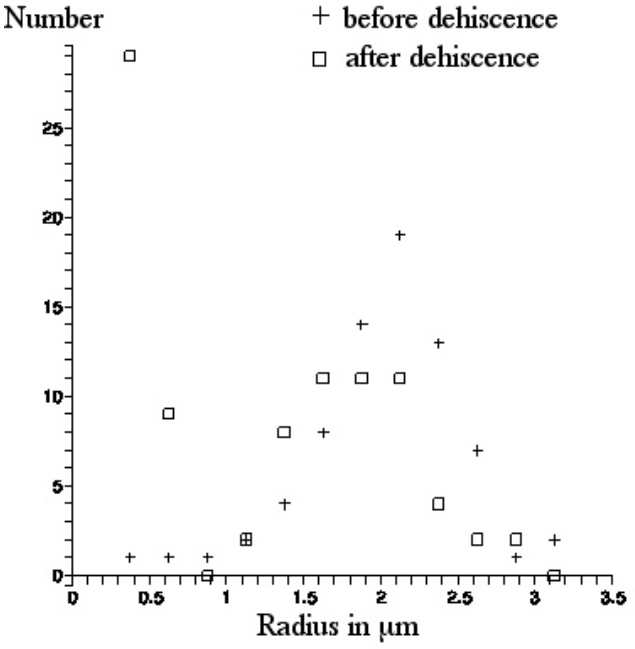

FIG. 10: Number of particles (in a radius bin .25 μm wide) vs radius in μm.

after dehiscence (and no such peak before dehiscence): these are the spherosomes.

Quantitatively, there is a discrepancy between Brown's observation of the sizes of the amyloplasts and spherosomes, and what is depicted here: his sizes are larger. As we have noted, Brown quotes the amyloplasts as having average radius (half the long axis length) $R \approx 3$ μm, with maximum $R \approx 4$ μm, whereas with our Olympus microscope, on average $R \approx 2$ μm, with maximum $R \approx 3$ μm. And, he quotes the spherosome radii as ranging from $R \approx .65$ μm to $R \approx .85$ μm, whereas with our Olympus microscope, most spherosomes appear to cluster around $R \approx .5 \pm .05$ μm, with maximum size about $R \approx .65 \pm .05$ μm.

To resolve this discrepancy in the case of the spherosomes, in section V C 2 below, lenses and their effect on the image of a round object are discussed. Essentially, due to diffraction, Brown's lens and the Olympus microscope both enhance the image beyond the actual size of the object, but the Olympus microscope enhances the image less than did Brown's microscope. The theory, described in section V C 3, is found to be in good agreement with observations, of polystyrene spheres of known radius, made with the Olympus microscope. Therefore, in section V C 4, the theory is applied to observations of spherosomes with the Olympus microscope, enabling estimation of the spherosome size. Then, Brown's observations of the spherosome size enables estimation of properties of his microscope!

Section V C 5 treats the Brownian motion and rotation evinced in Fig. 8.

Lastly, in section V D, the construction of a ball lens microscope with power close to that of Brown's lens is presented. Aided by a picture of amyloplasts taken with it, the amyloplast size discrepancy is discussed.

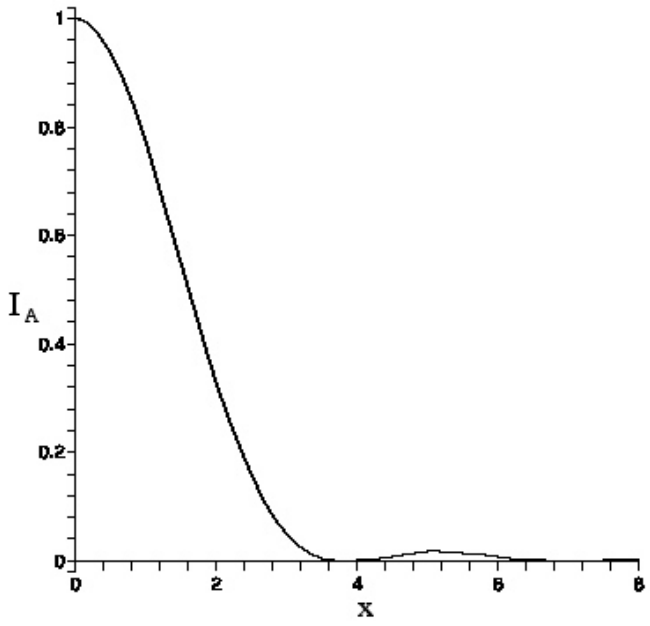

FIG. 11: Airy function intensity $I_A(x)$ vs x.

2. Lenses

Interestingly, Brown's hypothesis and conclusion, of the ubiquity and uniformity of the "molecules," although wrong, was so stimulating to him that it led to his famous discovery. As mentioned in the Introduction, when he was viewing objects smaller than the resolution of his lens, diffraction and possibly spherical aberration produced a larger, uniform, size[68].

We now discuss this further, summarizing mathematical results given in Appendices F, G. The main result is Fig. 12, which will enable us to find the radius a of a spherical object from the larger radius R of the image observed through a lens or microscope. The theory shall be compared to observations of polystyrene spheres made with the Olympus microscope. Then, the results shall be applied to the spherosome size discrepancy .

Also, using these ideas, we shall attempt a bit of historical detective work. From information supplied by Brown about the size of his "molecules," we can hazard a guess at the radius b of the circular aperture that backed his microscope lens, which is called the exit pupil.

For sufficiently small b, a point source of light's image is a diffracted intensity distribution, a circular pattern of light. The intensity as a function of radial distance r from the lens axis is given by the Airy function, Eq. (F5):

$$I_A(x) = \left[\frac{2J_1(x)}{x}\right]^2, \tag{3}$$

where $J_1(x)$ is the Bessel function and $x \equiv krb/f$. Here, f is the lens focal length and b/f is called the "numerical aperture" of the lens. $k = 2\pi/\lambda$, where λ is the wavelength of the light, traditionally taken for design purposes as green light with $\lambda = .55$ μm. This expression (and those which follow, such as Eq. (4)) give properly scaled dimensions of the image. Dimensions actually seen through the lens are larger by a factor of the lens magnification.

The Airy function (3) is graphed in Fig. 11. The intensity vanishes at the first zero of the Bessel function, $J_1(3.83...) = 0$. This defines the Airy radius r_A. Setting $kr_Ab/f = 3.83$ allows one to find the lens's Airy radius:

$$r_A = \frac{.61\lambda}{b/f}. \tag{4}$$

Since viewing is subjective, the Airy radius (4) may not be perceived as the boundary of the Airy pattern light intensity (the so-called "Airy disc"), but it is not far off. For consistency with the non–Airy intensity pattern that appears as b is increased, which also fall off rapidly with distance but does not vanish, we shall define the light boundary as occurring at 5% of peak value. Applied to the Airy function, since $I_A(3.01..) = .05$, this criterion puts the radius of the light boundary at $R \equiv (3.01/3.83)r_A \approx .8r_A$.

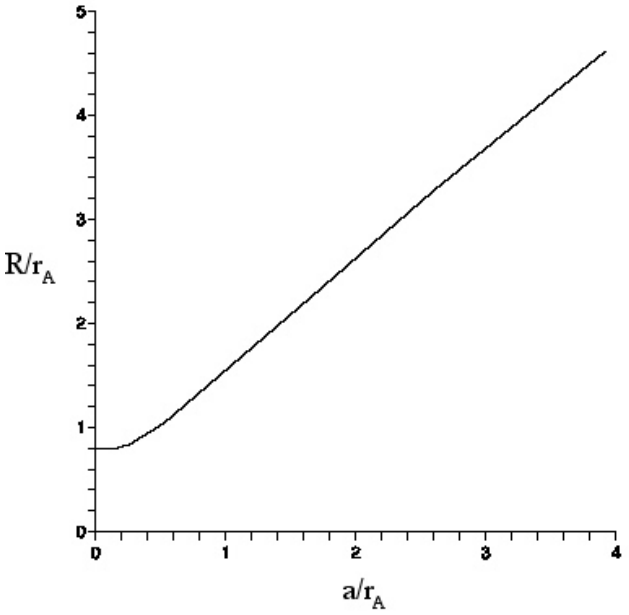

FIG. 12: For an object hole of radius a, R is the image circle's radius, defined as where the intensity is 5% of the intensity at the center of the image circle. r_A is the Airy radius.

As b grows, according to Eq.(4), the Airy radius r_A diminishes: this increases resolution. Moreover, as the aperture grows, more light exits the lens: this increases visibility. However, eventually as b is increased further, visibility and resolution start to decrease. The light intensity outside r_A grows, and light intensity inside r_A decreases. This is due to spherical aberration: rays at the outer edge of the exit pupil come to a focus closer to the lens than do paraxial rays. A design choice, called the Strehl criterion[70], suggests an optimal choice of b which keeps spherical aberration at a tolerable minimum while maximizing visibility: the intensity on the optic axis (in the image plane that minimizes the observed disc radius) should be 80% of $I_A(0)$. The intensity shape is then still close to the Airy distribution. In this case, the image is described as "diffraction limited": this shall be assumed hereafter.

Consider now, instead of a point source, an extended object, modeled by a hole of radius a illuminated by incoherent light. In geometrical optics, for *an ideal lens*, each point on the object plane is imaged onto a point on the image plane. Therefore, there will be a circular image which appears also to have radius a. But, with *an actual lens*, each point in the object plane becomes an Airy disc in the image plane. These discs add like little spotlights of radius r_A, with centers uniformly distributed throughout a circle of radius a. Therefore, the image radius R is larger than a.

Fig. 12 graphs R/r_A vs a/r_A. This was obtained by numerical evaluation of Eq.(G1), which gives the net in-

tensity of the image pattern at any radius in the image plane. Fig. 12 can be understood as follows.

For small a, $a/r_A \lesssim .25$, the centers of the Airy discs that contribute to the intensity are so close together that the intensity is essentially the Airy pattern. Thus, $R/r_A \approx .80$ as discussed following Eq.(4).

As a/r_A grows beyond $\approx .25$, R starts to grow as well, since the Airy disc centers are now spread out over a non-negligible range. For example, we see from Fig. 12, for $a/r_A \approx .5$ that $R/r_A \approx 1$, and for $a/r_A \approx 1$, that $R/r_A \approx 1.5$.

For very large a/r_A, the intensity at the center of the image circle is contributed mostly by Airy discs whose own centers lie within an Airy radius of the center. This is true for points somewhat farther out from the center so, at the center and to an extent beyond, the intensity remains essentially constant. But, at distance $a-r_A$ from the center, the intensity starts to drop.

At the "edge" (distance a from the center), the intensity is about half that in the center, because only Airy discs on the inner side of the edge contribute. The intensity drops off further as the distance from the center increases beyond a, reaching 5% of $I_A(0)$ at distance $R \approx a + r_A$. Thus $(R-a)/r_A$ asymptotically approaches 1.

In the graph of Fig.12, R/r_A has its largest value for $a/r_A = 4$, at which $(R-a)/r_A \approx .7$. Not shown on the graph are points $\{a/r_A, \approx (R-a)/r_A\} = \{8, .8\}, \{17, .9\}, \{30, .99\}$.

3. Polystyrene Spheres

To provide an experimental counterpart to these calculations, slides of .3 μm and 1 μm diameter polystyrene spheres[72] (diameter standard deviation less than than 3%) were prepared and digitally photographed using our Olympus BX-50 microscope, along with a scale whose line spacing is 2 μm. For this microscope, the manufacturer states the resolution is $r_A = .45$ μm.

For .3 μm diameter spheres, since $a = .15\mu$m and so $a/r_A = .33$, we find that $R/r_A \approx .86$ from Fig.12. Therefore, the spheres should appear as of diameter $2R \approx 2(.86r_A) \approx .77$ μm.

No pictures shall be given here, but the observations are summarized. The digital image was enlarged until it appeared as composed of pixels, each a .2 μm$\times$.2 μm square. Spheres which stood alone (for, many spheres cluster) typically appeared as 3×3 pixel grids (dark in the middle, and grey on the outside, with the surrounding pixels lighter and more-or-less randomly shaded), although a 4×4 grid for a few could not be ruled out. Thus the spheres appeared to be of diameter $\approx .6$ μm, with error of a pixel size, consistent with the estimate.

For 1 μm diameter spheres, since $a = .5$ μm and so $a/r_A = 1.1$, we find that $R/r_A \approx 1.7$ from Fig.12. Therefore, the spheres should appear as of diameter $2R \approx 2(1.7r_A) \approx 1.5$ μm.

In the unenlarged photograph, isolated spheres seemed to be only slightly larger than 1 μm, perhaps 1.2-1.3 μm, with a bright center (the spheres are transparent) and dark boundary. However, when enlarged so that the pixels could clearly be seen, particularly the outermost light grey ones, the spheres typically appeared as an 8×8 grid. Thus the spheres appeared to be of diameter 1.6 μm, with error of a pixel size, consistent with the estimate.

4. Spherosome Sizes and Brown's Lens

In the previous section we have seen that the polystyrene sphere sizes observed through our Olympus microscope are larger than the actual sizes . Therefore, we expect the same to be true of the spherosomes. Moreover we expect that the spherosome sizes observed by Brown will be even larger than what we observed, due to a larger Airy radius for Brown's lens than the .45 μm Airy radius for the Olympus microscope. The universal size of Brown's "molecules," regardless of their source, can be attributed to their being small enough so that their Airy disc is what Brown observed.

We do not have an electron microscope picture of spherosomes to indicate their actual sizes, as that proved to be very difficult to obtain: that is a challenging project for the future. Unlike amyloplasts which are structurally robust and whose electron microscope picture we succeeded in obtaining (see Fig. (16), spherosomes are membrane bound lipid droplets: when an attempt is made to concentrate them by filtering so that there are sufficient numbers to view, they coalesce, and appear as an amorphous mass.)

We therefore turn to estimate the actual spherosome sizes using our observations through the Olympus microscope As we have noted, according to Fig. 10, we observed that most spherosomes appeared to cluster about 1±.1 μm in diameter, the largest being perhaps 1.3±.1 μm in diameter.

For the smallest spherosomes, we have $R/r_A \approx (.9/2)/.45 \approx 1$. From Fig. 12 we read that therefore $a/r_A \approx .5$, so their radius is $a \approx .5 \times .45 \approx .2$ μm, i.e., their diameter is $\approx .4$ μm.

For most spherosomes, we have $R/r_A \approx (1/2)/.45 \approx 1.1$. From Fig. 12 we read that therefore $a/r_A \approx .6$, so their radius is $a \approx .6 \times .45 \approx .27$ μm, i.e., their diameter is $\approx .54$ μm.

For the largest spherosomes, we have $R/r_A \approx (1.4/2)/.45 \approx 1.6$. From Fig. 12 we read that therefore $a/r_A \approx 1.1$, so their radius $a \approx 1.1 \times .45 \approx .5$ μm, i.e., their diameter is ≈ 1 μm.

Armed with these results, we may try to find some properties of Brown's lens. We assume that the minimum size of his "molecules" corresponds to the Airy disc, i.e., they belong in the realm $a/r_A < .3$ in Fig. 12 for which $R/r_A \approx .8$. Since Brown quotes the minimum diameter of his "molecules" as $\approx 1/20,000$ in≈ 1.3 μm, half this is the radius $R \approx .65$ μm, and so the Airy radius of Brown's

lens is deduced to be

$$r_A = R/.8 \approx .65/.8. \approx .8\ \mu\text{m}.$$

Then, from Eq. (4) we may conclude that the radius of the exit pupil of his $f = 1/32$ in$\approx .8$ mm lens was

$$b = \frac{.61\lambda f}{r_A} = \frac{.61 \times .55 \times .8}{.8} \approx .35 \text{ mm}.$$

As a consistency check, we note that Brown quoted the maximum diameter of his "molecules" as $\approx 1/15,000$ in$\approx 1.7\ \mu$m. Then, $R/r_A \approx (1.7/2)/.8 \approx 1.1$. From Fig.12, we read that this corresponds to $a/r_A \approx .6$. Therefore, we deduce that the actual radius of these largest spherosomes is $a \approx .6 \times .8 \approx .5\ \mu$m. This agrees with the actual radius of the largest spherosomes we observed.

5. *Amyloplast Brownian Motion and Rotation*

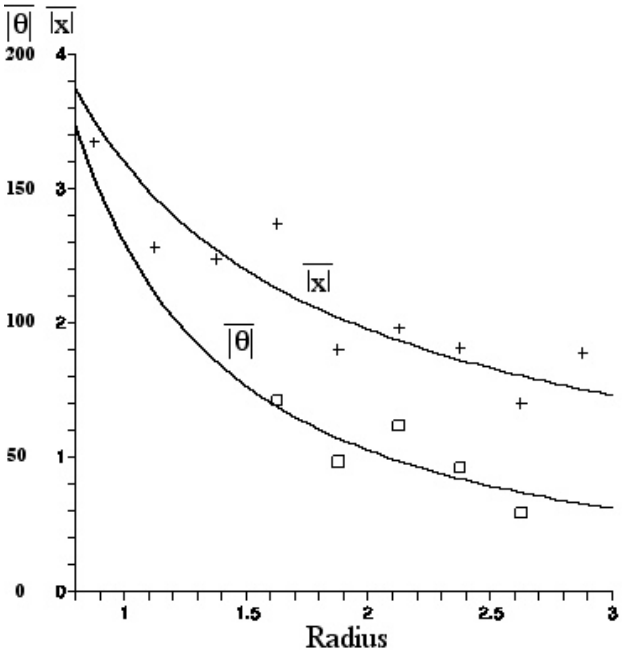

FIG. 13: Mean linear displacement $|\bar{x}|$ in μm and mean angular displacement $|\bar{\theta}|$ in degrees, vs R in μm, for amyloplasts undergoing Brownian motion for 60 sec. The least squares fit curves depicted here are given in Eq.(5).

We next turn to analysis of the observed Brownian motion of the amyloplasts. In what follows, R is half the length of the long axis of an amyloplast.

From Fig. 8, the x–displacement, y–displacement, and θ–displacement of each amyloplast, over the one minute interval, were found. Because of the possibility of overall fluid flow (assumed constant and irrotational in the region containing the observed particles), the mean displacement was calculated; it proved to be .053 μm in the x-direction (negligible flow) and -.847 μm in the y-direction. This was then subtracted from each displacement, to give the true Brownian contribution.

A plot of mean linear displacement and a graph of mean angular displacement for each R bin (.25 μm wide) appears in Fig. 13. Smallest and largest R values representing too few data points were omitted (which is why there are fewer data points representing $|\bar{\theta}|$ than $|\bar{x}|$). Fig. 13 was made with the Maple program (with labeling help from the Appleworks program), and includes graphs of the least squares fit to a power law A/R^B, for each set of data. The results, compared with the predictions given in Eqs. 1, 2 (setting $R_{\text{eff}} \equiv R$) are

$$\begin{aligned} |\bar{x}| &= \frac{3.2}{R_{\mu\text{m}}^{.7}}\mu\text{m} \quad \text{compared with} \quad |\bar{x}| = \frac{4.0}{R_{\mu\text{m}}^{.5}}\mu\text{m}, \\ |\bar{\theta}| &= \frac{130\ ^\circ}{R_{\mu\text{m}}^{1.3}} \quad \text{compared with} \quad |\bar{\theta}| = \frac{201\ ^\circ}{R_{\mu\text{m}}^{1.5}}\ . \end{aligned} \tag{5}$$

The powers in Eqs. (5) agree reasonably well, considering that no correction has been made for the ellipsoidal nature of the particles. As discussed in Section III B and Appendices B 5 and B 9, R_{eff} for translation and rotation of ellipsoids in Eqs. (1), (2) should be less than R for a sphere by a factor that is different for the long and short axes, and that varies with their ratio. No attempt was made to correct for this effect, nor for the fact that the observed amyloplast sizes are larger than the actual sizes, just as in the case of the spherosomes.

Interesting studies, with appropriate selection of uniform particle sizes, can be made. The subject of Brownian motion of ellipsoids, first studied by Perrin, is still of interest[71].

The numerical coefficients in the comparable Eqs.(5) differ because the last terms on the right–hand sides of Eqs.(1),(2) assume the fluid in which the particles are immersed is water. However, the amyloplasts move in a fluid that is a mixture of water and the intracellular medium, which emerged with the amyloplasts from the pollen. That is, the measured coefficients are proportional to $1/\sqrt{\eta_{\text{fluid}}}$ while the expressions based upon Eqs.(1),(2) are proportional to $1/\sqrt{\eta_{\text{water}}}$. From the displacement expressions in Eq.(5) we obtain for $\sqrt{\eta_{\text{fluid}}/\eta_{\text{water}}}$ the value $(4.0/3.2) \approx 1.3$, while from the angular displacements this is $(201/130) \approx 1.5$. These estimates of the fluid viscosity are in reasonable agreement, especially considering the omission of an ellipsoidal correction mentioned above.

One last qualitative observation is worth mentioning. Some wet-dry 400 grit sandpaper was used to grind to powder some of a seashell, a rock, and a nickel. In all cases, the powder (which was colored white or grey, while the sandpaper was colored black, so the sandpaper grit was not being observed), had some particles of apparent sizes $\lesssim 1\mu$m which were observed jiggling in water, just as Brown said occurred for anything he ground up fine

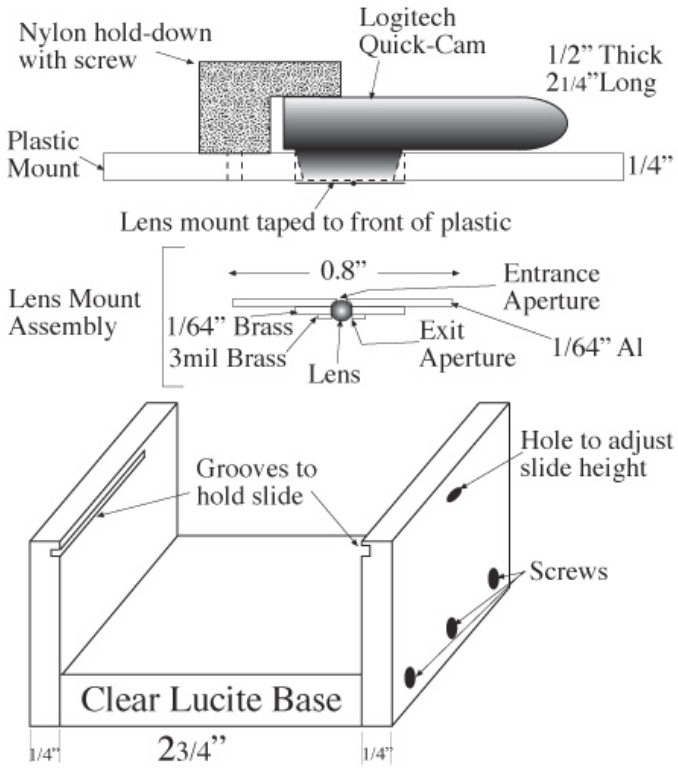

FIG. 14: Ball Lens Microscope Diagram

enough.

D. Ball Lens Microscope

Finally, we discuss construction of a single lens microscope with a magnification comparable to Brown's, and some observations made with it.

Ground lenses of high magnification such as those made by Bancks and Dollond are not readily available nowadays. However, fortunately, precision small glass spheres called ball lenses are readily available (they are used for coupling lasers to optical fibers) that can be used as high magnification lenses[73]. We purchased a ball lens of 1 mm diameter and index of refraction 1.517[74]. The focal length f of a sphere of radius R can be found from the lensmaker's formula[75] for a thick lens of radii R_1 and $-R_2$, thickness T and index of refraction n:

$$\frac{1}{f} = (n-1)\Big[\frac{1}{R_1} - \frac{1}{R_2} + \frac{(n-1)T}{nR_1R_2}\Big]. \qquad (6)$$

For $T = 2R$ and $R_1 = -R_2 = R$, Eq. (6) yields

$$f = nR/2(n-1). \qquad (7)$$

For our lens, f= .733 mm=1/34.6 inch, not far from the f=1/32 inch of Brown's lens.

The "microscope" is essentially the lens sandwiched between two perforated supports. One support was made as follows. A circle of 1" diameter was cut out of a 1/64" (≈0.4 mm) thick aluminum sheet. A 0.8 mm. diameter hole was drilled part way through its center, and then a 0.48 mm diameter hole was drilled all the way through. Thus, the exit pupil radius was constructed to be 0.24 mm. Then, a small washer was made from a piece of 1/64" brass with a 1 mm diameter hole drilled through it. The holes in the two pieces were aligned, and the pieces secured to each other with Kapton polyimide tape. The ball lens was placed in the resulting hole, supported by the edges of the 0.48 mm hole and surrounded by the washer.

The second support consisted of a piece of 3 mil (0.076 mm) brass shim stock with a 0.55 mm diameter hole in the center, It was secured over the lens with more Kapton tape to hold the lens in place and serve as the entrance aperture.

The assembled "microscope" was then mounted with more Kapton tape over the entrance aperture of a Logitech QuickCam Pro USB camera. This camera was chosen from a large number of such "webcams" because the front of its lens lies very close to the surface of the camera, allowing a very small separation between the microscope and the imaging camera. A 1/4" × 3" × 5" plastic sheet was fashioned, and a hole was drilled through its center, through which the microscope backed by the camera lens protrudes: the body of the camera rests upon the plastic. An inverted-L shaped bracket was attached to the plastic sheet to hold the camera .

A U-shaped plastic stand, of dimensions slightly less than 3" (the length of a microscope slide) was constructed from 1/4" plastic. Horizontal grooves (rabbets) to support the slide were cut in the sides of the U just

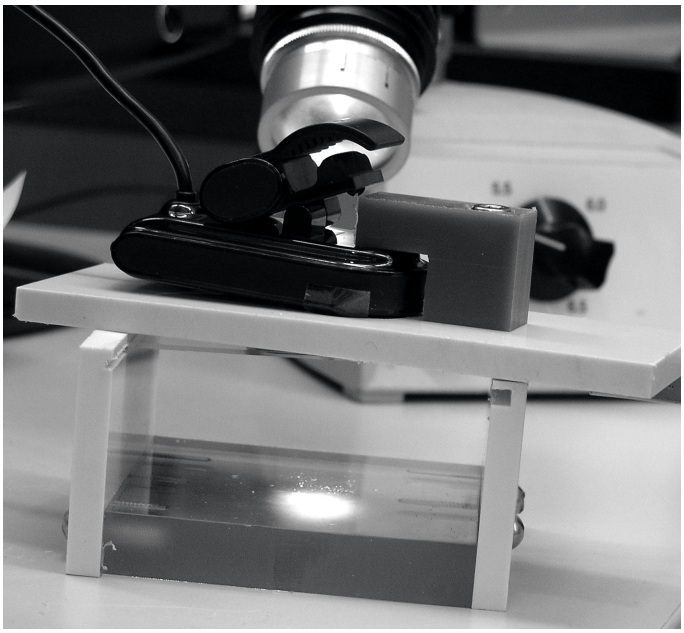

FIG. 15: Ball Lens Microscope Setup.

below the top edges. The plastic sheet holding the microscope/camera rests upon the top edges of the U, and can be moved freely over the slide.

A small hole was drilled through one side of the U, partly through and partly below the rabbet. Focus adjustment is achieved by placing a small wedge (e.g., a toothpick) through the hole and under the slide. As the wedge is moved in and out, it raises and lowers the slide by a fraction of a millimeter. Light from a small microscope illuminator, collimated to a 1" beam, is diffusely reflected from a white surface on which the plastic stand sits, through the slide and into the microscope/camera.

The setup is shown in Fig. 15. The plastic sheet supporting the camera (cable going off to the left) lies in the middle of the picture, slightly skewed to the stand. The ball lens and its support, attached to the camera aperture, lies within a hole in the middle of the plastic sheet, and so is not visible, nor is the focus adjustment hole in the side visible. The inverted L-shaped bracket that affixes the camera, the rabbets which support a slide, and a bit of a slide itself (just below the plastic sheet on the left), the inverted U stand, as well as the light source and its power supply, are visible.

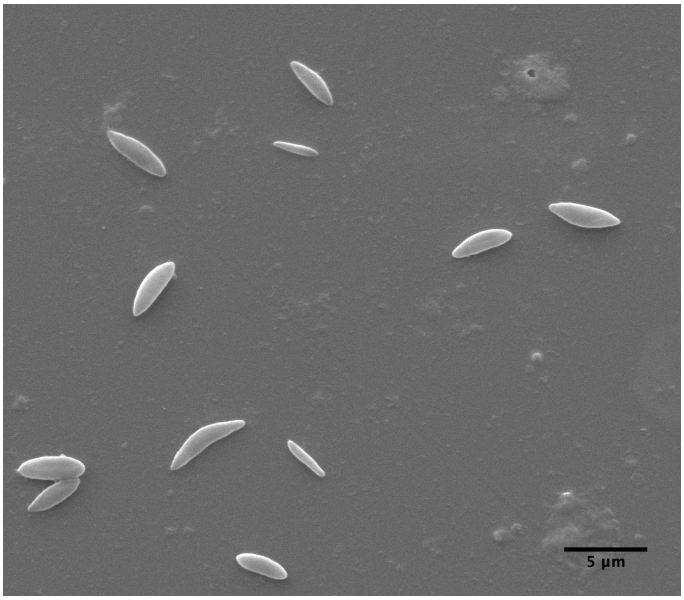

FIG. 16: Clarkia pulchella amyloplasts photographed with the electron microscope.

1. *Amyloplasts Seen With Ball Lens Microscope*

Now we address the discrepancy between our observations with the Olympus microscope, summarized in Fig. 10, that the amyloplasts appear to be of average radius (i.e., half-length) $\approx$ 2 μm, with maximum radius $\approx$ 3 μm, and Brown's observations with his microscope, that their radius range is $\approx$ 3–4 μm. We shall do so by showing that the observations with the ball lens are essentially the same as Brown's. But, also, the electron microscope picture Fig.16 of amyloplasts, while not depicting a large sample, suggests that the size distribution measured with the Olympus microscope is reasonably accurate.

For the ball lens, the Airy radius is $r_A = .61\lambda f/b = 1.0$ μm. This can also be seen in the graph of its intensity versus distance in Appendix F 2, Fig. 20 (the $\bar{B} = 2$ curve). The exit pupil b=.24 mm is not the ideal size to minimize spherical aberration according to the Strehl criterion (discussed in Section V C 2 and Appendix F 2). That ideal size is b=.19 mm, corresponding to the $\bar{B} = 1$ curve in Fig.20. However, its intensity is still reasonably approximated by the Airy function, so we shall assume that the considerations leading to Fig.12 are valid.

To check that $r_A = 1$ μm, a slide containing 1 μm diameter polystyrene spheres was observed and photographed. Another slide containing a scale with marks 10 μm apart was separately photographed. Both photographs were superimposed using the program Photoshop Elements 2. Using the program ImageJ, the image of the spheres was enlarged so that the pixels could be seen, and they were analyzed, as described for the spheres photographed with the Olympus microscope in section V C 3. The result was that the polystyrene spheres appeared to have diameter 2.1$\pm$.2μm.

For a theoretical comparison, with $a/r_A = .5/1 = .5$, one reads from Fig. 12 that $R/r_A \approx 1.1$. Therefore, it is predicted that the apparent radius of the spheres should be $R = 1.1r_A = 1.1\mu$m, or diameter 2.2μm, in good agreement with the observation discussed above.

Now we turn to compare the amyloplast sizes seen with the Olympus microscope and amyloplast sizes seen through the ball lens. Fig. 18 shows a portion of a photo taken through the ball lens, of a slide containing amyloplasts that had emerged from a pollen grain (whose out-of-focus edge appears at the lower left).

As described above, a photograph of a scale was superimposed and the photograph was further enlarged so that pixels were visible. The radius (half the length) of 44 amyloplasts was measured, 14 of which appear in Fig. 18 and 30 appear in another photograph of a different scene. Fig.17 contains a graph of number of amyloplasts in a .25 μm radius bin versus radius in μm.

From this graph, the amyloplasts appear through our ball lens as of average radius $\approx$ 3 μm, with maximum radius $\approx$ 4 μm. This is $\approx$ 1 μm larger than what was observed with the Olympus microscope, Fig. 10, but exactly what Brown said about the amyloplast sizes he observed through his lens!

This excellent agreement, between the observations with our ball lens and Brown's observations with his lens should be tempered by the realization that our lens has $r_A \approx 1$ μm and exit pupil $b = .24$mm, whereas we have deduced that Brown's lens had $r_A \approx .8$ μm and exit pupil $b = .35$ mm. However, it leaves little doubt that Brown was seeing enlarged amyloplasts on account of the diffraction and possible spherical aberration of his lens.

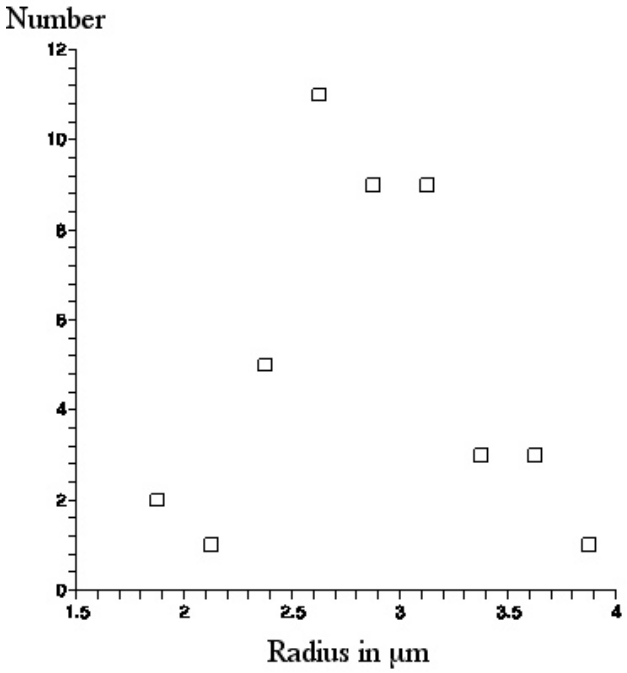

FIG. 17: Number of amyloplasts in a .25 μm radius bin vs amyloplast radius (= half amyloplast length).

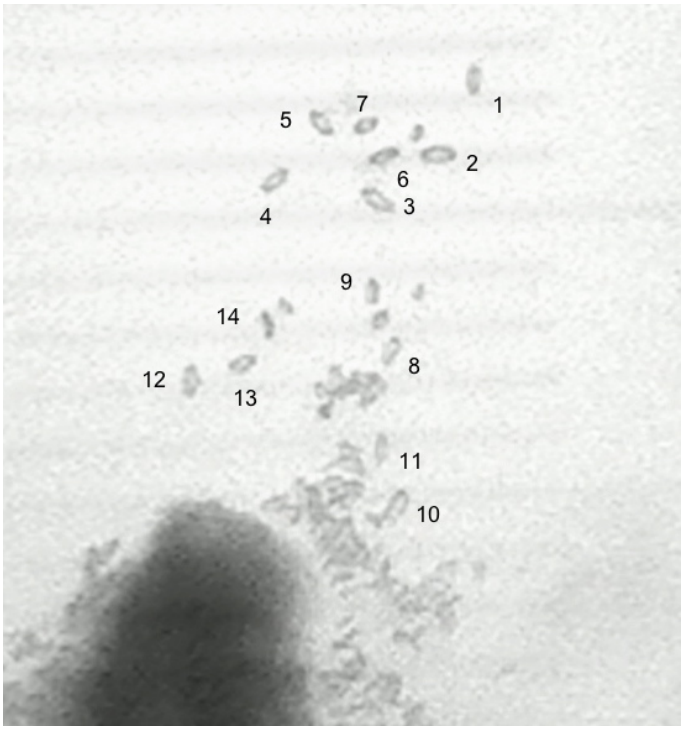

FIG. 18: Amyloplasts photographed with the ball lens microscope. The superimposed scale marks (the faint horizontal lines) are 10μm apart.

Acknowledgments

It is a pleasure to thank Diane Bilderback, Brent Elliot, Brian Ford, Armando Mendez, Michael Milder, Bill Pfitsch, Hilary Joy Pitoniak, Diana Pilson, Bronwen Quarry, James Reveal, Ann Silversmith, Ernest Small, and David Mabberley for help with this endeavor.

VI. THEORY

The appendices contain seven mathematical tutorials.

Appendix A contains a derivation due to Langevin, of the well known expression, given first by Einstein[76], for the mean-square displacement of an object undergoing Brownian motion[77]. The method is easily applied to give the mean-square angular displacement of an object undergoing Brownian rotation.

These expressions depend upon the viscous force or viscous torque on the object. Such fluid flow analysis is not treated in places which treat the material of Appendix A. The results for a sphere are derived in Appendix B[78]. For an ellipsoid, results are just cited[79].

Appendix C presents a derivation of geometrical optics starting from the wave equation. The discussion here, utilizing the WKB approximation in 3 dimensions, does not seem to be given elsewhere, although the result (the eikonal approximation of geometrical optics) is well known. Appendix D, a digression, applies this result to mirrors and lenses. It is emphasized, because of the approximate solution's abrupt discontinuities at the boundaries of mirrors and lenses, that it must be modified in order to better satisfy the wave equation.

Appendix E contains the modification, obtaining from Green's theorem, in a standard way, the Huyghens-Fresnel-Kirchhoff expression for a diffracted wave emanating a lens[80]. Then, in Appendix F, this theory is used to discuss lens imaging of a point source. Usually, books on optics discuss the diffraction of a lens (due to its limited aperture) and the spherical aberration of a lens (due to the image made by rays at the rim of the lens having a different focal plane than the image made by near-axial rays) separately. Then, no expression is given for their combined intensity. Here, diffraction and spherical aberration receive a unified treatment. As a concrete example, the theory is applied to what is seen through a 1mm diameter ball lens used as a microscope. The optimum choice for the exit pupil for such a lens, to minimize spherical aberration, is discussed.

Appendix G applies these results for a point source to an extended light source, an illuminated hole of radius a. The apparent radius of the image is discussed, for small and large a. As discussed in section III H, results are obtained which illuminate (sic) Brown's observations of "molecular" size,

APPENDIX A: BROWNIAN TRANSLATION AND ROTATION

1. Brownian Translation

The derivation of the expression for the mean square distance travelled, or mean square angle rotated, by an object undergoing Brownian motion, is surprisingly simple.

For motion in the x-direction, an object of mass m obeys Newton's second law

$$\begin{aligned} \frac{dx}{dt} &= v \\ m\frac{dv}{dt} &= -\beta v + f(t) \end{aligned} \tag{A1}$$

In Eq. (A1), the force on the object due to the impact of molecules is divided into two pieces. One is a steady viscous force $-\beta v$ (calculation of the constant β is discussed in Appendix B), the other is a random force $f(t)$, which is assumed uncorrelated with x. We imagine a collection of identical objects undergoing this motion. Each object suffers a different force, but the average force over the collection is $\overline{f}(t) = 0$. We wish to know the mean square distance $\overline{x^2}$ travelled in time t, for this collection. We assume that the molecules are in thermal equilibrium, with each other and with the objects, so by the equipartition theorem,

$$\frac{1}{2}m\overline{v^2} = \frac{1}{2}kT, \tag{A2}$$

where k is Boltzmann's constant and T is the temperature.

Consider the equations for x^2 and xv, which follow from Eqs. (A1):

$$\begin{aligned} \frac{1}{2}\frac{dx^2}{dt} &= xv \\ m\frac{dxv}{dt} &= mv^2 - \beta xv + xf(t) \end{aligned} \tag{A3}$$

Upon taking the average, over the collection, of Eqs. (A3), one obtains

$$\begin{aligned} \frac{1}{2}\frac{d\overline{x^2}}{dt} &= \overline{xv} \\ m\frac{d\overline{xv}}{dt} &= m\overline{v^2} - \beta\overline{xv} \end{aligned} \tag{A4}$$

since $\overline{xf(t)} = \overline{x}\overline{f}(t) = 0$. Surprisingly, this force, which causes the Brownian motion, appears to plays no role in the subsequent mathematics. However, it does play a role: it is responsible for Eq. (A2), as can be seen by calculating $\overline{vf}(t) \neq 0$ (which we shall not do here, as it is not needed).

One readily sees from the second of Eqs. (A4) that $\overline{xv}$ exponentially decays to a constant, so that the right side vanishes,

$$\overline{xv} = \frac{m}{\beta}\overline{v^2} = \frac{kT}{\beta}, \tag{A5}$$

where Eq. (A2) is utilized in the second step. Putting Eq. (A5) into the first of Eqs. (A4) and integrating, we obtain the desired result:

$$\overline{x^2} = \frac{2kTt}{\beta}. \tag{A6}$$

It is useful to have an expression for the mean distance $\overline{|x|}$. It can be argued that the particle position probability density distribution is well approximated by a gaussian distribution,

$$P(x) = \frac{1}{\sqrt{2\pi\overline{x^2}}}e^{-x^2/2\overline{x^2}}$$

which yields the result

$$\overline{|x|} = 2\int_0^\infty dx x P(x) = \sqrt{\frac{2}{\pi}\overline{x^2}} \approx .80\sqrt{\overline{x^2}}.$$

It is also useful to have an expression for the mean distance $\overline{|r|}$ travelled when there is motion in two dimensions. Then

$$\overline{|r|} = \int_0^\infty r^2 dr \int_0^{2\pi} d\theta \frac{1}{2\pi\overline{x^2}} e^{-r^2/2\overline{x^2}} = \sqrt{\frac{\pi}{2}\overline{x^2}} \approx 1.25\sqrt{\overline{x^2}}.$$

2. Brownian Rotation

For Brownian rotation through angle θ about an axis, for an object of moment of inertia I, the Newtonian equations are

$$\begin{aligned} \frac{d\theta}{dt} &= \omega \\ I\frac{d\omega}{dt} &= -\beta'\omega + \tau(\omega), \end{aligned} \tag{A7}$$

where the equipartition theorem implies $(1/2)I\omega^2 = (1/2)kT$, and the random torque satisfies $\overline{\tau}(\omega) = 0$. Eqs. (A1) and (A7) are precisely analogous, so the result (A6) in this case becomes

$$\overline{\theta^2} = \frac{2kTt}{\beta'}. \tag{A8}$$

APPENDIX B: VISCOUS FORCE AND TORQUE ON A SPHERE AND ELLIPSOID

1. Fluid Flow Equations

The derivation of the expression for the viscous force, felt by an object moving with constant velocity through a fluid, is surprisingly complicated. First one finds the fluid

velocity and pressure in an equivalent situation, where the object is at rest and the fluid asymptotically flows with constant velocity. Then one finds the force.

Any fluid obeys the conservation of mass equation,

$$\frac{\partial \rho}{\partial t} + \nabla \cdot \rho \mathbf{v} = 0.$$

If the fluid is incompressible, then the mass density ρ is constant, so

$$\nabla \cdot \mathbf{v} = 0. \tag{B1}$$

The next equation, the Navier-Stokes equation, is Newton's second law for a bit of fluid,

$$\begin{aligned} \rho \frac{D\mathbf{v}}{Dt} &= -\nabla P + \eta \sum_{i=1}^{3} \frac{\partial}{\partial x_i}\Big[\frac{\partial \mathbf{v}}{\partial x_i} + \nabla v_i\Big] \\ &= -\nabla P + \eta \nabla^2 \mathbf{v}. \end{aligned} \tag{B2}$$

(Eq. (B1) has been used in the second step of Eq. (B2)). In Eq. (B2), P is the pressure, η is the coefficient of viscosity, and $D\mathbf{v}/Dt$ denotes the rate of change of velocity while moving with the fluid. For an area of fluid whose normal points in the i-direction, the normal force/area is -P while the shear force/area in the j-direction ($j \neq i$) is

$$f_{ij} = \eta\Big[\frac{\partial v_i}{\partial x_j} + \frac{\partial v_j}{\partial x_i}\Big]. \tag{B3}$$

The sum of the pressure and viscous forces on two opposing faces of an infinitesimal cube of fluid give the pressure and viscous force/volume on the cube: these are the two terms on the right side of Eq. (B2). For our application, we assume that the fluid velocity is small enough that the left side of Eq. (B2) is negligibly small compared to either of the two terms on the right side, so (B2) becomes

$$+\eta \nabla^2 \mathbf{v} = \nabla P. \tag{B4}$$

We must solve Eqs. (B1), (B4), subject to the boundary conditions.

2. Boundary Conditions

We shall consider that the object is a sphere of radius R. Far from it, the boundary conditions, which obviously satisfy Eqs. (B1), (B4), are that the fluid velocity and pressure are constant, say

$$\lim_{r\to\infty} \mathbf{v} = w\mathbf{i}_z = w[\mathbf{i}_r \cos\theta - \mathbf{i}_\theta \sin\theta], \quad \lim_{r\to\infty} P = Q.$$

Here, $\mathbf{i}_z$, $\mathbf{i}_r$ and $\mathbf{i}_\theta$ are respectively the unit vectors in the z-direction and in the spherical coordinate r and θ directions, and w is the constant asymptotic fluid speed, while Q is the constant asymptotic pressure. There is no loss in generality in observing that, for $r > R$, the solution may be written

$$\begin{aligned} \mathbf{v} &= \mathbf{i}_r[w\cos\theta + v'_r(r,\theta)] + \mathbf{i}_\theta[-w\sin\theta + v'_\theta(r,\theta)], \\ P &= Q + p(r,\theta). \end{aligned}$$

where v'_r, v'_θ and p all vanish for large r. Nothing depends upon the azimuthal angle ϕ because the solution must be rotationally symmetric about the z-axis.

The boundary condition at the surface $r = R$ of the sphere is that $\mathbf{v} = 0$. But this is only possible if $v'_r(r,\theta) = wf(r)\cos\theta$, $v'_\theta(r,\theta) = wg(r)\sin\theta$, where $f(R) = -1$, $g(R) = 1$. Any additional terms must vanish both at infinity and on the sphere's surface, but that is the solution for a fluid at rest, vanishing everywhere. Thus we look for solutions of the form

$$\begin{aligned} \mathbf{v} &= \mathbf{i}_r w\cos\theta[1 + f(r)] + \mathbf{i}_\theta w\sin\theta[-1 + g(r)], \\ P &= Q + p(r,\theta). \end{aligned} \tag{B5}$$

3. Fluid Velocity and Pressure

First, consider the constraint of Eq. (B1). Putting Eq. (B5) into Eq. (B1) gives

$$\begin{aligned} \nabla \cdot \mathbf{v} &= \frac{1}{r^2}\frac{\partial}{\partial r} r^2 \{w\cos\theta[1 + f(r)]\} + \\ &\quad \frac{1}{r\sin\theta}\frac{\partial}{\partial\theta}\sin\theta\{w\sin\theta[-1 + g(r)]\} = 0 \end{aligned} \tag{B6}$$

(expressions for vector operators in spherical coordinates can be found, e.g., on the back cover of Jackson's book[81]). This tells us that

$$\begin{aligned} \frac{1}{r^2}\frac{d}{dr} r^2 f(r) + \frac{2}{r} g(r) &= 0 \quad \text{or} \\ g(r) &= -f(r) - \frac{r}{2} f'(r) \end{aligned} \tag{B7}$$

Next we apply Eq. (B4). This can be rewritten as a first order equation in terms of $\mathbf{B} \equiv \nabla \times \mathbf{v}$, by means of the identity $\nabla \times (\nabla \times \mathbf{v}) = \nabla(\nabla \cdot \mathbf{v}) - \nabla^2 \mathbf{v} = -\nabla^2 \mathbf{v}$ (using (B1)):

$$\eta \nabla \times \mathbf{B} = -\nabla P. \tag{B8}$$

Eq. (B8) looks like Maxwell's equation for a magnetic field caused by an azimuthally symmetric current $\sim \nabla P$. Thus we expect that $\mathbf{B} \sim \mathbf{i}_\phi$, and this is borne out by calculation. Using Eqs. (B5) and (B7),

$$\begin{aligned} \mathbf{B} &\equiv \nabla \times \mathbf{v} = \mathbf{i}_\phi \frac{1}{r}\Big[\frac{\partial}{\partial r} r v_\theta - \frac{\partial}{\partial\theta} v_r\Big] \\ &= -\mathbf{i}_\phi w \frac{\sin\theta}{r}\Big[\frac{r^2}{2} f''(r) + 2r f'(r)\Big]. \end{aligned} \tag{B9}$$

Write Eq. (B9) as $\mathbf{B} = \mathbf{i}_\phi B(r)\sin\theta$, and insert this into Eq. (B8):

$$\begin{aligned} \nabla \times \mathbf{B} &= \Big[\mathbf{i}_r \frac{1}{r\sin\theta}\frac{\partial}{\partial\theta}\sin\theta - \mathbf{i}_\theta \frac{1}{r}\frac{\partial}{\partial r} r\Big] B(r)\sin\theta \\ &= \mathbf{i}_r \frac{1}{r} 2\cos\theta B(r) - \mathbf{i}_\theta \sin\theta \frac{1}{r}\frac{\partial}{\partial r} r B(r) \\ &= -\frac{1}{\eta}\nabla P = -\mathbf{i}_r \frac{1}{\eta}\frac{\partial}{\partial r} p - \mathbf{i}_\theta \frac{1}{\eta r}\frac{\partial}{\partial\theta} p. \end{aligned} \tag{B10}$$

Eq. (B10) can only be satisfied if $p/\eta = h(r)\cos\theta$, where B, h satisfy the two equations

$$B(r) = -\frac{r}{2}h'(r), \quad h(r) = -B(r) - rB'(r). \tag{B11}$$

Combining Eqs. (B11) yields the second order differential equation for $B(r)$,

$$\frac{d^2}{dr^2}rB(r) - \frac{2}{r}B(r) = 0.$$

The solutions are $B(r) = Cr^{-2}$, and $B(r) \sim r$ (which we discard). Then, from (B11), we find $h(r) = B(r)$.

Returning to Eq.(B9), we now have a differential equation for $f(r)$,

$$\frac{C}{r^2} = -\frac{w}{r}\Big[\frac{r^2}{2}f''(r) + 2rf'(r)\Big]. \tag{B12}$$

The inhomogeneous solution is C/wr, and the two solutions of the homogeneous equation are $C'r^{-3}$ and ~ 1 (which we discard). Thus we obtain $f(r)$, and then get $g(r)$ from Eq. (B7):

$$f(r) = \frac{C}{wr} + \frac{C'}{r^3}, \quad g(r) = -\frac{C}{2wr} + \frac{C'}{2r^3}.$$

Finally, the boundary conditions $f(R) = -1$, $g(R) = 1$ determine the constants:

$$C = -\frac{3wR}{2}, \quad C' = \frac{R^3}{2}.$$

Putting these results into Eq. (B5) gives the velocity and the pressure:

$$\begin{aligned}\mathbf{v} &= \mathbf{i}_r w\cos\theta\Big[1 - \frac{3R}{2r} + \frac{R^3}{2r^3}\Big] \\ &+ \mathbf{i}_\theta w\sin\theta\Big[-1 + \frac{3R}{4r} + \frac{R^3}{4r^3}\Big] \\ P &= Q - \cos\theta\frac{3w\eta R}{2r}\end{aligned} \tag{B13}$$

4. Force on Sphere

First, we calculate the force due to the pressure. This force PdA, on an area dA of the sphere's surface, points radially inward. Because of the symmetry, the integrated force only has a net component in the $-\mathbf{i}_z$ direction. The component of the force in that direction is $PdA\cos\theta$. Therefore, the net pressure force is

$$\begin{aligned}\mathbf{F}_p &= -\mathbf{i}_z\int_0^{2\pi}\int_0^{\pi}\int_0^{2\pi} R^2\sin\theta d\theta d\phi\Big[Q - \cos\theta\frac{3w\eta}{2}\Big]\cos\theta \\ &= \mathbf{i}_z 2\pi w\eta R.\end{aligned} \tag{B14}$$

Second, we calculate the viscous force/area, on an element of surface area oriented along $\mathbf{i}_r$. It is in the direction $\mathbf{i}_\theta$, and is found from Eq. (B3):

$$\begin{aligned}\sum_{i,j=1}^{3}\mathbf{i}_{ri}f_{ij}\mathbf{i}_{\theta j} &= \eta\sum_{i=1}^{3}[(\mathbf{i}_\theta\cdot\nabla v_i)\mathbf{i}_{ri} + (\mathbf{i}_r\cdot\nabla v_i)\mathbf{i}_{\theta i}] \\ &= \eta\Big[\frac{1}{r}\frac{\partial}{\partial\theta}v_r - \sum_{i=1}^{3}v_i\frac{1}{r}\frac{\partial}{\partial\theta}\mathbf{i}_{ri} + \frac{\partial}{\partial r}v_\theta - \sum_{i=1}^{3}v_i\frac{\partial}{\partial r}\mathbf{i}_{\theta i}\Big],\end{aligned}$$

where the second step uses $\mathbf{i}_r\cdot\nabla = \partial/\partial r$ and $\mathbf{i}_\theta\cdot\nabla = r^{-1}\partial/\partial\theta$ and we have differentiated by parts. Using $(\partial/\partial\theta)\mathbf{i}_r = \mathbf{i}_\theta$, and $(\partial/\partial r)\mathbf{i}_\theta = 0$ and inserting the velocity components from (B13), we obtain

$$\begin{aligned}\sum_{i,j=1}^{3}\mathbf{i}_{ri}f_{ij}\mathbf{i}_{\theta j} &= \eta\Big[\frac{1}{r}\frac{\partial}{\partial\theta}v_r + \frac{\partial}{\partial r}v_\theta - \frac{1}{r}v_\theta\Big]_{r=R} \\ &= \eta\Big[\frac{\partial}{\partial r}v_\theta\Big]_{r=R} = -\eta w\sin\theta\frac{3}{2R},\end{aligned} \tag{B15}$$

Since (B15) is the viscous force/area in the $\mathbf{i}_\theta$ direction, it must be multiplied by $-\sin\theta dA$ to get the projection of the force on a surface element in the $\mathbf{i}_z$ direction. Thus, the net viscous force is

$$\begin{aligned}\mathbf{F}_v &= \mathbf{i}_z\int_0^{2\pi}\int_0^{\pi}\int_0^{2\pi} R^2\sin\theta d\theta d\phi\Big[-\eta w\sin\theta\frac{3}{2R}\Big](-\sin\theta) \\ &= \mathbf{i}_z 4\pi w\eta R.\end{aligned} \tag{B16}$$

Therefore, from Eqs. (B14) and (B16), the net force is

$$\mathbf{F} = \mathbf{F}_p + \mathbf{F}_v = \mathbf{i}_z 6\pi w\eta R.$$

Of course, here $\mathbf{v} = \mathbf{i}_z w$ is the asymptotic velocity of the water with respect to the sphere at rest, while $\mathbf{v}_s = -\mathbf{v}$ is the velocity of the sphere with respect to the asymptotically resting water, so the force on the moving sphere (Stokes' law) is

$$\mathbf{F}_s = -\mathbf{v}_s 6\pi\eta R. \tag{B17}$$

Thus, in Eq. (A6), $\beta = 6\pi\eta R$.

5. Force on Ellipsoid

When the shape of the object is not a sphere, still one expects from dimensional considerations that the expression for the force is of the same form as (B17). However, the radius R is replaced by a much more complicated function of the dimensions, an effective radius. For an ellipsoid $z^2/a^2 + (x^2+y^2)/b^2 = 1$ ($a \geq b$), moving in the z-direction, the result is[79]

$$\begin{aligned}R_{\rm eff}^{-1} &= \frac{3}{8}\int_0^\infty d\lambda\frac{2a^2+\lambda}{(a^2+\lambda)^{3/2}(b^2+\lambda)} \\ &= \frac{3}{8}\left[\frac{2a^2-b^2}{(a^2-b^2)^{3/2}}\ln\frac{a+\sqrt{a^2-b^2}}{a-\sqrt{a^2-b^2}} - \frac{2a}{a^2-b^2}\right].\end{aligned} \tag{B18}$$

For $b \to a$, this becomes $a^{-1}+(2/5a^3)(a^2-b^2)+...$ which, of course, reduces to the Stokes value a^{-1} when $b = a$. A good fit for $.2 \le b/a \le 1$ is $R_{\rm eff} \approx .8b + .2a$. With $b = a/2$, (B18) gives $R_{\rm eff} \approx .60a$.

For the ellipsoid moving in the x or y-direction, the result is

$$R_{\rm eff}^{-1} = \frac{3}{8}\int_0^\infty d\lambda \frac{2b^2+\lambda}{(a^2+\lambda)^{1/2}(b^2+\lambda)^2}$$
$$= \frac{3}{8}\left[\frac{a^2-(3/2)b^2}{(a^2-b^2)^{3/2}}\ln\frac{a+\sqrt{a^2-b^2}}{a-\sqrt{a^2-b^2}} + \frac{a}{a^2-b^2}\right]. \quad \text{(B19)}$$

For $b \to a$, this becomes $a^{-1} + (3/10a^3)(a^2-b^2) + ...$ A good fit for $.2 \le b/a \le 1$ is $R_{\rm eff} \approx .6b + .4a$. With $b = a/2$, (B19) gives $R \approx .69a$.

The area moving through the water is, in increasing order, that of the the ellipsoid moving parallel to its long axis, the ellipsoid moving perpendicular to its long axis, and the moving sphere of radius a. It is reasonable that the force in these three cases is also in increasing order.

6. Rotational Boundary Conditions

The calculation of the viscous torque, felt by a sphere rotating with constant angular velocity through a fluid asymptotically at rest, follows the same lines as for the translating sphere, and is simpler. First comes the boundary conditions. As before, we consider the problem from the reference frame of the sphere, so that the fluid's asymptotic velocity is

$$\lim_{r\to\infty}\mathbf{v} = \mathbf{i}_\phi \Omega r\sin\theta \qquad \lim_{r\to\infty} P = Q. \quad \text{(B20)}$$

Ω is the constant asymptotic fluid angular velocity about the z-axis, while Q is the constant asymptotic pressure. (B20) satisfies Eqs. (B1), (B4). The general solution has the form

$$\mathbf{v} = \mathbf{i}_\phi[\Omega r\sin\theta + v'_\phi(r,\theta)], \quad P = Q + p(r,\theta)$$

where v'_ϕ and p vanish for large r and satisfy Eqs. (B1), (B4).

The boundary condition at the surface $r = R$ of the sphere is that $\mathbf{v} = 0$. But this is only possible if $v'_\phi(r,\theta) = \Omega f(r) r\sin\theta$, where $f(R) = -1$. Any additional terms must vanish both at infinity and on the sphere's surface, but that is the solution for a fluid at rest, vanishing everywhere. Thus we look for solutions of the form

$$\mathbf{v} = \mathbf{i}_\phi \Omega r\sin\theta[1+f(r)], \quad P = Q + p(r,\theta). \quad \text{(B21)}$$

7. Fluid Velocity and Pressure

The constraint of Eq. (B1) is identically satisfied, since

$$\nabla\cdot\mathbf{v} = r\sin\theta\frac{\partial}{\partial\phi}v_\phi = 0.$$

Next we apply Eq. (B4), in the form (B8). First we calculate

$$\mathbf{B} \equiv \nabla\times\mathbf{v}$$
$$= \Big[\mathbf{i}_r\frac{1}{r\sin\theta}\frac{\partial}{\partial\theta}\sin\theta - \mathbf{i}_\theta\frac{1}{r}\frac{\partial}{\partial r}r\Big]\Omega r\sin\theta[1+f(r)]$$
$$= 2\Omega[\mathbf{i}_r\cos\theta(1+f) - \mathbf{i}_\theta\sin\theta(1+f+\frac{r}{2}f')]. \quad \text{(B22)}$$

Then, according to (B8),

$$\nabla\times\mathbf{B} = \mathbf{i}_\phi 2\Omega\frac{1}{r}\Big[\frac{\partial}{\partial r}r[-\sin\theta(1+f+\frac{r}{2}f')]$$
$$-\frac{\partial}{\partial\theta}[\cos\theta(1+f)]\Big]$$
$$= -\mathbf{i}_\phi 4\Omega\sin\theta[f'+\frac{r}{4}f'']$$
$$= -\frac{1}{\eta}\nabla P = -\frac{1}{\eta}\Big[\mathbf{i}_r\frac{\partial}{\partial r}p + \mathbf{i}_\theta\frac{1}{r}\frac{\partial}{\partial\theta}p\Big]. \quad \text{(B23)}$$

From Eq. (B23), it follows that

$$f' + \frac{r}{4}f'' = 0, \quad p = 0.$$

The two solutions are $f(r) = C/r^3$ and ~ 1 (which we discard). The boundary condition $f(R) = -1$ determines the constant, $C = -R^3$. Thus, we obtain from Eq. (B21), the velocity

$$\mathbf{v} = \mathbf{i}_\phi\Omega r\sin\theta[1-\frac{R^3}{r^3}]. \quad \text{(B24)}$$

8. Torque on Sphere

First we find the force in the ϕ-direction, using Eq. (B3), and then we can calculate the torque. The force/area, on the surface area dA oriented along $\mathbf{i}_r$, in the direction $\mathbf{i}_\phi$ is

$$\sum_{i,j=1}^3 \mathbf{i}_{ri}f_{ij}\mathbf{i}_{\phi j} = \eta\sum_{i,=1}^3[(\mathbf{i}_\phi\cdot\nabla v_i)\mathbf{i}_{ri} + (\mathbf{i}_r\cdot\nabla v_i)\mathbf{i}_{\phi i}]$$
$$= \eta\Big[\frac{1}{r\sin\theta}\frac{\partial}{\partial\phi}v_r - \sum_{i,=1}^3 v_i\frac{1}{r\sin\theta}\frac{\partial}{\partial\phi}\mathbf{i}_{ri}$$
$$+\frac{\partial}{\partial r}v_\phi - \sum_{i,=1}^3 v_i\frac{\partial}{\partial r}\mathbf{i}_{\phi i}\Big].$$

Since $v_r = 0$, $(\partial/\partial\phi)\mathbf{i}_r = \sin\theta\mathbf{i}_\phi$ and $(\partial/\partial r)\mathbf{i}_\phi = 0$, we have from (B24),

$$\sum_{i,j=1}^3 \mathbf{i}_{ri}f_{ij}\mathbf{i}_{\phi j} = \eta\Big[-\frac{1}{r}v_\phi + \frac{\partial v_\phi}{\partial r}\Big]_{r=R} = 3\eta\Omega\sin\theta. \quad \text{(B25)}$$

The torque/area on the surface of the sphere is this force/area multiplied by the moment arm $R\sin\theta$, and

it points in the $\mathbf{i}_z$ direction, so the net viscous torque is

$$\begin{aligned}\mathcal{T} &= \mathbf{i}_z \int_0^{2\pi}\int_0^{\pi}\int_0^{2\pi} R^2 \sin\theta d\theta d\phi [R\sin\theta][3\eta\Omega\sin\theta] \\ &= \mathbf{i}_z 8\pi\eta\Omega R^3.\end{aligned}$$

Of course, here $\omega = \mathbf{i}_z\Omega$ is the asymptotic angular velocity of the water with respect to the sphere at rest, while $\omega_s = -\mathbf{i}_z\Omega$ is the angular velocity of the sphere with respect to the asymptotically resting water, so the torque on the moving sphere is

$$\mathcal{T}_s = -\omega_s 8\pi\eta R^3. \tag{B26}$$

Thus, in Eq. (A8), $\beta' = 8\pi\eta R^3$.

9. Torque on Ellipsoid

When the shape of the object is the ellipsoid $z^2/a^2 + (x^2+y^2)/b^2 = 1$ ($a \geq b$), the expression for the torque is of the same form as (B26), but the radius R is replaced by another expression. For rotation about the long (a) axis, the result is[79]

$$\begin{aligned}R_{\rm eff}^{-3} &= \frac{3}{2}\int_0^\infty d\lambda \frac{1}{(a^2+\lambda)^{1/2}(b^2+\lambda)^2} \\ &= \frac{3}{2}\left[\frac{a}{(a^2-b^2)b^2}\right. \\ &- \left.\frac{1}{2(a^2-b^2)^{3/2}}\ln\frac{a+\sqrt{a^2-b^2}}{a-\sqrt{a^2-b^2}}\right].\end{aligned} \tag{B27}$$

For $b \to a$, this becomes $a^{-3} + (6/5a^5)(a^2-b^2) + ...$ A good fit for $.2 \leq b/a \leq 1$ is $R_{\rm eff} \approx .84b + .16a$. With $b = a/2$, (B27) gives $R_{\rm eff} \approx .59a$.

For rotation about either of the other axes,

$$\begin{aligned}R_{\rm eff}^{-3} &= \frac{3}{2}\int_0^\infty d\lambda \frac{1}{(a^2+\lambda)^{3/2}(b^2+\lambda)^2}\left[\lambda + \frac{2a^2b^2}{a^2+b^2}\right] \\ &= \frac{3}{2(a^2+b^2)}\left[\frac{-a}{(a^2-b^2)}\right. \\ &+ \left.\frac{(a^2-(1/2)b^2)}{(a^2-b^2)^{3/2}}\ln\frac{a+\sqrt{a^2-b^2}}{a-\sqrt{a^2-b^2}}\right].\end{aligned} \tag{B28}$$

For $b \to a$, this becomes $a^{-3} + (9/10a^5)(a^2-b^2) + ...$ A good fit for $.2 \leq b/a \leq 1$ is $R_{\rm eff} \approx .56b + .44a$. With $b = a/2$, (B28) gives $R_{\rm eff} \approx .72a$.

APPENDIX C: GEOMETRICAL OPTICS FROM THE WKB APPROXIMATION

1. The Problem To Be Solved

The problem addressed in the next four appendices is to find the image of a point source of light, made by a ball lens of limited aperture. This is used to discuss the optimal choice of aperture radius.

Consider a ball lens of radius R (diameter D) and index of refraction $n = 3/2$. ($n = 1.5$ is close enough to the BK7 glass index $n = 1.517$ of the ball lens of our experiments.) It follows from Eq. (7) that the focal length of the lens is $f = 3R/2$.

The point source of light has wave-number $k \equiv 2\pi/\lambda$, where $\lambda = .55\mu$m (green light). It is placed at the focal distance f from the center of the lens. Rays pass through the lens and then through a coaxial hole of radius b in a screen (the so-called exit pupil), and proceed onwards.

The light does not converge to a point at infinity, as predicted by geometrical optics for an ideal lens. Instead, the light intensity distribution which appears on a screen at infinity (placed such as to make the image as sharp as possible) is a circular blob, Although it sounds like something used by a racetrack oddsmaker, this light intensity distribution is called the *point spread function* because it describes how the light from a point source is spread out by the lens.

But, first, the connection should be made between this problem and the one we actually want to solve. The latter is to use the lens as a magnifying glass. That is, one places the point source on the optic axis slightly closer to the lens than f, so that the sharpest image is on a plane at 25cm on the *same* side of the lens as the source. One then divides this magnified image intensity by the lens magnification, $m \approx 25/f$ ($f << 25$cm), to obtain the apparent image intensity to scale (i.e., as if there was in fact a spread-out object of that size being precisely imaged, instead of a point source being imprecisely imaged.)

However, if the source is instead put at the focal length, with the image at $-\infty$, the angular magnification is still m. But, this is the same angular magnification as when the image is at $+\infty$, on the *opposite* side of the lens from the source. It is this simpler problem we are addressing.

The point spread function for this simpler problem can be readily utilized to find the intensity distribution for the magnifier application. For example, suppose we find a ring of light at infinity, with a dark boundary which makes angle β_0 with a point at the center of the lens. The magnifier usage has this circle of vanishing intensity appearing on the 25cm image plane with radius $25\beta_0$. Therefore, the apparent radius of the circle of light is $25\beta_0/m = \beta_0 f$.

2. Light Field in the WKB Approximation

We shall accept the argument[82] that there is no appreciable error in calculating the light intensity by taking the monochromatic light amplitude to be described by a complex scalar field $U(\mathbf{x})\exp -i\omega t$, instead of the actual vector electromagnetic field, with the time average intensity given by $|U(\mathbf{x})|^2$.

The wave equation for $U(\mathbf{x},t)$ with a point source of

light of constant amplitude C at the origin is

$$\nabla^2 U(\mathbf{x},t) - \frac{n^2(\mathbf{x})}{c^2}\frac{\partial^2}{\partial t^2}U(\mathbf{x},t) = -4\pi\delta(\mathbf{x})C.$$

We permit the speed of light $c/n(\mathbf{x})$ to vary throughout space except in the neighborhood of the origin where the speed is that of vacuum, c, and the index of refraction $n(\mathbf{x}) = 1$. Later we shall specialize to $n(\mathbf{x})$ describing a ball lens, i.e., $n(\mathbf{x}) = 1$ everywhere except within a sphere where $n(\mathbf{x}) = n$ is constant. With $U(\mathbf{x},t) = U(\mathbf{x})\exp -i\omega t$ and $\omega = kc$, the wave amplitude is the solution of

$$\nabla^2 U(\mathbf{x}) + k^2 n^2(\mathbf{x})U(\mathbf{x}) = -4\pi\delta(\mathbf{x})C. \qquad \text{(C1)}$$

Away from the source, Eq. (C1) may be written in Schrödinger-like form

$$-\nabla^2 U(\mathbf{x}) - k^2[n^2(\mathbf{x}) - 1]U(\mathbf{x}) = k^2 U(\mathbf{x})$$

It is amusing that turn-of-the-last century physicists got their insights into quantum theory through optics, while we get our insights into optics through quantum theory. The quantum problem, analogous to our optical ball lens problem, is for a particle of mass 1/2 and momentum magnitude k ($\hbar = 1$) emerging from a point and scattering from a spherical potential well of radius R and constant depth $k^2[n^2 - 1]$, The wave function is to have the form $r^{-1}\exp ikr$ in the neighborhood of $r = 0$, a point which lies a distance f from the center of the well. Although this is an exactly solvable problem, it is difficult to obtain physical results from the analytic expression, which is expressed as an infinite series of partial waves[83].

For this reason we shall apply the approximate WKB method. Quantum texts seem to universally discuss this method for one-dimensional motion only. However, the three dimensional problem has been treated[84].

We write $U = \exp i[k\Phi_0 + \Phi_1 + k^{-1}\Phi_2 + ...]$ and substitute into Eq. (C1). Gathering terms of like powers in k, we obtain (away from $\mathbf{x} = 0$ which shall be handled later):

$$k^2\nabla\Phi_0\cdot\nabla\Phi_0 = k^2 n^2, \qquad \text{(C2)}$$
$$2k\nabla\Phi_1\cdot\nabla\Phi_0 = ik\nabla^2\Phi_0 \qquad \text{(C3)}$$

Eq. (C2) implies that

$$\nabla\Phi_0(\mathbf{x}) = n(\mathbf{x})\hat{\mathbf{v}}(\mathbf{x}), \quad \hat{\mathbf{v}}(\mathbf{x})\cdot\hat{\mathbf{v}}(\mathbf{x}) = 1. \qquad \text{(C4)}$$

To find $\hat{\mathbf{v}}(\mathbf{x})$ requires implementing the restriction that Eq. (C4) is a gradient. To do that, consider

$$[\hat{\mathbf{v}}\cdot\nabla]n\hat{\mathbf{v}} = [\hat{\mathbf{v}}\cdot\nabla]\nabla\Phi_0 = \sum_{i=1}^{3}\hat{v}^i\nabla\frac{\partial}{\partial x^i}\Phi_0$$
$$= \sum_{i=1}^{3} v^i\nabla n v^i = \frac{1}{2n}\nabla[n^2\hat{\mathbf{v}}\cdot\hat{\mathbf{v}}] = \nabla n \qquad \text{(C5)}$$

Imagine space filled with the vector field $\hat{\mathbf{v}}$. Picture a line passing through a point parallel to the vector $\hat{\mathbf{v}}$ at that point, and continuing on parallel to the vectors it encounters on its path. Such lines are like the flow lines of a fluid in steady state flow, with $\hat{\mathbf{v}}(\mathbf{x})$ as the (constant speed) velocity field.

Now, if one imagines moving along a particular flow line with the fluid, the rate of change of any function $f(\mathbf{x})$ is given by the substantial derivative

$$\frac{D}{Dt}f(\mathbf{x}) \equiv \frac{f(\mathbf{x}+\hat{\mathbf{v}}dt) - f(\mathbf{x})}{dt} = [\hat{\mathbf{v}}\cdot\nabla]f(\mathbf{x}).$$

We see that the left side of Eq. (C5) is the substantial derivative of $n(\mathbf{x})\hat{\mathbf{v}}(\mathbf{x})$.

So, for a fictitious particle of fluid moving with velocity $\hat{\mathbf{v}}(t)$ along a single flow line $\mathbf{x}(t)$, according to Eq. (C5), it satisfies the equation of motion

$$\frac{d}{dt}[n(\mathbf{x}(t))\hat{\mathbf{v}}(t)] = \frac{D}{Dt}n(\mathbf{x})\hat{\mathbf{v}}(\mathbf{x}) = \nabla n(\mathbf{x}(t)) \quad \text{or}$$
$$\frac{d}{dt}\hat{\mathbf{v}} = -\hat{\mathbf{v}}\frac{d}{dt}\ln n + \nabla\ln n. \qquad \text{(C6)}$$

Given a surface, once one specifies the initial velocity vectors on it, the Newton-type law Eq. (C6) then gives the velocity of the fluid elsewhere.

The force in Eq. (C6) ensures that the particle keeps moving with constant speed: the scalar product of Eq. (C6) with $\hat{\mathbf{v}}(t)$ is

$$\frac{1}{2}\frac{d}{dt}[\hat{\mathbf{v}}(t)\cdot\hat{\mathbf{v}}(t)] = [1 - \hat{\mathbf{v}}(t)\cdot\hat{\mathbf{v}}(t)]\frac{d}{dt}\ln n(\mathbf{x}(t))$$

($\hat{\mathbf{v}}\cdot\nabla = \sum_i [dx^i/dt][\partial/\partial dx^i] = d/dt$ has been used), so if $\hat{\mathbf{v}}\cdot\hat{\mathbf{v}} = 1$ initially, that speed is maintained.

It is easily seen that Snell's law is obtained as a consequence of Eq. (C6). If a particle moves in a medium with constant $n = n_1$ (a straight line trajectory since the force vanishes) and passes through a plane interface beyond which $n = n_2$, it receives an impulse perpendicular to the plane. Thus, from the first of (C6), the component of $n\hat{\mathbf{v}}$ parallel to the plane does not change:

$$n_1\hat{\mathbf{v}}_{1,||} = n_2\hat{\mathbf{v}}_{2,||} \quad \text{or} \quad n_1\sin\theta_1 = n_2\sin\theta_2,$$

where θ is the angle made by $\hat{\mathbf{v}}$ and the normal to the plane

We wish to find the solution of Eq. (C4) when $\hat{\mathbf{v}}(\mathbf{x})$ is the velocity field whose flow lines are described by Eq. (C6). We shall now see that Φ_0 is the least action for this motion. For, consider the principle of minimizing the particular action

$$\mathcal{A}(\mathbf{x}) \equiv \int_{\mathbf{x}_0}^{\mathbf{x}} dt\mathcal{L}(\mathbf{x}(t),\dot{\mathbf{x}}(t)) \equiv \int_{\mathbf{x}_0}^{\mathbf{x}} dt n(\mathbf{x}(t))[\dot{\mathbf{x}}(t)\cdot\dot{\mathbf{x}}(t)]^{1/2} \qquad \text{(C7)}$$

We note for later use that t can be replaced by any function of t without altering the action. The principle of least action gives rise to Lagrange's equation,

$$\frac{d}{dt}\frac{n(\mathbf{x})\mathbf{v}}{[\mathbf{v}\cdot\mathbf{v}]^{1/2}} = [\nabla n(\mathbf{x})][\mathbf{v}\cdot\mathbf{v}]^{1/2}, \qquad \text{(C8)}$$

where $\mathbf{v} = \dot{\mathbf{x}}(t)$. By choosing $t = s$, where s is the distance travelled by the particle, so $ds^2 = d\mathbf{x} \cdot d\mathbf{x}$, the velocity $\mathbf{v} = d\mathbf{x}/ds$ has speed $\mathbf{v} \cdot \mathbf{v} = 1$. Then, Eq. (C8) is identical to the equation of motion Eq. (C6).

Imagine the vector field passing through an initial surface, labeled by coordinate $s = 0$ and proceeding onward. Since each member of the family of subsequent s = constant surfaces is perpendicular to $\hat{\mathbf{v}}$, we have $\nabla s(\mathbf{x}) = C(\mathbf{x})\hat{\mathbf{v}}(\mathbf{x})$, where C is some function. However,

$$\hat{\mathbf{v}} \cdot \nabla s = \sum_i \frac{dx^i}{ds}\frac{\partial}{\partial x^i}s = \frac{ds}{ds} = 1,$$

so $C = 1$ and $\nabla s = \hat{\mathbf{v}}$.

Then, Eq. (C7) may be written:

$$\mathcal{A}_0(\mathbf{x}) \equiv \int_0^{s(\mathbf{x})} ds\mathcal{L}(\mathbf{x}(s), \hat{\mathbf{v}}(s)) = \int_0^{s(\mathbf{x})} dsn(\mathbf{x}(s)), \tag{C9}$$

where it is understood that $\mathbf{x}$, $\hat{\mathbf{v}}$ depend not only upon s, but also on two other coordinates, say ξ, η, laid out upon the constant s surfaces. So, from (C9),

$$\nabla\mathcal{A}_0(\mathbf{x}) = n(\mathbf{x}(s))\nabla s = n(\mathbf{x}(s))\hat{\mathbf{v}}(s). \tag{C10}$$

This is the same as (C4), so $\Phi_0 = \mathcal{A}_0$.

Φ_0 is called the optical path length. A light ray follows the flow line of the fictitious particle we have been considering but, of course, it moves along that path with the speed of light c/n. So, when a light ray moves through the distance ds, that takes time dt=dsn/c. Thus, according to Eq. (C9), the optical path length Φ_0 is just the integrated time that light takes to go from one place to another, multiplied by c. (The "principle of least time," the idea that the actual path light takes between two points is the path which takes the least time, is due to Fermat in 1662.) As a consequence, all rays of light which have the same phase at the surface $s = 0$ and travel to the surface s have the same phase there. The surface of constant s is called a "wave front."

To complete the WKB approximation, we need to find Φ_1. Setting $\Phi_1 = i\Phi_1^I$ in Eq. (C3), with use of (C4), we have that

$$2n\hat{\mathbf{v}} \cdot \Phi_1^I = 2n\frac{d}{ds}\Phi_1^I = \nabla \cdot (n\hat{\mathbf{v}}) = \frac{d}{ds}n + n\nabla \cdot \hat{\mathbf{v}}.$$

From the second and fourth terms of this equation,

$$\Phi_1^I(\mathbf{x}) = \ln n^{1/2}(\mathbf{x}) + \frac{1}{2}\int_0^{s(\mathbf{x})} ds\nabla \cdot \hat{\mathbf{v}}(\mathbf{x}(s)). \tag{C11}$$

Thus, from Eqs.(C9),(C11), we obtain the WKB approximate solution of the wave equation:

$$U(\mathbf{x}) = n^{-1/2}(\mathbf{x})e^{-\frac{1}{2}\int_0^{s(\mathbf{x})} ds\nabla\cdot\hat{\mathbf{v}}(\mathbf{x}(s))}e^{ik\int_0^{s(\mathbf{x})} dsn(\mathbf{x}(s))} \tag{C12}$$

Eq. (C12) is what shall be used in what follows. It requires specifying an initial surface for $s = 0$. From this, at any point $\mathbf{x}_0$ on this surface, the initial veocity field $\hat{\mathbf{v}}(\mathbf{x}_0)$ can be determined, since it is perpendicular to the surface and of unit length. Then, one can solve the dynamical equation (C6) to obtain the velocity field elsewhere, and find the specific trajectories $\mathbf{x}(s, \mathbf{x}_0)$. This allows calculation of the integrals in (C12), resulting in the WKB solution $U(\mathbf{x})$. If $n(\mathbf{x}_0) = 1$, this solution has $U(\mathbf{x}_0) = 1$. If a solution with any other value $U_0(\mathbf{x}_0)$ on the $s = 0$ surface is desired, it is $U_0(\mathbf{x}_0)U(\mathbf{x})$.

The last factor in Eq. (C12) is well known in optics, as the eikonal or ray approximation. What has been shown here is that it is justified as the WKB approximate solution of the wave equation.

For our problem, of a point source at $\mathbf{x} = 0$, we choose the $s = 0$ surface to be spherical, of infinitesimal radius, centered at $\mathbf{x} = 0$. Therefore, the initial velocity emanates radially out from $\mathbf{x} = 0$. We assume $n = 1$, for at least a small volume around $\mathbf{x} = 0$. Then, by Eq. (C6), $d\mathbf{v}/dt = 0$ so $\hat{\mathbf{v}}(\mathbf{x}) = \mathbf{r}/r = \hat{\mathbf{r}}$, where $\mathbf{r}$ is the radial vector. Since $\nabla \cdot \hat{\mathbf{r}}f(r) = r^{-2}d^2[r^2f(r)]/dr^2$, with $f = 1$ we get $\nabla \cdot \hat{\mathbf{v}} = 2/r$. The distance travelled from $s = 0$, along the velocity field, is $s = r$. Putting this into Eq. (C12) gives, in this volume,

$$U(\mathbf{x}) = \frac{1}{r}e^{ikr}. \tag{C13}$$

This satisfies the wave equation Eq. (C1), with a unit point source at the origin.

APPENDIX D: REFLECTION FROM LENSES AND MIRRORS

This subsection is a diversion from our main argument, and may be skipped. It is here for logical completeness, and to make some pedagogical points.

In applications to optical systems, light, initially in vacuum, encounters an abrupt change of index of refraction, in the form of lenses or mirrors. The latter may be accommodated by setting $n = -\infty$ in the volume of the mirror. This may be understood from the quantum theory analogy, where $n = -\infty$ turns the potential well into an infinite potential barrier.

How good is the WKB approximation in this case? For completely empty space, Eq. (C13) is the exact solution of Eq. (C1). However, in non-empty space, there is an obvious failure when two rays cross. In that case, from (C4), $\nabla\Phi_0 \sim \hat{\mathbf{v}}$ would then have two possible values, which is impossible.

1. Mirrors

This is what occurs at the surface of a mirror. For example, for a plane mirror at $z = 0$, and an incoming plane wave of wave number k and direction $\hat{\mathbf{v}} = \hat{\mathbf{j}}a + \hat{\mathbf{k}}b$, we know the solution of the wave equation. It is the sum

of incident and reflected waves which vanishes at $z = 0$:

$$\begin{aligned} U &\sim e^{ik(ay+bz)} - e^{ik(ay-bz)} \sim e^{ikay} e^{\ln \sin kbz} \\ &\sim e^{ikay + \ln(kbz) - (kbz)^2/6 + \ldots}, \end{aligned}$$

Obviously, the wave amplitude can no longer be described by a single term of the form $\exp ik\Phi$, where Φ can be expanded in inverse powers of k.

But, the resolution of this difficulty is apparent from the example. It is to find the solution of the wave equation as the *sum* of WKB terms. After all, the wave equation is linear, so a sum of solutions is a solution.

For the case of a finite sized mirror, rays which don't hit the mirror can continue on their merry way. Those incident rays $U_{\rm i}$ which do hit the mirror surface are used to obtain the reflected solution $U_{\rm r}$. That is, the solution is $U = U_{\rm i} + U_{\rm r}$, where $U_{\rm r}$ is to be constructed. This requires, on the mirror surface, knowing $U_{\rm r}$ and the direction of the outgoing vector field $\hat{\mathbf{v}}_{\rm r}$. These are obtained by requiring the wave equation to be satisfied through the mirror surface, that is, by requiring $U = 0$ and $\nabla_{||} U = 0$ on the mirror surface.

The first condition implies $U_{\rm r} = -U_{\rm i}$ at the surface. The second condition implies

$$\nabla_{||} U = ik[U_{\rm i} \nabla_{||} \Phi_{\rm i} + U_{\rm r} \nabla_{||} \Phi_{\rm r}] = ikU_{\rm i}[\hat{\mathbf{v}}_{{\rm i}||} - \hat{\mathbf{v}}_{{\rm r}||}] = 0$$

(the last step uses the WKB approximation of Φ_0 replacing Φ, and (C4)). Thus, $\hat{\mathbf{v}}_{{\rm r}||} = \hat{\mathbf{v}}_{{\rm i}||}$. Since $\hat{\mathbf{v}}_{\rm r}$ is a unit vector, this implies $\hat{\mathbf{v}}_{{\rm r}\perp} = -\hat{\mathbf{v}}_{{\rm i}\perp}$. Thus, the law of reflection is obtained. This completes the specification of the initial conditions for the reflected WKB solution, which can now be constructed using (C12)

The reflected part of U is non-zero within the volume enclosed by the mirror surface and the outermost reflected rays, and abruptly jumps to zero outside. More will be said about this discontinuity at the end of this Appendix.

2. Lenses

A similar situation prevails for a finite sized lens. The WKB approximation's rays travel past or through the lens and beyond. However, even before the WKB solution breaks down (where the focused rays which emerge from the lens eventually cross), something is missing. Light reflects from glass. The single WKB solution does not take that into account.

Accordingly, another solution $U_{\rm r}$ to represent the reflected light must be added. We shall only discuss how to find the light which reflects from the entrance lens surface: light also reflects from the exit lens surface, and that light reflects off the entrance surface, etc: using the method of our discussion, one could do these other calculations if one chose.

Reflected energy means decreased refracted energy. We shall take the refracted solution to be $U_{\rm R} = AU_{\rm i}$ within the lens, where $0 < A < 1$ is real. Likewise, within the lens, take $\hat{\mathbf{v}}_{\rm R}$ to be identical to $\hat{\mathbf{v}}$, the (refracted) continuation through the lens of the incident solution. So, we just need to determine A to complete the specification of $U_{\rm R}$. In addition, we must find the initial conditions for $U_{\rm r}$ and $\hat{\mathbf{v}}_{\rm r}$ on the surface, to construct $U_{\rm r}$ elsewhere.

As with the case of a mirror, this information is supplied by requiring the wave equation be satisfied. That is, U and ∇U must be continuous across the lens surface. The first condition implies $U_{\rm i} + U_{\rm r} = U_{\rm R}$ on the surface, i.e., $U_r = -(1 - A)U_{\rm i}$. The second condition is $U_{\rm i} ik\nabla\Phi_{\rm i} + U_{\rm r} ik\nabla\Phi_{\rm r} = U_{\rm R} ik\nabla\Phi_{\rm R}$ on the surface. With use of Eq. (C4), this gives

$$\hat{\mathbf{v}}_{\rm r} = \frac{\hat{\mathbf{v}}_{\rm i} - An\hat{\mathbf{v}}_{\rm R}}{1 - A}. \tag{D1}$$

We can find A by taking the scalar product of (D1) with itself. Since $\hat{\mathbf{v}}_{\rm i} \cdot \hat{\mathbf{v}}_{\rm R} = \cos(\theta_{\rm i} - \theta_{\rm R})$, where the angles are those the incident and refracted rays make with the normal to the surface at a point of the surface, we obtain

$$A = \frac{2}{n^2 - 1}[n \cos(\theta_{\rm i} - \theta_{\rm R}) - 1]. \tag{D2}$$

Putting (D2) into (D1) and taking (D1)'s scalar product with a unit vector parallel to the surface and in the plane of $\hat{\mathbf{v}}_{\rm i}$ and $\hat{\mathbf{v}}_{\rm R}$, results in the law of reflection:

$$\sin\theta_{\rm r} = \frac{\sin\theta_{\rm i} - An\sin\theta_{\rm R}}{1 - A} = \sin\theta_{\rm i}$$

(using $\sin\theta_{\rm i} = n\sin\theta_{\rm R}$, Snell's law). This completes the specification of the initial conditions for the reflected and refracted WKB solutions from the entrance surface of the lens.

For normally incident light, $\theta_{\rm i} = \theta_{\rm R}$, it follows from (D2) that $A = 2/(n + 1)$: this is also the result given by electromagnetic theory. Therefore, for $n = 3/2$, the magnitude of the reflected light intensity is $(1 - A)^2 = 1/25$. The intensity of reflected light at any other angle is less than this 4% value. Because it is so small, it shall be unnecessary to consider this reflected solution in subsequent sections.

The purpose of this discussion was not just to show that reflected light can be neglected in considering refracted light through a lens. It was also to emphasize that the sum of WKB solutions is a solution, and that it can be accurate to use the WKB solution up to a surface, and then consider another WKB solution as a continuation of it. Both ideas shall be needed, because something still is missing.

If the lens is backed by an screen containing an aperture (the exit pupil), $U_{\rm R}$ beyond the lens abruptly jumps from its WKB value to zero at the edge of the "ray bundle." Since $\nabla^2 U_{\rm R}$ is singular there, this cannot satisfy the wave equation. There has to be a modified $U_{\rm R}$ which smooths out this abrupt transition. This brings us to considerations of diffraction.

APPENDIX E: HUYGHENS-FRAUNHOFER-KIRCHHOFF APPROXIMATION

We shall use the WKB (eikonal) approximation up to the exit surface of the lens, but construct a solution of the wave equation which is better than the WKB expression in the space beyond the lens. This requires input of just the WKB values for U and ∇U values at the exit surface of the lens. The solution beyond the lens is provided by Green's theorem:

$$U(\mathbf{x}) = \frac{1}{4\pi}\int_{\Sigma_0} d\mathbf{\Sigma_0}\cdot[U(\mathbf{x_0})\nabla_0 G(\mathbf{x},\mathbf{x}_0) - G(\mathbf{x},\mathbf{x}_0)\nabla_0 U(\mathbf{x_0})]. \tag{E1}$$

In what follows, it is helpful to use symbols illustrated in Fig. (19), although the details associated with this particular lens are not needed. In Eq. (E1), $\mathbf{x} = \mathbf{r}$ is the observation point beyond the lens. $\mathbf{x}_0 = -L\hat{\mathbf{k}} + \mathbf{r}_1$ represents a point on Σ_0, the exit surface of the lens. (It also includes the screen, but on it U and ∇U are taken to vanish). $d\mathbf{\Sigma}_0 = d\Sigma_0\hat{n}$ is the surface element of the lens, whose normal $\hat{n}$ points radially outward from it. $G(\mathbf{x},\mathbf{x}_0)$ is the Green's function for the vacuum, given by Eq. (C13) with $r = |\mathbf{x}-\mathbf{x}_0| \equiv D$. It satisfies the wave equation with a point source (Eq. (C1), with $n = 1$ and with the argument of the delta function changed to $\mathbf{D}$). Thus, Eq. (E1) describes U as a continuous sum (integral) of solutions of the wave equation so, of course, it is a solution of the wave equation.

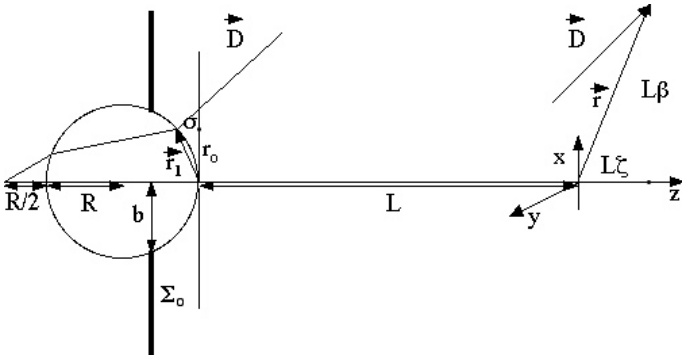

FIG. 19: Ray geometry for a ball lens

Eq. (E1) can be simplified. From (C13),

$$\nabla_0 G = -G\hat{\mathbf{D}}[ik - D^{-1}] \approx -G\hat{\mathbf{D}}ik,$$

where the approximation is valid for $D >> \lambda$. From (C12),

$$\nabla_0 U(\mathbf{x}_0) = ikG(\mathbf{x}_0)\nabla_0\Phi(\mathbf{x}_0) \approx ikG(\mathbf{x}_0)\hat{\mathbf{v}}_0,$$

where the approximation replaces Φ by Φ_0 (since Φ_1 is quite constant over the lens exit surface) and uses (C4). Thus, (E1) becomes:

$$U(\mathbf{x}) = \frac{-ik}{4\pi}\int_{\Sigma_0} d\Sigma_0 U(\mathbf{x_0})\frac{1}{D}e^{ikD(\mathbf{x},\mathbf{x}_0)}\hat{n}\cdot[\hat{\mathbf{v}}_0 + \hat{\mathbf{D}}].$$

We are interested in the solution for large L, on the image plane far from the lens. There, D^{-1} varies slowly, and may be taken out of the integral.

As shown at the end of section (B 7), the outgoing ray from the lens surface satisfies is almost parallel to the z-axis (the optic axis), i.e., $\hat{\mathbf{v}}_0 \approx \hat{\mathbf{k}}$. (For a perfect lens, $\hat{\mathbf{v}}_0 = \hat{\mathbf{k}}$ since then the source point is imaged at ∞.) Similarly, $\hat{\mathbf{D}} \approx \hat{\mathbf{k}}$ since the intensity at $\mathbf{x}$ we wish to explore is not very much off-axis. The normal to the exit lens surface is not parallel to $\hat{\mathbf{k}}$, but $d\mathbf{\Sigma_0}\cdot\hat{\mathbf{k}} = d\Sigma_0\hat{n}\cdot\hat{\mathbf{k}} = dA_0$, where dA_0 is the surface element of S_0, the plane tangent to the exit surface of the lens at the point where it intersects the optic axis and perpendicular to the optic axis (the "tangent plane"). Therefore, the surface integral can be converted from being over the exit surface of the lens to being over the tangent plane. With $U(\mathbf{x_0}) \sim \exp ik\Phi_0(\mathbf{x_0})$ given by the WKB approximation, the approximate solution to be evaluated is

$$U(\mathbf{x}) \sim \int_{S_0} dA_0 e^{ik[\Phi_0(\mathbf{x_0}) + |\mathbf{x}-\mathbf{x}_0|]}. \tag{E2}$$

Eq. (E2) is what we need hereafter. Since we are only interested in relative values of $|U(\mathbf{x})|^2$, constant factors may be dropped or chosen at pleasure.

It is worth re-emphasis, that $\Phi_0(\mathbf{x_0})$ in Eq. (E2) is the optical path length (C9), from the source to the exit surface of the lens, at height r_0 above the optic axis. It is *not* the optical path length from the source to the tangent plane whose surface area element is integrated over in Eq. (E2).

APPENDIX F: POINT SPREAD FUNCTION AND CONSEQUENCES

1. The Diffraction Integral

To integrate (E2), we need $D = |\mathbf{x}-\mathbf{x}_0|$. Again, refer to Fig.(19). The origin of the coordinate system is on the optic axis, a large distance L away from the exit surface of the lens. $\mathbf{D}$ makes a small angle β with respect to the optic axis, and its horizontal component extends a small distance ζL beyond the origin. Therefore, the observation point is

$$\mathbf{x} = \mathbf{r} = \hat{\mathbf{i}}L\beta + \hat{\mathbf{k}}L\zeta.$$

The point on the surface of the lens is

$$\mathbf{x}_0 = \hat{\mathbf{i}}r_0\cos\phi + \hat{\mathbf{j}}r_0\sin\phi - \hat{\mathbf{k}}[L+\sigma]$$

where ϕ is the azimuthal angle in the tangent plane and

$$\sigma = R - \sqrt{R^2 - r_0^2} \approx \frac{r_0^2}{2R^2} + \frac{r_0^4}{8R^3}$$

is the "sagitta," the horizontal distance between the surface of the lens and the tangent plane, at height r_0 above the optic axis. With $D = [(\mathbf{x} - \mathbf{x}_0)^2]^{1/2}$, dropping terms of order L^{-1}, we obtain:

$$e^{ikD} = e^{ikL\{1+(1/2)[\beta^2-\zeta+\frac{1}{2}\zeta^2]\}} e^{ik[-\beta r_0 \cos\phi+(-\zeta+1)\sigma]},$$

and (E2) becomes

$$U(\beta) \sim \int_0^b r_0 dr_0 \int_0^{2\pi} d\phi e^{ik[\Phi_0(\mathbf{x_0})-\beta r_0 \cos\phi+(1-\zeta)\sigma]}, \tag{F1}$$

where b is the radius of the exit pupil.

The purpose of section F 4 is to show that the optical path length from the source point to the exit surface of the lens at distance r_0 from the optic axis is

$$\Phi_0 = 3.5R - \frac{r_0^2}{2R} - \frac{37R}{216}\Big[\frac{r_0}{R}\Big]^4 = 3.5R - \sigma - \frac{R}{21.6}\Big[\frac{r_0}{R}\Big]^4. \tag{F2}$$

Suppose a ray exits the lens at at distance r_0 from the optic axis in a direction almost parallel to $\hat{\mathbf{k}}$, and travels the distance σ further to the tangent plane. As Eq. (F2) shows, it still has to travel a bit further than that to achieve the same optical path from source to tangent plane as the axial ray ($r_0 = 0$), whose optical path is $(R/2) + n2R = 3.5R$. Thus, the wavefront is slightly converging.

With change of variable to $\rho \equiv r_0/b$ and

$$\bar{b} \equiv b/R, \quad \bar{\sigma}(\rho) \equiv \frac{(\bar{b}\rho)^2}{2} + \frac{(\bar{b}\rho)^4}{8},$$

Eq. (F1) becomes

$$U(\beta) \sim \int_0^1 \rho d\rho \int_0^{2\pi} d\phi e^{-ikR\Big[\rho^4 \frac{\bar{b}^4}{21.6} + \rho\beta\bar{b}\cos\phi + \zeta\bar{\sigma}(\rho)\Big]}. \tag{F3}$$

The integral over ϕ is readily performed:

$$U(\beta) \sim \int_0^1 \rho d\rho e^{-ikR\Big[\rho^4 \frac{\bar{b}^4}{21.6} + \zeta\bar{\sigma}(\rho)\Big]} J_0(kR\rho\beta\bar{b}), \tag{F4}$$

where J_0 is the Bessel function.

We note that if we choose the observation plane to be $\zeta = 0$ and neglect the exponent (a good approximation for sufficiently small exit pupil radius b), the result can be integrated using the identity $d[xJ_1(cx)]/dx = cxJ_0(x)$, with resulting intensity

$$I_{\rm A}(kb\beta) \sim |U(\beta)|^2 \sim \left[\frac{2J_1(kb\beta)}{kb\beta}\right]^2. \tag{F5}$$

$I_{\rm A}(kb\beta)$ is the well known and important Airy point spread function of a circular perfect lens or aperture, discussed in Section III H and illustrated in Fig.11.

The exponent in (F4) is responsible for spherical aberration. In geometrical optics, this is caused by the rays at the outer edge of a lens coming to a focus on the optic axis closer to the lens than the paraxial ray focus. In our calculation, this is represented by the converging wavefront. As a result, as one moves a plane along the optic axis, one sees a circle of light of varying radius. One tries to choose the best effective focal plane, the plane where there is the "circle of least confusion" or the plane where the on-axis intensity is largest. The value of the present discussion is that it gives the intensity of the combined diffraction and spherical aberration, something not given by geometrical optics.

In order to slickly choose the best plane of focus, one needs to introduce a complication, We express the exponent in (F4) in terms of orthogonal Zernike polynomials (designed just for this purpose!), $R_{2n}(\rho) \equiv P_n(2\rho^2 - 1)$, where the P_n are the Legendre polynomials. The first three, which we shall need, are $R_0 = 1$, $R_2 = 2\rho^2 - 1$, $R_4 = 6\rho^4 - 6\rho^2 + 1$. They obey the orthogonality relations $\int_0^1 \rho d\rho R_{2n} R_{2m} = \delta_{nm}(4n+2)^{-1}$. They also obey the neat relation $\int_0^1 \rho d\rho R_{2n}(\rho) J_0(c\rho) = (-1)^n J_{2n+1}(c)/c$.

In terms of these polynomials, (F4) becomes

$$U(\beta) \;=\; \sim \int_0^1 \rho d\rho e^{-ikR\Big[R_4\bar{b}^4\left(\frac{1}{130}+\frac{\zeta}{48}\right)+R_2\bar{b}^2\frac{1}{4}(\zeta+\frac{6\bar{b}^2}{65})\Big]} \times J_0(kR\rho\beta\bar{b}). \tag{F6}$$

(In obtaining (F6), we have set $\zeta[1 + \bar{b}^2/4] \approx \zeta$, a few percent error).

It is apparent that one can choose ζ so that the R_2 term vanishes. Moreover, this is essentially the plane of largest intensity on the optic axis ($\beta = 0$). Upon setting $J_0(0) = 1$ in Eq.(F6), expanding the exponential to second order, and using the orthogonality relations, the result is

$$|U(0)|^2 = \Big|2\int_0^1 \rho d\rho e^{-i[pR_4+qR_2]}\Big|^2 = 1 - \frac{p^2}{5} - \frac{q^2}{3}.$$

Since $dp^2/d\zeta << dq^2/d\zeta$ the intensity is maximized to a high degree of accuracy by setting $\zeta = -6\bar{b}^2/65$ and thus making the q^2 term vanish. This best focus plane is closer to the lens, consistent with the spherical aberration effect. When this value is put into the first term, it becomes $R_4\bar{b}^4[1 + \bar{b}^2/4]/130 \approx R_4\bar{b}^4/130$, using the same approximation already made.

2. The Point Spread Function

Defining

$$\bar{\beta} \equiv kR\beta\bar{b}, \quad \bar{B} \equiv kR\bar{b}^4/130, \tag{F7}$$

we arrive finally at the amplitude which combines diffraction and spherical aberration,

$$U(\bar{\beta}) \sim \sqrt{2}\int_0^1 \rho d\rho e^{i\bar{B}R_4(\rho)} J_0(\rho\bar{\beta}). \tag{F8}$$

Fig. (20) contains plots of $I(r)$, the intensity of light due to a point source imaged by the lens on the image plane, i.e., the point spread function,

$$I(r) = \sqrt{\bar{B}}|U(kbr/f)|^2, \tag{F9}$$

for various exit pupil radii b, for our 1mm diameter lens. r is the distance from the optic axis. (F7) has been used (with $\beta = r/f$, as discussed at the end of the introduction to this Appendix), with $\lambda = .55\mu$m, and $f = (3/2)R = .75$mm.

The reason for the factor $\sqrt{2}$ in Eq. (F8) and the factor $\sqrt{\bar{B}}$ in Eq. (F9) are as follows.

Using the Fourier-Bessel relation

$$\int_0^\infty \bar{\beta} d\bar{\beta} J_0(\rho\bar{\beta}) J_0(\rho'\bar{\beta}) = \rho^{-1}\delta(\rho - \rho'),$$

because of the factor $\sqrt{2}$ in (F8), an integral proportional to the total energy emerging from the lens (proportional to the intensity integrated over the area of the image plane) is conveniently normalized to 1:

$$\int_0^\infty \bar{\beta} d\bar{\beta} |U(\bar{\beta})|^2 = 2\int_0^1 \rho d\rho = 1$$

(the maximum $\bar{\beta}$ allowed by our limitation $\sin\beta \approx \beta$, is large enough to allow the integral to be extended to ∞ with good accuracy).

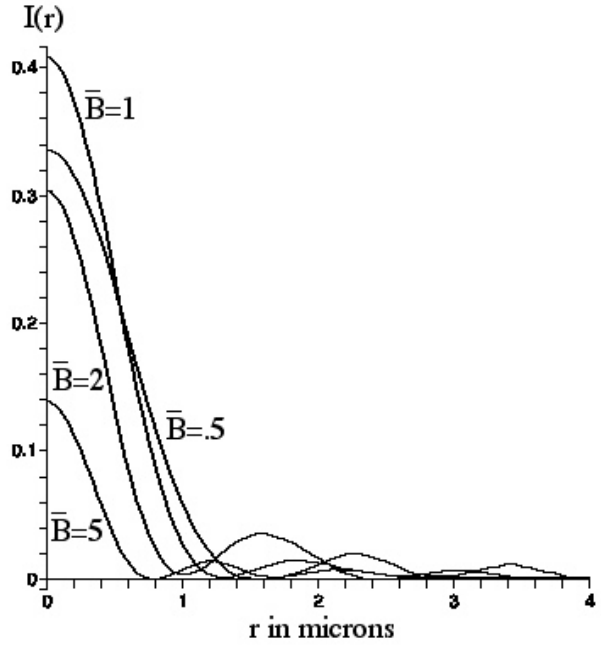

FIG. 20: Point spread functions $I(r)$ for $b = .16\mu$m ($\bar{B} = .5$), $b = .19\mu$m ($\bar{B} = 1$), $b = .23\mu$m ($\bar{B} = 2$), $b = .29\mu$m ($\bar{B} = 5$).

However, the total energy emerging from the lens should be proportional to the exit pupil area, $\sim b^2$. Since $\sqrt{\bar{B}} \sim b^2$ (see (F7)), this factor is included in the definition (F9) of the point spread function.

It is useful to have an approximate analytic expression for the point spread function, at least for small values of $\bar{B}$. Expansion of (F8) to second order in $\bar{B}$ gives

$$U(\bar{\beta}) \sim \sqrt{2}\int_0^1 \rho d\rho [1 - i\bar{B}R_4 - \frac{1}{2}(\bar{B}R_4)^2] J_0(\rho\bar{\beta}).$$

A little algebra shows that $R_4^2 = (18/35)R_8 + (2/7)R_4 + (1/5)$ so, dropping the R_8 term,

$$U(\bar{\beta}) \sim \sqrt{2}\left\{\left[1 - \frac{\bar{B}^2}{10}\right]\frac{J_1(\bar{\beta})}{\bar{\beta}} - \frac{\bar{B}^2}{7}\frac{J_5(\bar{\beta})}{\bar{\beta}} - i\bar{B}\frac{J_5(\bar{\beta})}{\bar{\beta}}\right\}.$$

Thus, to second order in $\bar{B}$ (neglecting the small $\sim J_1 J_5$ term), the point spread function is, approximately,

$$I(r)/\sqrt{\bar{B}} \sim \frac{1}{2}\left(\frac{2J_1(\bar{\beta})}{\bar{\beta}}\right)^2\left(1 - \frac{\bar{B}^2}{5}\right) + \frac{\bar{B}^2}{2}\left(\frac{2J_5(\bar{\beta})}{\bar{\beta}}\right)^2 \tag{F10}$$

The normalized total energy is still 1 in this approximation:

$$\int_0^\infty \bar{\beta} d\bar{\beta} I(r)/\sqrt{\bar{B}} = \frac{1}{2}\left\{2\left(1 - \frac{\bar{B}^2}{5}\right) + \bar{B}^2\frac{2}{5}\right\} = 1.$$

Eq. (F10) shows that, for small $\bar{B}$ (small b), the point spread function is essentially the Airy function. As $\bar{B}$ grows, the amplitude of the Airy function decreases, with concomitant growth of a fifth order Bessel function contribution which vanishes for $r = 0$, and whose oscillations are displaced to larger r values than the oscillations of the Airy function.

Eq. (F10) has good accuracy for $\bar{B} = 1$: it is $\approx 2.5\%$ low at $\bar{\beta} = 0$, improving to negligible inaccuracy at $\bar{\beta} = 1$ and beyond. (For $\bar{B} = 1.3$ and 1.5, these percentages are 6% and 12% at $\bar{\beta} = 0$, with negligible inaccuracy beyond $\bar{\beta} = 2.5$, 3 respectively.)

3. The Exit Pupil

These results may be used to choose the optimum exit pupil radius b for our lens.

As can be seen from Fig. (20), as b is increased from a small value, the intensity on the optic axis $r = 0$ initially grows, because the exit pupil is allowing more light to exit the lens. For small values of b ($\bar{B} < 1$), the intensity distribution (F10) is essentially $\sim I_{\rm A}(\bar{\beta})$, the Airy function, variously given in (F5) or Eq. (3), and illustrated in Fig.11 and the $\bar{B} = .5$ curve in Fig. (20). The Airy radius for our lens is, from Eq. (4),

$$r_A = .61\frac{\lambda}{b/f} = \frac{.50}{\bar{b}}\mu\text{m}. \tag{F11}$$

b/f is called the lens "numerical aperture."

For the Airy function, ≈84% of the light energy lies within the Airy disc. But, as b increases further, spherical aberration kicks in, the intensity on the optic axis starts to diminish and a greater percentage of light energy appears beyond r_A. For the values b =.16, .19, .23 and .29μm, used in Fig. (20), Eq. (F11) gives r_A =1.56, 1.3, 1.1 and .86μm respectively. The first two curves appear to reach 0 at these values of r_A, whereas the last two curves deviate somewhat.

One wants b to be as large as possible, to decrease r_A and thus increase resolution, and to let as much light as possible exit the lens. However, as b grows, spherical aberration grows, as seen in Fig. (20): $I(r)$ decreases for $r < r_A$ and more light appears for $r > r_A$, so resolution decreases. A rule of thumb, called the Strehl criterion, suggests increasing b until the maximum intensity, the intensity on the optic axis $I(0)$, is reduced to 80% of the maximum intensity on the optic axis without any spherical aberration. Then, the image is considered still *diffraction limited*, i.e., the image is still essentially the Airy disc. From (F9), we see $I(0) \approx 1/2[1-(\bar{B})^2/5]$. Thus, the Strehl criterion implies $\bar{B} = 1$. It does seem from Fig. (20) that this is an optimal choice.

For $\bar{B} = 1$, the wavefront (the surface of constant phase), for a ray exiting the lens a distance $\equiv \rho b$ above the optic axis, goes beyond the tangent plane by the distance $R\rho^4\bar{b}^4/21.6 = \rho^4 6\bar{B}/k \approx \lambda\rho^4$, according to Eq.(F4). Thus, the wavefront at the edge of the exit pupil, $\rho = 1$, is about a wavelength in front of the tangent plane. For $\bar{B} > 1$, images are available[85] showing appreciable spherical aberration, for path differences from $1.4\lambda\rho^4$ to $17.5\lambda\rho^4$.

4. Optical Path Calculation

The unfinished business remains of showing that the optical path length, of a ray emerging from the source at the lens focal length, passing through the lens and up to its exit surface, is given by Eq. (F2). For the following discussion, refer to Fig. (21). The focal length of the lens, according to Eq. (4), is $f = nR/2(n-1) = 1.5R$ for $n = 1.5$. Thus, the point source at a is at a distance $R/2$ to the left of the lens surface. We shall follow a ray which leaves the source at angle α to the optic axis.

A simplifying feature, which occurs only for $n = 1.5$, is that the angle of refraction cde also happens to be α. That can be seen as follows. The angle of incidence θ and the angle of refraction θ' are related by Snell's law, $\sin\theta = n\sin\theta'$. By the law of sines applied to the triangle adc, $\sin\alpha/R = \sin(\pi-\theta)/f$, or $\sin\theta = (f/R)\sin\alpha$. This is the same as Snell's law provided $f = nR$, which is only true for n=1.5.

The axial ray, $\alpha = 0$, obviously has optical path length $(R/2) + n2R = 3.5R$. For arbitrary α, the optical path length Φ_0 is ad+$n$de or, as can readily be seen from

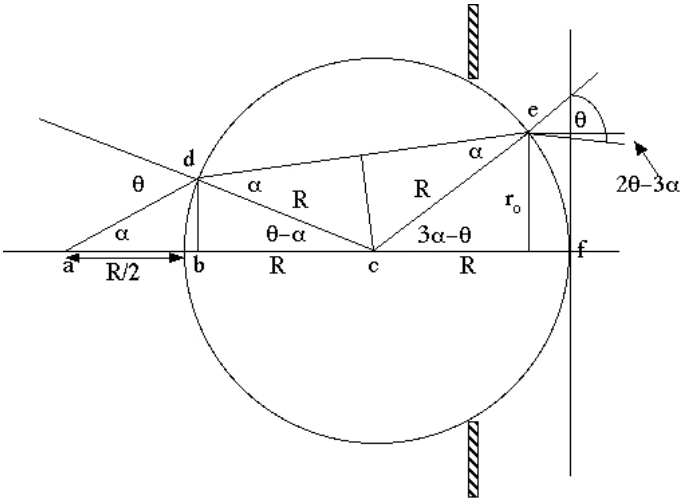

FIG. 21: Optical path length geometry

Fig.(21),

$$\begin{aligned}\Phi_0 &= \frac{R\sin(\theta-\alpha)}{\sin(\alpha)} + (1.5)2R\cos\alpha \\ &= 4.5R\cos\alpha - R\cos\theta \\ &= 4.5R\cos\alpha - R\sqrt{1-(1.5\sin\alpha)^2} \\ &\approx R[3.5-(9/8)\alpha^2+(57/128)\alpha^4+....] \quad \text{(F12)}\end{aligned}$$

The approximation (F12) is good to about 1% at $\alpha = .6 \approx 34°$. We want to express Φ_0 in terms of the distance r_0 between the optic axis and the exit point e. In terms of α, r_0 is

$$\begin{aligned}r_0 &= R\sin(3\alpha-\theta) \\ &= R\sin 3\alpha\sqrt{1-(1.5\sin\alpha)^2} - R1.5\cos 3\alpha\sin\alpha \\ &\approx R[1.5\alpha-(7/8)\alpha^3+...].\end{aligned}$$

This equation can be inverted,

$$\alpha = R^{-1}[(2/3)r_0 + (14/81)r_0^3 + ...]$$

and inserted into Eq. (F12), with the result (F2).

It was mentioned earlier that the angle γ the exiting ray makes with the horizontal is quite small. Here is the argument. From Fig. (21), $\gamma = 2\theta - 3\alpha$. From Snell's law, $\theta - \theta^3/6 \approx (3/2)[\alpha - \alpha^3/6]$, or $\theta \approx (3/2)\alpha + (5/16)\alpha^3$, so $\gamma \approx (5/8)\alpha^3$. Thus, the horizontal distance σ from e to the tangent plane differs from the actual distance $\sigma[1+(1/2)\gamma^2]$ by a negligibly small amount.

APPENDIX G: EXTENDED OBJECT

Having treated the image of a point source, we shall now consider the image of a uniformly illuminated hole of radius a. The hole models a transparent object such as a spherosome or a polystyrene sphere. We shall suppose

that the lens is diffraction limited, i.e., the exit pupil has been chosen so that the image of a point source is the Airy intensity distribution.

But first, we remark that the intensity in this problem is related to that of the complementary case, the image of an opaque disc of radius a. According to *Babinet's principle*, the sum of the light amplitudes for these two cases is the constant light amplitude without either. (This is easy to see from the linearity of the Huyghens-Fresnel-Fraunhofer expression discussed in Appendix B 3). So, where one is light, the other is dark.

Suppose the hole is illuminated with incoherent light, as in ordinary microscopy. If $a < \lambda/4$, the illumination is nonetheless effectively coherent, since any incident plane wave of random phase will have little phase difference across the hole. If $a > \lambda/2$, the illumination may be considered incoherent. This is the case considered here.

1. Incoherent Illumination

If this were geometrical optics, light from each uniformly illuminated point of the object plane would pass through the lens and be focused as an illuminated point on the image plane. The properly scaled image of all these illuminated points would be a uniformly illuminated circle of radius a. We shall call the circumference of this circle the "image circle edge." The new wrinkle is that diffraction surrounds each imaged point with its own Airy disc (assuming that spherical aberration is negligible), so that the image extends beyond the image circle edge. The intensities add so, at a point $\mathbf{r}$ on the image plane, the net intensity is

$$I(r) \sim \frac{1}{\pi}\int_{A_0} dA_0 \left[\frac{J_1(k\tilde{b}|\mathbf{r}-\mathbf{r_0}|)}{|\mathbf{r}-\mathbf{r_0}|}\right]^2, \qquad \text{(G1)}$$

where A_0 is the area of the image circle, and $\tilde{b} \equiv b/f$ is called the numerical aperture.

For $a >> r_A$, where r_A is the Airy radius, the intensity at the center point of the image circle is, by (G1),

$$I(0) \sim \frac{1}{\pi}\int_0^a r_0 dr_0 \int_0^{2\pi} d\phi \left[\frac{J_1(k\tilde{b}r_0)}{r_0}\right]^2 \approx 1.$$

In this equation, the limit a has been extended to ∞ with no appreciable error, since the major contribution is from Airy discs centered within distance r_A of the origin.

As the point of interest moves off center, the intensity remains essentially constant, until at a distance $\approx a - r_A$ from the center, a distance r_A from the image circle edge. Then I starts to decrease, reaching the value $\approx .5$ at the edge. This is because, at the edge, ≈half the Airy discs contribute intensity, compared to the discs which contribute intensity at a point well inside the image circle.

Now, we turn to quantitative analysis of the general case, with no restriction of the relative sizes of a and r_A. We shall calculate the intensity (G1) outside the image circle, at $r = 0$ which is placed a distance z beyond the image circle edge, i.e., the center of the image circle in this coordinate system is at $r = a + z$. The contributing Airy disc centers lie within the image circle, between radius r_0 ($z \le r_0 \le 2a + z$) and radius $r_0 + dr_0$, along an arc subtending an angle 2ϕ. The hole circumference $(x-a-z)^2 + y^2 = a^2$ cuts this arc at two points. Setting $x = r_0\cos\phi$ and $y = r_0 \sin\phi$ in this expression allows one to find $\cos\phi$. Eq. (G1) becomes

$$I_{\rm out}(z) \sim \frac{2}{\pi}\int_z^{2a+z} dr_0 \cos^{-1}\left[\frac{r_0^2 + z^2 + 2az}{2r_0(a+z)}\right]\frac{J_1^2(k\tilde{b}r_0)}{r_0} \qquad \text{(G2)}$$

For completeness, we put here the comparable expression for the intensity inside the image circle. Again, we calculate the intensity (G1) at $r = 0$, where this new coordinate system origin is a distance z away from the center of the image circle. There are two contributions, one from a circular area of radius $a - z$, the other from the rest of the disc ($a - z \le r_0 \le a + z$):

$$I_{\rm in}(z) \sim 2\int_0^{a-z} dr_0 \frac{J_1^2(k\tilde{b}r_0)}{r_0} + \frac{2}{\pi}\int_{a-z}^{a+z} dr_0 \cos^{-1}\left[\frac{r_0^2 + z^2 - a^2}{2r_0 z}\right]\frac{J_1^2(k\tilde{b}r_0)}{r_0}. \qquad \text{(G3)}$$

For large a, (G2) becomes

$$I_{\rm out}(z) \approx \frac{2}{\pi}\int_z^{\infty} dr_0 \cos^{-1}\left[\frac{z}{r_0}\right]\frac{J_1^2(k\tilde{b}r_0)}{r_0}$$

This is a function of $k\tilde{b}z = 3.83(z/r_A)$. Numerical evaluation shows $I_{\rm out}(z)$ drops from .5 at $z = 0$ to $\approx .05$ at $z = r_A$. While it is somewhat subjective, this suggests that we take the perceived edge of the image of the hole to be located where the intensity is 5% of its maximum value at the center of the image circle. Thus, diffraction increases the radius of a large hole from a to $R \approx a + r_A$.

By changing the variable of integration in (G2) to r_0/a, one sees that the intensity is a function of two variables, z/a and $k\tilde{b}a/3.83 = a/r_A$. For each value of a/r_A, one can numerically solve Eq. (G2) for the value of z/a for which $I(z) = .05I(0)$. This is the ratio R/a, where R is defined as the radius of the image. A graph of R/r_A vs a/r_A is given in Fig. 12, and is discussed in section III H.

[1] P. W. van der Pas, Scientiarum Historia **13**, 127 (1971): see [68] for a more detailed discussion.

[2] A transcript of an interesting historical talk about

the Lewis and Clark expedition and its genesis, by Robert S Cox, given at Monticello in 2004, may be found at http://www.monticello.org/streaming /speakers/transcripts/cox.html

[3] *Original Journals of the Lewis and Clark Expedition, 1804-1806* (Dodd, Mead and Company, New York, 1905), edited by R. G. Thwaites, Volume 5, p.95.

[4] A wealth of material on the Lewis and Clark expedition and related topics appears at http://www.lewis-clark.org/. For a discussion of Clarkia pulchella, a picture of the plant, and Pursh's drawing of it which appeared in his *Flora*, click on "Natural History," then "Plants," then "Clarkia." It is also interesting to read here about the lives (and tragic deaths of the first three) of Lewis (see also http://www.prairieghosts.com/meriwet.html), Pursh (see also J. Ewan, Proc. Amer. Phil. Soc, **96** # 5, 599 (1952)), available at Googlebooks), Douglas (see also http://www.coffeetimes.com/daviddouglas.htm) and Barton, all by the American botanist J. Reveal.

[5] J. Loudon, *The Ladies Flower Garden of Ornamental Annuals* (W. Smith, London 1842), pp. 56-57 and her beautiful illustration of Clarkia plants between these two pages. It may be viewed at http://books.google.com/. A biography of Jane Loudon may be found at http://www.shigitatsu.com/LOUDON%201.htm.

[6] D. Douglas, *Journal kept by David Douglas during his travels in North America 1823-1827* (W. Wesley and son, London 1914), W. Wilks and H. R. Hutchinson eds. This is a marvelous first-hand adventure story. It can be read or downloaded at the Washington State historic site, http://www.secstate.wa.gov/history/publications.aspx (click on Exploration and Early Travel).

[7] Ibid, p. 57.

[8] Ibid, pp. 130-131.

[9] Ibid, p. 146.

[10] We are indebted to Bronwen Quarry of the Hudson's Bay Company archives for furnishing information about the dates of travel and fate of the William and Ann.

[11] Ibid, pp. 71-72.

[12] D. J. Mabberley, *Jupiter Botanicus: Robert Brown of the British Museum* (J. Cramer, Braunschweig 1985). The biographical details given in this paper are almost exclusively from this authoritative source.

[13] Wikipedia contains a short biography of Robert Brown, as does the Australian dictionary of Biography, http://www.adb.online.anu.edu.au/biogs/A010149b.htm, each with pictures of Brown, old and young respectively. See also http://www.answers.com/topic/robert-brown.

[14] B. J. Ford, http://www.brianjford.com/wbbrowna.htm. This web site also contains a photograph of the Bancks-made Linnean Society microscope of Brown's, as well as a comparison of a view with a single lens and a compound microscope of the time, and a short video of Brownian motion of milk fat droplets.

[15] http://www.microscopy-uk.org.uk/dww/home /hombrown.htm also has a video of milk fat droplets undergoing Brownian motion, of sizes .5 to 3μm, with tips on how to duplicate the observation. It incorrectly states: "... he noticed the motion in tiny particles suspended within the medium of living pollen grains." although correctly adding "Some texbooks, even to university level, incorrectly state that he observed the movement of the pollen grains themselves. Most pollen grains are too large to exhibit noticeable Brownian motion."

[16] Robert M. Mazo, *Brownian Motion: Fluctuations, Dynamics and Applications* (Clarendon Press, Oxford 2002). The first few pages, available at google-books, http://books.google.com/, and also at Amazon, http://www.amazon.com/, contains a brief treatment of the first two sections of this paper. See also Edward Nelson, *Dynamical Theories of Brownian Motion* (Princeton University Press, Princeton 1967), which is available at http://www.math.princeton.edu/ nelson/books/bmotion.pdf, Chapter 2. Both are excellent texts on "mathematical" Brownian motion.

[17] A biography of John Lindley is available at the orchid information web site http://www.orchids.co.in/: select orchidolologists.

[18] The Horticultural Society garden in Chiswick was part of the 655 acre estate of the lessee, William Spencer Cavendish (1790-1858), the 6th Duke of Devonshire, with a gate to the garden installed for the Duke's use. The physicist Henry Cavendish (1731-1810) was related, a grandson of the 2nd Duke. What remains of this estate, Chiswick House on 68 acres, a fine example of Palladian architecture, is being restored and can be visited (http://www.chgt.org.uk). More of the acreage exists as a Chiswick public park, Dukes Meadows (http://www.dukesmeadowstrust.org/). However, the Horticultural Society garden is no more, replaced by city streets.

[19] We are indebted to David Mabberley for "strongly" suggesting that the slips catalog be looked into, and to Armando Mendez, of the Botany Library of the Natural History Museum, for finding this sheet and mailing us a copy.

[20] We are indebted to Brent Elliot, Historian of the Royal Horticultural Society, for this information. The society does not have any surviving plant receipt books for the garden at Chiswick until the 1840s, so one cannot track Clarkia pulchella into or out of the garden. Lindley was in overall supervision of the gardens, with Donald Munro as head gardener, and a staff of under-gardeners. It was common for botanists to share plants of interest.

[21] The complete entries for both dates are reproduced in J. Ramsbottom, Journ. of Bot. **70** 13, (1932).

[22] E. Small, I. J. Bassett, C. W. Crompton, and H. Lewis, *Pollen Phylogeny in Clarkia*, Taxon **20**, 739 (1971) contains detailed dimensional measurements on many species of Clarkia, including pulchella.

[23] R. Brown, Edinburgh New Philos. Journ. **5** 358, (1828) and Philos. Mag. **4** 161, (1828). This, and the addendum published a year later, Edinburgh Journ. Sci **1** 314, (1829), can be downloaded from the New York Botanical Gardens, at sciweb.nybg.org/science2/pdfs/dws/Brownian.pdf.

[24] B. J. Ford, *Single Lens: the Story of the Simple Microscope* (Harper and Row, New York 1985), pp. 152-153.

[25] B. J. Ford, Microscopy **34** 406, (1982); The Linnean **1** 12, (1985). These describe the loving restoration of the Linnean Society microscope, with the first paper giving quantitative measurements on the lenses. See also B. J. Ford, Infocus **15**, 18 (2009).

[36] Mabberley, Ibid, p. 389.

[27] This is a translation from the French. The original appears in Mabberley, Ibid, pp. 270-271.

[28] H. Loncke, "Making a von Leeuwenhoek microscope

lens," Microscope **138** (April, 2007): this is an online article available at http://www.microscopy-uk.org.uk. Select the Library/Issue Archive.

[29] J. J. Lister, Phil. Trans. Roy. Soc. London, **120** 187, (1830).

[30] W. A. Newman in *History of Carcinology* (CRC Press, 1993), F. Truesdale, ed., p. 357, available at Googlebooks.

[31] D. Layton, Journ. Chem. Ed. **42**, 367 (1965).

[32] A casual on–line search turns up many examples. J. Bernstein Am. Jour. Phys. **74**, 863 (2006), in a fine, authoritative assessment of Einstein's 1905 Brownian motion paper and its impact, nonetheless writes on p.85, about Brown: "He noticed that if pollen grains of a few ten-thousands of a centimeter were suspended in water, they executed an incessant jigging motion." The size is right, but it is not the Clarkia pollen size; Einstein year website, http://www.einsteinyear.org/facts: "In 1827 the biologist Robert Brown noticed that if you looked at pollen grains in water through a microscope, the pollen jiggles about."; Announcement of Gauss Prize (2006) for Kiyoshi Itô, http://www.mathunion.org/Prizes/Gauss/index.html. "In Itô's case, this way begins with a look into a microscope showing pollen grains or dust particles in water moving around in an erratic way."; T. Spencer, power point lecture "Random Walk from Einstein to the Present" at the educational arm of the Institute for Advanced Study at Princeton, http://pcmi.ias.edu/, type in Brownian motion: "Around 1827 Brown made a systematic study of the swarming motion of microscopic particles of pollen."; Wikipedia Dictionary, http://en.wiktionary.org/wiki/Brownian, "1. Pertaining to botanist Robert Brown (1773-1858), who investigated the movement of pollen suspended in water."; http://www.wisegeek.com/what-is-brownian-motion.htm, "As a botanist, Brown first observed the effect in pollen floating in water, where it is visible with the naked eye." ; Univ. of St. Andrews, School of Mathematics and Statistics, http://www-groups.dcs.st-and.ac.uk/ history/Biographies/Ito.html, "Brown, a botanist, discovered the motion of pollen particles in water."; http://physicsworld.com/cws/article/print/21146, "Most of us probably remember hearing about Brownian motion in high school, when we are taught that pollen grains jiggle around randomly in water due the impacts of millions of invisible molecules."; http://www.math.utah.edu/ carlson/teaching/java/prob/brownianmotion/1/, "In 1827 the English botanist Robert Brown noticed that pollen grains suspended in water jiggled about under the lens of the microscope, following a zigzag path like the one pictured below."

[33] Born and E. Wolf, *Principles of Optics* (Pergamon, Oxford 1983), sixth (corrected) edition, p. 234.

[34] B. J.Ford, The Microscope **40**, 235 (1992) verified that Brown could have seen motion with his Linnean x170 lens, writing: "The Clarkia pollen was obtained from anthers of C. pulchella at the Botanical Garden at Cambridge University, and pollen specimens from other species within the Oenotheraceae were also utilized. Exactly as Brown recorded, the experiments were carried out in the month of June and the pollen grains were mounted in water after removal from pre-dehiscent anthers. ... The phenomenon of Brownian movement was well resolved by the original microscope lens. Within the pollen grains, ceaseless movement could be observed." However, while the author saw the contents of the pollen, he did not see them undergoing Brownian motion, as this appears to suggest. Rather, with this lens, he observed the Brownian motion of similarly sized milk fat droplets (private communication from B. J. Ford). Presumably, what was meant is that "ceaseless movement *could have been* observed" with that lens. Perhaps this led to the erroneous statement in an article reporting on this work, Science News **142** (Aug. 15), 109 (1992): "Each grain contains a thick liquid ... When Brown looked inside the pollen grains with his microscope, he could see tiny particles, each about 1 micron across, suspended in the liquid and constantly in motion."

[35] At the web site of the Scuola Normale of Pisa, http://gbamici.sns.it/eng/osservazioni, select osservazionibiologiche.htm.

[36] Mabberley, Ibid.

[37] John Lindley, *An Introduction to Botany*, Fourth edition, Volume 1 (Longman, Brown Green and Longmans, London 1848), p. 361, available at the Googlebooks site.

[38] J. Heslop-Harrison, *Pollen: Development and Physiology* (Butterworths, London 1971).

[39] A. Frey-Wyssling, *Die Pflanzliche Zellwand* (Springer-Verlag, Berlin 1959).

[40] Y. Heslop Harrison and K. R. Shivanna, Ann. Bot. **41**, 1233 (1977).

[41] U. Kirsten, M. Beidermann, G. Liebezeit, R. Dawson and L. Bohm , Eur. J. Cell Biol. **19**, 281(1979).

[42] L. L. Hoefert, Am. J. Bot. **56**, 363 (1969).

[43] W. A. Jensen and D. B. Fisher, Planta bf 84,158(1969).

[44] J. Tupy, Biol. Plant. 4, bf 69 (1962).

[45] J. P. Mascarenhas and E. Bell, Biochim. Biophys. Acta.**179**, 199 (1969).

[46] J. P. Mascarenhas, Am. J. Bot. **53**, 563 (1966).

[47] W. G. Rosen, S. R. Gawlik, W. W. Dashek and K. A. Siegesmond, Am. J. Bot. **51**, 61 (1964).

[48] W. W. Dashek and W. G. Rosen, Protoplasma **61**, 192 (1966).

[49] R. G. Stanley and H. F. Linskens, Nature **203** , 542 (1964).

[50] L. Jost, Ber. Deutsch. Bot. Ges. **23**, 504 (1905).

[51] D. E. Bilderback, Environ. Health Perspect. **37**, 95 (1981).

[52] T. Schumucker, Planta **23**, 264 (1935).

[53] D. B. Dickinson, J. Am. Soc. Hort. Sci. **103**, 263 (1978).

[54] J. L. Brewbaker and B. H. Kwack, Am. J. Bot. **50**, 859 (1963).

[55] J. P. Mascarenhas, Ibid.

[56] D. E. Bilderback, Ibid.

[57] M. H. Weisenseel and L. F. Jaffe, Planta **133**, 1 (1976).

[58] K. R. Robinson and M. A. Messerli, Sci. STKE **2002**, pe51 (2002). The article in this electronic journal may be downloaded from the web site of one of the authors: http://www.biology.purdue.edu /people/faculty/robinson/Lab/publications.htm.

[59] X. Chao-Tian, Q. Yi-Lan , C. Su-Hong and T. Hui-Qiao, J. Pl. Physiol. and Molec. Biol. **31**, 53 (2005).

[60] N. A. Eckardt, The Plant Cell bf 17, 327 (2005).

[61] Here are some web sites that describe how to observe pollen tubes in the laboratory: http://www-saps.plantsci.cam.ac.uk/pollen/pollen2.htm,

http://www-saps.plantsci.cam.ac.uk/worksheets/ssheets/ssheet4.htm, and http://www.microscopy-uk.org.uk/mag/artdec99/jgpollen.html.

[62] H. Lewis and M. E. Lewis, *The Genus Clarkia* (University of California Publications in Botany **20**, pp. 241-392, 1955), p. 356.

[63] I grew Clarkia plants from Diane's seeds, http://www.dianeseeds.com: packets of C. pulchella (containing ≈1000 seeds), C. amoena (≈1800 seeds) and C. elegans (≈1500 seeds) each cost $2.00. Everwilde farms, http://www.everwilde.com sells packets (≈2000 seeds) of the latter two species for $2.50. Thompson and Morgan, http://www. tmseeds.com, a British company, sells packets of C. pulchella and C. elegans (≈400 seeds) for $2.55. Monticello sells a packet of seeds of C. pulchella (a plant cultivated by Thomas Jefferson) for $2.50, but I did not have good results with these seeds.

[64] The U. S. Department of Agriculture site, http://plants.usda.gov/, has much general information on species. Under Scientific Name, type in Clarkia, and then choose Clarkia Pursh.

[65] http://www.leevalley.com. The Lee Valley Seed Starter costs $22.50 plus shipping. One can purchase 25 plastic pots for $9.50, and a plastic tray which holds 24 such pots for $26.50.

[66] Hydrofarm Green Thumb or Jump Start (they seem to be the same) fixtures with bulbs are available from various vendors. For example, DirtWorks, http://www.dirtworks.net/Grow-Lights.html, sells the fixture, the 2 foot version (which will light one Lee Valley Seed Starter) costs $69 plus shipping and the 4-foot version (which I bought and which lights three Lee Valley Seed Starters) costs $89 plus shipping.

[67] ImageJ is available from the National Institutes of Health web site http://rsbweb.nih.gov/ij/.

[68] P. W. van der Pas, Scientiarum Historia **13**, 127 (1971): Of Brown's molecules, van der Pas says: " ... they were approximately of the same size; their diameter varying between 1.26 and 1.6 microns. These statements are not true, BROWN was led to them because he worked with an imperfect lens at the border line of its magnifying power." This seems to be the only place to find this latter assertion which, however, van der Pas did not enlarge upon. He wrote this paper to call attention to a rather throw-away paragraph in a paper in 1784 by Jan Ingenhousz, thereby intimating Ingenhousz's priority over Brown. The purpose of Ingenhousz's paper was to introduce the idea of a transparent cover slip in microscopy to prevent water evaporation. Unlike others who had seen Brownian motion before Brown, but attributed it to life, Ingenhousz observed and clearly asserted in this paragraph that nonliving matter underwent the motion, but he did no systematic investigation.

Citing van der Pas, Mabberley (Op. Cit. p. 272) says: "It has been shown that Brown's 'molecules' were artifacts, there being no particles 1.26-1.6 μm across in pollen grains or elsewhere." However, this statement is only partially correct. While there are not *universal* particles of this size range as Brown supposed, spherosomes imaged to such size were certainly seen by Brown. Spherosomes have been observed in various plant tissues of diameter .4-4 μm[69].

[69] T. J. Jacks, L. Y. Yatsu and A. M. Altschul, Plant Physiol. **42**, 585 (1967), L. Y. Yatsu, T. J. Jacks and T. P Hensarling, Plant Physiol. **48**, 675 (1971).

[70] K. W. A. Strehl, Zeit. fur Instr. **22**, 213 (1902). The Strehl criterion is mentioned in most books on optical design, e.g., D. Malacara and Z. Malacara, *The Handbook of Optical Design, 2nd Edition* (Marcel Dekker, New York 2003), p. 211.

[71] F. Perrin, Journ. Phys. radium **V**, 497 (1934); R. Vasanthi, S. Rarichandran and B. Bagchi, Journ. Chem. Phys. **114**, 7989 (2001); Y. Han et. al., Science **314**, 626 (2006).

[72] The polystyrene latex spheres were obtained from Ted Pella, Inc., http://www.tedpella.com/.

[73] Two web sites that describe construction of such microscopes are http://www.microscopy-uk.org.uk/mag/artjul06/aa-lens3.html and http://www.funsci.com/fun3_en/usph/usph.htm.

[74] Edmund Optical Company, 1 mm diameter ball lens #NT43-708, costing $22.

[75] A. C. Hardy and F. H. Perrin, *The Principles of Optics* (McGraw-Hill, New York 1932), p. 58, Eq. (71).

[76] A. Einstein, Ann. d. Phys. **17**, 549 (1905).

[77] P. M. Morse *Thermal Physics* (Benjamin, New York 1969), p. 228; C. Kittel *Elementary Statistical Physics* (Wiley, New York 1958), p. 153; a recent paper in this journal, D. Jia et. al., Am. J. Phys **75**, 111 (2007) (see also textbook references therein).

[78] K. Huang *Statistical Mechanics* (Wiley, New York 1965), p. 119 and and L. D. Landau and E. M. Lifshitz, *Fluid Mechanics* (Pergamon, Oxford 1978), p.63: the latter also contains a problem that discusses the viscous torque on a sphere, p. 68.

[79] The viscous force on an ellipsoid moving parallel to an axis is discussed in Lamb's classic volume, H. Lamb *Hydrodynamics* (Dover, New York 1945), section 339. The viscous torque on an ellipse rotating about an axis is calculated in a 1922 paper, G. B. Jeffery, Proc. Roy. Soc. London, series A **102**, 161(1922), Eq. (36).

[80] See chapter IX of M. Born and E. Wolf, *Principles of Optics* (Pergamon, Oxford 1983), sixth (corrected) edition, p. 459.

[81] J. D. Jackson *Classical Electrodynamics* (Wiley, New York 1975).

[82] M. Born and E. Wolf, Ibid, p. 387.

[83] A simpler problem is the scattering of a plane wave by a sphere. The solution for our problem (scattering of a wave emerging from a point source) is a superposition of solutions of the plane wave problem. However, this "simpler" problem is itself quite complicated. Its solution can be written exactly, as an infinite sum of angular momentum eigenstates, each with a spherical Bessel function giving the radial behavior. Since $\lambda << R$, one cannot truncate the series at a few terms. Sophisticated techniques (such as the Watson transform, Regge pole theory, method of steepest descent) are used to sum appropriate terms corresponding to the physical behavior of rays, first discussed by Debye. The first sum corresponds to reflection from the sphere, the second to the geometrical optics refraction and its attendant aberrations, the third to one internal reflection (responsible for the behavior of the rainbow), the fourth to two internal reflections (responsible for the behavior of the glory), etc: H. M. Nussenzveig, Journ. Math. Phys. **10**, 82 & 125 (1969). The sum for the electromagnetic field is called the Mie solution. Mie solution calculators, which sum the terms

numerically, are available on the web. For an analytic treatment, see W. T. Grandy Jr., *Scattering of waves from large spheres* (Cambridge U. P., Cambridge 2005).

[84] H. M. van Horn and E. E. Salpeter, Phys. Rev. **157**, 751(1967): this discusses the pioneering 1928 work of J. H. van Vleck.

[85] Born and Wolf, Ibid, opposite p. 478. See also http://en.wikipedia.org/wiki/Spherical_aberration.